ASSESSMENT OF THE SURFACE ENERGY OF POWDERS AND ITS USE IN PREDICTING THE STABILITY OF NONPOLAR NONAQUEOUS SUSPENSIONS

By

GARY EDWARD PARSONS

B.Pharm., MRPharmS

THESIS SUBMITTED FOR THE DEGREE OF DOCTOR OF PHILOSOPHY IN THE UNIVERSITY OF LONDON

SEPTEMBER, 1992

The School of Pharmacy,
29/39 Brunswick Square,
London,
WC1N 1AX.

ACKNOWLEDGEMENTS

I am indebted to Graham Buckton for his constant encouragement and guidance throughout the course of this work. His enthusiasm for the subject was a continual source of motivation.

I would like to thank Professor Newton and the staff of the pharmaceutics department for providing the facilities and resources necessary to complete this work. In particular I would like to thank Mr. Don Hunt for constructing much of the equipment used during this period of research, and Mr. John McAndrew and his staff for their technical support.

Thanks are also due to Dr. Sarah Chatham for her valuable and welcome advice over the past three years. The technical and financial support provided by Eli Lilly is also greatly appreciated.

I would like to thank my family for their interest in this work and the motivation they provided. I would also like to thank Alasdair MacKellar, Anthony Murray and Ken MacRitchie whose friendship made this work all the more enjoyable.

Finally, I would like to thank Ruth, without your encouragement, support and patience this work would not have been possible.

ABSTRACT.

The concept and application of solid surface energy values have been studied from a pharmaceutical perspective.

The derivation of solid surface energy is usually based on the contact angle formed between a liquid of known surface energy and the test solid.

Three commonly used methods of contact angle determination have been investigated, namely the Wilhelmy plate and sessile drop techniques (which utilise the sample in the form of a flat plate), and the liquid penetration technique which utilises a powdered sample of the solid. A system of model particles and plates has been used which allows systems of differing geometry to be studied, without altering the surface energy.

Contact angles obtained by the Wilhelmy plate and sessile drop techniques were found to be in good agreement with, but consistently lower than, those obtained by liquid penetration experiments.

A linear relationship was found to exist between the liquid penetration and Wilhelmy plate results, suggesting that the rate of liquid penetration through a

packed powder bed is not adequately described by the Washburn model of a bundle of parallel capillaries.

Surface energy values have been derived for the model systems studied by a variety of methods.

The harmonic and geometric mean variants of the theory of surface energy components, the theory of nonadditive surface energy components and an equation of state have been applied.

The derived values of surface energy were comparable for the theoretical models studied. Values for individual components of surface energy were dependent upon both the theoretical model and liquid pair used.

The stability of pharmaceutical nonaqueous nonpolar suspensions has been studied. The ease of dispersion, degree of aggregation and extent of powder adhesion to the container wall has been investigated for five solids (indomethacin, isoprenaline, aspirin, PTFE and beclomethasone) and related to surface energy data.

Each phenomenon could be related to calculated surface and interfacial parameters.

CONTENTS. PAGE

LIST OF FIGURES

LIST OF TABLES

LIST OF SYMBOLS.

a	=	constant
b	=	constant
β	=	constant
d	=	diameter of base of drop
f	=	fraction of surface
F	=	force on a Wilhelmy plate
G	=	Gibbs free energy
ΔG	=	change in Gibbs free energy under standard state conditions
g	=	acceleration due to gravity
h	=	height of capillary rise
ht	=	height of sessile drop
H	=	enthalpy
ΔH	=	change in enthalpy
l	=	distance of penetration
p	=	vapour pressure
ΔP	=	pressure difference
r	=	capillary radius
Sa	=	ratio of true and geometric surface area
S	=	entropy
ΔS	=	change in entropy
T	=	absolute temperature
t	=	time
V	=	volume of displaced liquid
Wa	=	work of adhesion
Wc	=	work of cohesion

W_i = work of immersion

W_s = work of spreading

Z_v = volume porosity

ϕ = interaction parameter

γ = interfacial or surface tension

γ_c = critical surface tension

γ_{sl} = solid/liquid interfacial energy

γ_{sv} = solid/vapour interfacial energy

γ_{lv} = liquid/vapour interfacial energy

γ^d = dispersion component of surface energy

γ^p = polar component of surface energy

γ^{p+} = electron acceptor (Lewis acid) parameter of polar forces

γ^{p-} = electron donor (Lewis base) parameter of polar forces

π_e = film pressure

ρ = density of solution

θ = undefined contact angle

θ_a = advancing contact angle

θ_d = dynamic contact angle

θ_e = equilibrium contact angle

θ_I = intrinsic contact angle

θ_r = receding contact angle

θ_y = Young contact angle

θ_w = Wenzel contact angle

λ_{12} = spreading coefficient of phase 1 over phase 2.

η = viscosity of solution

u = chemical potential

Γ = surface excess

Chapter 1

Introduction.

1. INTRODUCTION.

1.1. The Interface.

Any chemical or physical reaction involving a solid occurs at an interface (Veale, 1972). The nature of the interface is therefore of uppermost importance in this work.

Interfacial interactions influence the behaviour of many pharmaceutical formulations. The wetting of a tablet, the formation and subsequent stability of an emulsion and the dispersion and aggregation of particles in suspension, for example, all depend on favourable interfacial interactions.

An interface may be defined as the common boundary formed when two phases co-exist. The nature of the two phases determines the type of interface formed (table 1.1.1).

Table 1.1.1 Classification of interfaces.

Phases	Example
Gas/Gas	Does not exist
Gas/Liquid	Liquid surface
Gas/Solid	Solid surface
Liquid/Liquid	Emulsion
Liquid/Solid	Suspension
Solid/Solid	Powder particles in contact

Of most interest pharmaceutically are the solid/liquid, solid/solid and liquid/liquid interfaces. However, in order to understand the nature and behaviour of interfaces involving just solids and/or liquids, it is first necessary to consider the nature of liquid and solid surfaces (i.e. the solid/vapour and liquid/vapour interfaces).

1.1.1. Liquid surfaces.

Small drops of liquid spontaneously tend to assume the shape of a sphere, thereby minimising their surface area. Similarly, a stretched soap film will tend to become less extended. This tendency to contract to the smallest possible area is a fundamental property of liquid surfaces, and results in the apparent existence of a "tension" in the surface.

1.1.1.1. Molecular theory of surface tension and surface free energy.

The tendency of a liquid surface to contract in area can be simply explained by considering the behaviour of the molecules of the liquid. Liquids are distinguished from solids by the ability of the liquid molecules to move freely relative to one another. The cohesive forces between adjacent molecules in the liquid, however, are sufficiently strong to prevent more than a few molecules escaping into vapour, and distinguish the liquid from a gas.

Molecules in the bulk of the liquid are surrounded in all directions by similar molecules. Therefore, over a period of time, the net attraction on a molecule in any one direction is zero. A molecule in the surface, however, is subjected to attractive forces inwards towards the bulk and sideways by its neighbours in the surface. Since little outward attraction opposes the inward attraction, the resultant net force acting on a molecule in the surface is towards the bulk, perpendicular to the surface. Consequently as molecules move from the surface into the bulk at a faster rate than they are replaced, the number of molecules in the surface continually decreases until ultimately the surface area:volume ratio is at a minimum.

As a result of the discrepancy between the intermolecular forces in the bulk and surface, and the subsequent tendency to contract, a liquid surface behaves as if it were in a state of tension. If an imaginary cut were made in the surface, a force proportional to the length of the cut would be required to hold the molecules along both sides of the cut together. The value of this force per unit length is called the *surface tension*, γ, (mN/m). The surface tension may be defined as the force per unit length that must be applied parallel to the surface in order to counterbalance the net inward pull.

Any spontaneous process occurring at constant temperature and pressure must be accompanied by a decrease in free energy. The spontaneous contraction of

a liquid surface must therefore be associated with a free energy change. This can again be explained at a molecular level; work must be done in order to increase the surface area, since molecules must be brought from the bulk into the surface, against the inward attractive force, to a position less thermodynamically favoured. The work required to increase the surface by $1cm^2$ is called the *surface free energy* (mN/m), and is mathematically equivalent to the surface tension.

1.1.2. Solid surfaces.

The solid surface is far more difficult to characterise than the liquid surface. Although many of the principles pertaining to liquid surfaces also apply to solid surfaces, a fundamental difference between them is the mobility of their constituent molecules. The solid state is characterised by a rigidity of form and a tendency to maintain a definite shape, in contrast to a liquid in which the molecules are able to move relatively long distances quite freely.

The typical solid state is associated with a defined crystalline form, i.e. an ordered arrangement of the constituent atoms or molecules in the substance. Amorphous solids, such as glass, are essentially intermediate between the solid and liquid state, with only a partial degree of regularity of internal structure. The crystalline solid form can be distinguished from the amorphous solid form in many ways. Crystals, for example, possess a sharply defined

melting point whereas amorphous solids do not. One of the most fundamental differences, however, is the manifestation of regularity in the external form, (as well as in the internal arrangement), of crystals. Nearly all crystals have properties that vary with the direction in which they are measured, (exceptions to this are those crystals belonging to the cubic or regular system). Such substances are described as *anisotropic* , as opposed to cubic crystals and amorphous materials (and liquids) which are *isotropic*.

The major implication of the difference in molecular mobility, however, is that solids cannot exhibit those properties of liquids which involve molecular movement. For example, solids are unable to contract spontaneously. Secondly, the solid surface is usually extremely irregular. Solid surfaces are often rough because molecules are not free to move after new surface is formed, for example after grinding. The chemical nature of the molecules at the surface may then vary, as may the stress to which each molecule is subjected (Bikerman, 1957).

1.1.2.1. Solid surface cleanliness.

Another important difference between solid and liquid surfaces is that most solid surfaces are contaminated with a thin layer of foreign matter (Parfitt & Sing, 1976). The deposition of a greasy layer on the surface of solids left unprotected in air was first observed and reported in 1859 by Quincke.

Adsorption of gas at various regions of the surface can also occur and although the adsorbed/deposited layers may only be monomolecular in nature, they can have a profound effect on the physical chemistry of the surface by, for instance, reducing the overall surface free energy.

1.1.2.2. Solid surface energy.

The surface energy of a solid is well known to be one of the most important properties influencing colloidal behaviour (Martin et al., 1983). Indeed, the outcome of any process involving a solid/liquid or solid/solid interface will be determined by the respective surface energies.

Unfortunately, for direct measurement of surface or interfacial tension, a reversible deformation of the surface is necessary - the surface must be extended or contracted - which is obviously not possible for the majority of solids. Therefore, properties that are easily measured for liquid/liquid and liquid/gas interfaces are not measureable for solid/liquid and solid/solid interfaces or the solid/gas interface (i.e. the surface energy of the solid).

Also, the shape of a crystal of a given compound or element often varies with the conditions under which crystallisation occurs, (although the angles between the faces are always constant). A solid will crystallise in such a conformation as to minimise its surface free energy, analogically to liquids which tend to contract

in order to reduce the surface free energy of the system, (cf. section 1.1.1.). The preponderance of one crystal face at the expense of another, however, may significantly affect the overall surface energy of the solid.

Similarly, Lavielle and Schultz (1985) have shown how polymer surfaces can rearrange depending on their environment and consequently can exhibit a range of surface tensions.

It is apparent then, that the surface free energy of a solid will vary from region to region due to surface roughness, varying crystal faces, adsorbed layers etc., hence any reference to the surface free energy of a solid must be an average surface free energy for a large area of surface.

For these reasons, indirect means of estimating solid surface energy have to be used (see section 1.3).

1.2. Interfacial phenomena.

Since this work is, in the main, concerned with the wettability of solids, the solid/vapour, solid/liquid and liquid/vapour interfaces are of most interest.

1.2.1. The liquid/vapour interface.

The interfacial free energy of the liquid/vapour interface is equivalent to the surface tension of the liquid in the presence of its vapour. Since liquid surfaces are deformable, the interfacial free energy of the liquid/vapour interface is easily measured. Padday

(1963) has reviewed a variety of methods of liquid surface tension measurement.

1.2.2. The solid/vapour interface.

The interfacial free energy at the solid/vapour interface, γ_{sv}, provides a measure of the affinity of the vapour for the solid surface. It can also be related to the wettability of the solid surface (see section 1.3.1).

The forces of attraction between solid and adsorbed vapour are of two types; physical and chemical, giving rise to physical and chemical adsorption, respectively.

Physical adsorption occurs with all substances. It is associated with van der Waals forces of attraction (Glasstone and Lewis, 1960), and is reversible.

Chemical adsorption is exhibited by fewer substances than physical adsorption, and is associated with irreversible chemical forces of attraction.

1.2.2.1. Thermodynamics of solid/vapour adsorption.

It is possible to quantify physical adsorption in terms of changes in enthalpy (H), entropy (S) and Gibbs free energy (G) within the system.

The adsorption process at constant temperature may be followed by the measurement of the decrease in pressure (and/or volume) of the gas or the increase in weight of the solid. The relationship between the amount of gas adsorbed and the equilibrium pressure at a known

constant temperature is known as the adsorption isotherm.

Since physical adsorption is a spontaneous process, it is accompanied by a decrease in the free energy of the system. A decrease in entropy also occurs as the molecules of gas become more ordered when adsorbed to the solid surface.

The enthalpy change is related to the change in entropy and free energy by the general equation

$$\Delta G = \Delta H - T\Delta S$$

and must therefore be negative. Physical adsorption therefore is an exothermic process. This was demonstrated by Schroder (1984). In contrast, the process of chemical adsorption is often found to be endothermic.

1.2.3. The solid/liquid interface.

The solid/liquid interface is critical in determining whether a liquid spreads over a solid surface, thereby 'wetting' the surface. Spreading will only occur if it is energetically profitable. Detergency, lubrication and the wetting of powders are all examples of processes involving the solid/liquid interface.

The solid/liquid interfacial tension opposes the spreading of liquids across a solid surface, thus inhibiting wetting (see figure 1.3.2).

1.3. Methods for estimating solid surface energy.

1.3.1. The contact angle.

The most common approach to estimating the surface free energy of a solid is to consider the angle of contact formed between a liquid drop on a flat solid substrate, in equilibrium with the liquid vapour. The *contact angle* is measured through the liquid at the line of contact between three phases; the solid (S), the liquid (L) and the corresponding equilibrium vapour (V) (Fig.1.3.2).

As described previously (section 1.1.1), a free liquid drop assumes the shape which minimises the free energy of the system. This principle can be extended to the situation where a small liquid droplet is put in contact with a flat solid surface. Two distinct equilibrium states may be observed; i) partial wetting, with a finite contact angle, θ_e, (Fig.1.3.1(a) & 1.3.1(b)) and ii) in certain circumstances, complete wetting, where $\theta_e=0$, (Fig.1.3.1(c)),(de Gennes, 1985). In most instances the drop will not spread over the solid, but will remain as a drop with a definite angle of contact between itself and the solid. As such, the contact angle provides a convenient and useful measure of wettability, giving information on surface energetics, surface roughness and surface heterogeneity (Johnson and Dettre, 1969).

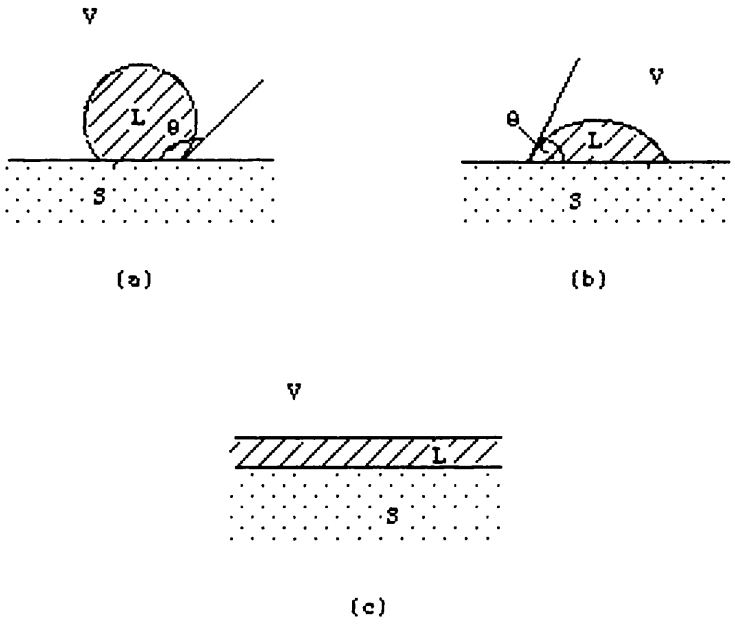

Figure 1.3.1 A small droplet in equilibrium on a horizontal surface: (a) and (b) correspond to partial wetting, the trend towards wetting being stronger in (b) than (a). (c) corresponds to complete wetting (θ = 0) (from de Gennes, 1985).

1.3.2. The Young equation.

All methods of contact angle interpretation start with the Young equation which relates the interfacial free energies of the three phases present with the Young contact angle, θ_y;

$$\gamma_{sv} = \gamma_{sl} + \gamma_{lv}.\cos\theta_y \qquad \text{Eqn.1.3.1}$$

where γ_{sv}, γ_{sl}, and γ_{lv} are the interfacial free energies of the solid/vapour, solid/liquid and liquid/vapour phases respectively.

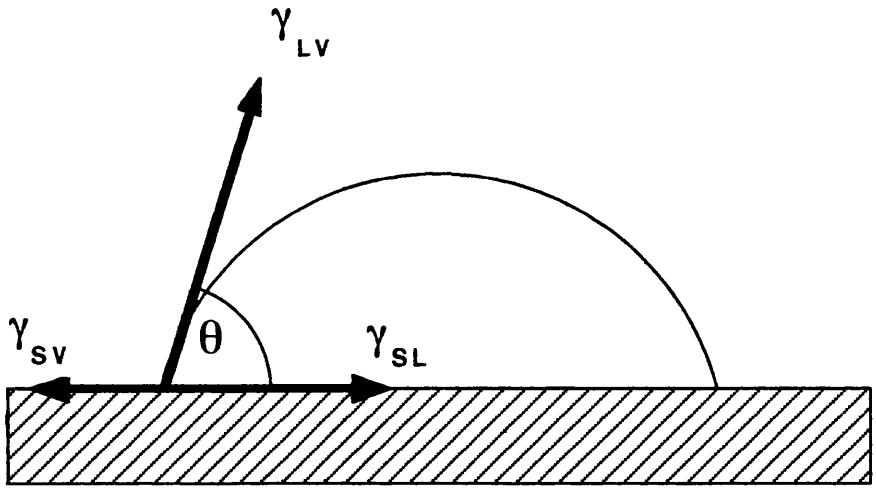

Figure 1.3.2. The contact angle.

From Fig.1.3.2, it can be seen that Young's equation is obtained by resolving the forces acting about the three phase contact line in a horizontal direction.

Of the terms in the Young equation, γ_{sl} is of most use as it can be related to the surface energy of the solid, γ_s, by the so-called film pressure, π_e, such that;

$$\gamma_s - \pi_e - \gamma_{sl} = \gamma_{lv} \text{ Cos } \theta_y \qquad \text{Eqn.1.3.2}$$

The film pressure term, π_e, relates the surface free energy of the solid in vacuo γ_s, to the surface free energy of the solid after adsorbtion of liquid vapour, γ_{sv}, i.e. $\gamma_s - \pi_e = \gamma_{sv}$.

The value of γ_{sv} may be considerably lower than γ_s, however, in the case of nonvolatile liquids, π_e is generally assumed to be negligible.

The validity of the Young equation has long been a topic for debate, but its scientific basis is now generally accepted provided θ is a Young contact angle, θ_y. The Young contact angle, θ_y, can essentially be regarded as equivalent to the equilibrium contact angle, θ_e, although Neumann (1974), Neumann and Ward (1974) and Good (1979) have proposed that, in certain cases, advancing, nonequilibrium contact angles may be applied to the Young equation, based on thermodynamic arguments (see section 1.4.1.2.).

Young's equation is often combined with Dupré's equation (1869);

$$W_a^{sl} = \gamma_{sv} + \gamma_{lv} - \gamma_{sl} \qquad \text{Eqn.1.3.3}$$

to give;

$$W_a^{sl} = \gamma_{lv}.(1 + \text{Cos } \theta) \qquad \text{Eqn.1.3.4}$$

(where W_a^{sl} is the work of adhesion between the solid and liquid), to provide a valuable means of calculating the strength of attraction between the solid and liquid.

The derivation of solid surface energy data from contact angle measurements is reviewed in more detail in chapter 3.

1.4. Contact angle hysteresis.

The derivation of Young's equation assumes that the liquid is spreading on a smooth, flat, nondeformable solid. In this idealised situation only one equilibrium

contact angle should exist. In practice it is found that, in most cases, a number of different angles can be measured, bounded by an upper and lower limit known as the advancing, θ_a, and receding, θ_r, angles respectively. Johnson and Dettre (1969) referred to the difference, $\theta_a-\theta_r$, as the *hysteresis*. Penn and Miller (1980a) suggest that a "stable" equilibrium contact angle θ_e, distinct from the advancing or receding angle does not exist. They proposed that through evaporation of the liquid, the contact angle will tend towards the receding angle. On the other hand, if evaporation is eliminated and the liquid is in the advancing mode, the advancing angle will persist even if advancement is stopped.

Hysteresis can be studied by considering a drop on a tilted plate (McDougall and Ockrent, 1942) as illustrated in figure 1.4.1.

Similar hysteresis can be seen by using a syringe to increase or decrease the volume of a drop on a solid surface such that the three phase boundary moves over the surface. Elliot and Riddiford (1967) have shown that the speed at which this is performed can affect the degree of hysteresis.

The extent of hysteresis can vary widely depending upon the liquid used and the surface studied. Birdi (1982) showed that if $\gamma_s^p = 0$ (i.e. the solid surface is apolar), then $\theta_a = \theta_e$. Penn and Miller (1980) reported a contact angle hysteresis of 50° for water on graphite

but no hysteresis at all for hexadecane on the same surface.

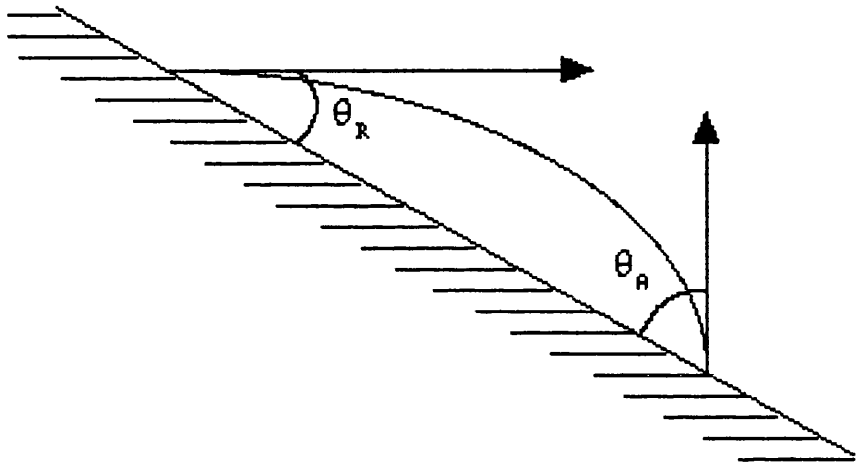

Figure 1.4.1 A drop on a tilted surface, showing an advancing and a receding contact angle.

1.4.1. Causes of contact angle hysteresis.

Contamination of the liquid or solid surface, surface chemical heterogeneity and surface roughness are generally accepted as the three main causes of contact angle hysteresis, although van Damme et al. (1986) have investigated the effect of polymer surface chain mobility on contact angle hysteresis. They concluded that it was a possible cause although the magnitude of the effect was also a function of temperature and chain length.

1.4.1.1. Surface contamination.

Surface contamination can affect contact angle values by virtue of the fact that the solid surface initially wetted by the liquid may differ from that

emerging from it. For example, a thin film of oil on a solid substrate may spread on the liquid surface, altering the interfacial values γ_{lv} and γ_{sv}. Rigorous cleaning has in some instances practically eliminated hysteresis (Fowkes and Hawkins, 1940).

1.4.1.2. Surface heterogeneity.

Cassie (1948) performed many of the early investigations into hysteresis. He originally proposed that the equilibrium contact angle of a smooth, patchy heterogenous surface could be described by an area-weighted average;

$$\text{Cos } \theta_C = f_1.\text{Cos } \theta_C + f_2.\text{Cos } \theta_C \qquad \text{Eqn.1.4.1}$$

where f_1 and f_2 are the area fractions of type 1 and 2.

Pease (1945) advanced the Cassie approach somewhat, by associating the advancing angle with the line of least work of adhesion and the receding angle with the line of most work of adhesion that the three phase junction can assume. The equilibrium contact angle, θ_e, is then defined by Pease (1945) as the line of least possible mean work of adhesion. Pease concluded that advancing contact angles measured on heterogenous surfaces were associated with the nonpolar portion of the surface and that receding angles were a measure of the polar portion.

This theory was essentially reiterated by Good (1979) who proposed that for a patchwise heterogenous

surface, "θ_a is related to, if not equal to, the equilibrium contact angle that would be observed on a homogenous, flat surface composed of the lower energy component". The receding angle is then taken to characterise the high energy component. A logical extension of Good's (1979) argument is that for a heterogenous surface, both the advancing angle and the receding angle can be used as a Young's contact angle, θ_y, when considering the low energy (most hydrophobic) and high energy (most hydrophilic) components of the surface respectively.

Shuttleworth and Bailey (1948) introduced the concept of an energy barrier between metastable states, which has been shown (Johnson And Dettre, 1964) to be one of the most important factors influencing hysteresis. Likewise, Neumann and Good (1972) showed that certain thermodynamic states are only possible when the liquid drop is advancing or receding, or has previously advanced or receded. Good (1953) and Johnson and Dettre (1964) demonstrated this effect using a model system of concentric rings.

1.4.1.3. Surface roughness.

Penn and Miller (1980b) report that heterogeneity is the most important factor influencing contact angle hysteresis, and that the significance of rugosity is questionable. Figure 1.4.2 shows the potential effect of surface roughness on contact angles.

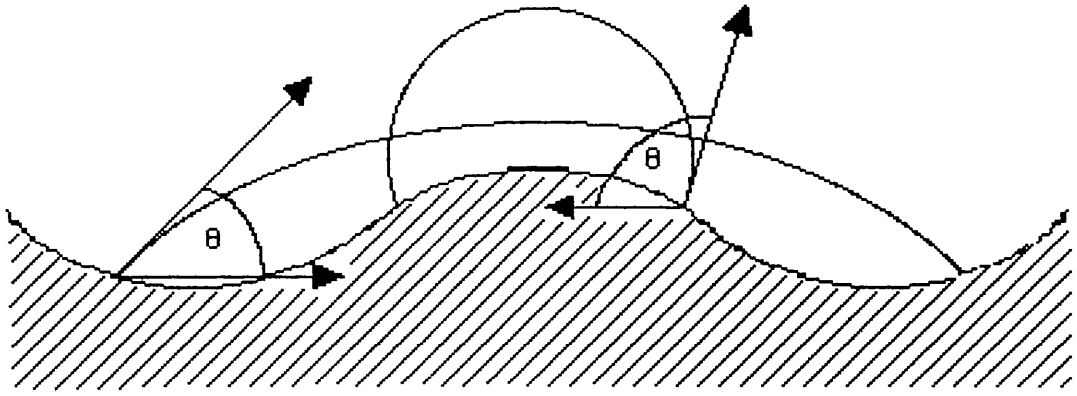

Figure 1.4.2 The effect of surface roughness on contact angle.

Zografi and Johnson (1984) investigated the effect of surface roughness on contact angle hysteresis using pharmaceutical powder compacts and found that although roughness had a significant effect on the receding angle, the advancing angle was virtually unaffected. They therefore proposed using θ_a as an estimate of the equilibrium contact angle, θe.

Hysteresis on rough surfaces would be expected to be large since a drop spreading on a rough surface has to overcome higher energy barriers than on a corresponding flat surface. This has in fact been demonstrated by Johnson and Dettre (1964) using both idealised and real systems. Several workers have attempted to quantify the effect of surface roughness on contact angle hysteresis using surfaces with various defined degrees of roughness, including Wenzel (1936), Cassie and Baxter (1944), Shepard and Bartell (1953a,

1953b) and Bikerman (1950). Wenzel (1936) proposed the following relationship;

$$S_a\ (\gamma_{sv} - \gamma_{sl}) = \gamma_{lv}\ \mathrm{Cos}\ \theta_w \qquad \text{Eqn.1.4.2}$$

where S_a is the ratio of the true and geometric surface area, and θ_w is the Wenzel contact angle.(equivalent to θ_e for the wetting of a rough surface).

If θ_I is the true contact angle, which locally satisfies Young's equation (eqn.1.3.1) then;

$$\mathrm{Cos}\theta_I = \frac{\gamma_{SV} - \gamma_{SL}}{\gamma_{LV}} \qquad \text{Eqn.1.4.3}$$

combining equations 1.4.2 and 1.4.3;

$$\mathrm{Cos}\ \theta_w = S_a\ \mathrm{Cos}\ \theta_I \qquad \text{Eqn.1.4.4}$$

Erick et al. (1975) proposed a model of an idealised rough surface (see fig.1.4.3) (similar to the model proposed by Neumann and Good (1972) for heterogenous surfaces (see section 1.4.1.2)), and demonstrated the existence of a large number of metastable states, i.e. the existence of a large number of distinct contact angles between θ_a and θ_r. Unfortunately it is not possible to attach any particular relevance to θ_a and θ_r, unlike the case for heterogenous surfaces (cf. section 1.4.1.2). Contact

angles measured on rough surfaces are generally advancing contact angles which cannot therefore be considered equilibrium contact angles. Consequently equation 1.4.4. cannot be applied as θ_w is impossible to determine.

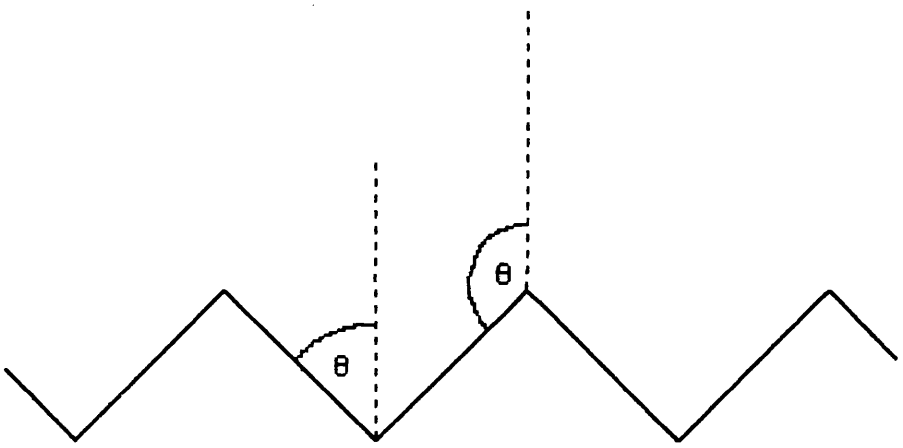

Figure 1.4.3 Contact angles on an idealised rough surface.

1.4.1.4. The critical size of rugosities/heterogeneities

In sections 1.4.1.2 and 1.4.1.3, the effect of surface roughness and heterogeneity on contact angles was discussed. However, in practice, all surfaces must contain some degree of rugosity and heterogeneity, even if only at a molecular level. Since not all surfaces exhibit hysteresis, there must be a certain magnitude of rugosity/heterogeneity below which hysteresis is not apparent (or measurable).

The critical size in the case of rugosities has been shown by Neumann et al. (1971) to be in the region

of 0.1μm, although this value may be affected by the type of system and the shape of the rugosity.

In the case of heterogeneity, a critical size is difficult to determine. The model system described by Neumann and Good (1972) consisting of a surface comprised of vertical strips of high and low energy material, exhibits hysteresis only in one configuration, that is when the line of contact has the potential to distort. The critical heterogeneity size therefore remains unknown.

1.5. Techniques of measuring contact angle.

The previous section dealt with the relationship between contact angle data and solid surface energy. This section will deal with the type of technique that may be employed for measuring contact angles.

Many of the methods that exist for the measurement of contact angles have been reviewed in detail by Neumann and Good (1979). The ultimate choice depends on the gross geometry of the sample under investigation with techniques existing for the measurement of contact angles on, for example, flat plates, the inner surface of capillary tubes, fibres and powders. From a pharmaceutical point of view, techniques utilising a smooth flat sample, the solid in powder form or a compressed disc or plate of powder are of most interest and these methods will be considered here.

1.5.1. Measurements on a flat plate.

1.5.1.1. Sessile drop or adhering gas bubble.

The direct measurement of a contact angle from the profile of a sessile drop or adhering gas bubble is the most widely used technique, employed extensively by Zisman (1964) and Fox and Zisman (1950) who made direct measurements using a telescope equipped with a goniometer eye-piece. Alternatively measurements can be made from a photograph of the drop or bubble. A photographic approach offers greater precision and convenience and dynamic effects can be followed through multiple exposures. For high accuracy, a large number of photographs are necessary.

An alternative approach to obtaining a contact angle from a sessile drop or adhering bubble was proposed by Bartell and Zuidema (1936), whereby basic rules of trigonometry are applied to the drop shape (assuming that the drop is sufficiently small that gravitational distortion is negligible). If **d** is the chord of a segment of a circle (in this case the diameter of the base) and **h** is the height, then;

$$\frac{2h}{d} = \mathrm{Tan}\frac{\theta}{2} \qquad \text{Eqn.1.5.1}$$

For gravitational effects to be negligible, however, the drop must be very small, which is likely to make h and d too small to measure accurately. Similar

derivations for larger nonspherical drops have been attempted (Padday 1963).

Recently, Duncan-Hewitt et al. (1989) have applied computer analysis to the drop shape (modified axisymmetric drop shape analysis, ADSA) to improve precision and increase objectivity.

1.5.1.2. Tilting plate method.

This classic method for determining accurate contact angles was developed by Adams and Jessop (1925). A plate approximately 2cm wide is dipped into the liquid and its tilt is altered until the angle is such that the liquid surface remains flat right up to the solid surface, in other words until the meniscus becomes flat. The angle between the plate and the horizontal is then equivalent to the contact angle.

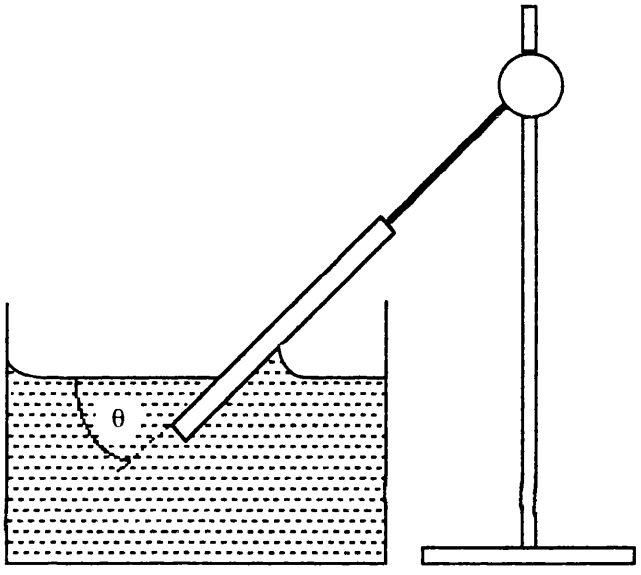

Figure 1.5.1 The tilting plate method for contact angle measurement.

This method allows simple and accurate measurements to be made. However, it is difficult to measure advancing and receding angles and it is likely that the angle obtained lies somewhere between θ_a and θ_r. Consequently the method has limited use (Adamson 1982).

1.5.1.3. Wilhelmy-gravitational method.

The basic premise for this technique is that proposed by Wilhelmy (1863). When a smooth, vertically suspended flat plate is brought into contact with a liquid, a downward force is exerted on it, given by;

$$f = p\gamma_{lv}\cos\theta \qquad \text{Eqn.1.5.2}$$

where p is the perimeter of the plate.

A correction can be made if the depth of immersion is not zero, such that;

$$F = p.\gamma_{lv}.\cos\theta - V.\rho.g \qquad \text{Eqn.1.5.3}$$

where V is the volume of displaced liquid, and ρ is the density of the liquid.

With the advent of sensitive microbalances and microprocessors, this technique has become extremely simple and convenient to perform. The plate is suspended from a microbalance above a liquid of known surface tension. The liquid is raised by means of a motorised platform up to and beyond the first point of contact with the solid. Meanwhile the force acting on the plate

is measured continuously by the microbalance. The change in force with time can subsequently be computer processed to give a value for the force at the point of zero depth of immersion i.e. the point at which the only force acting on the plate is due to a function of the surface tension of the liquid and its contact angle with the plate. Equation 1.5.2 then applies.

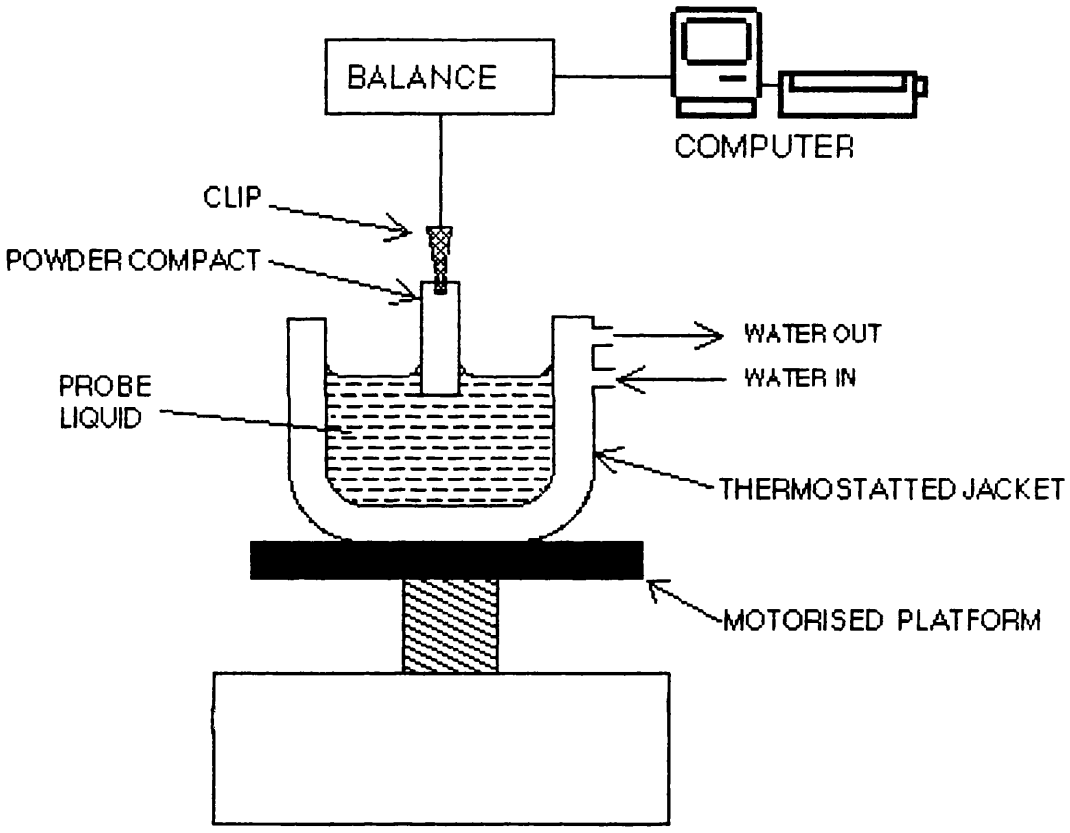

Figure 1.5.2 The wilhelmy method for contact angle measurement.

The advantages of this arrangement are related to its versatility. Contact angles can be monitored over time which, for example, allows changes due to temperature or adsorption to be monitored. Advancing and

receding contact angles can readily be established and the consistency of the contact angle over the length of the specimen can be tested. This technique has the added advantages of being fast, precise and operator independent.

1.5.1.4. Capillary rise at a vertical plate.

This method is a derivation of the Wilhelmy method, credited to Neumann (Padday, 1969). The plate is again aligned vertically and brought into contact with the liquid. However, unlike the Wilhelmy method, the pull on the plate is not measured. Instead, the capillary rise (**h**) at the vertical surface is recorded.

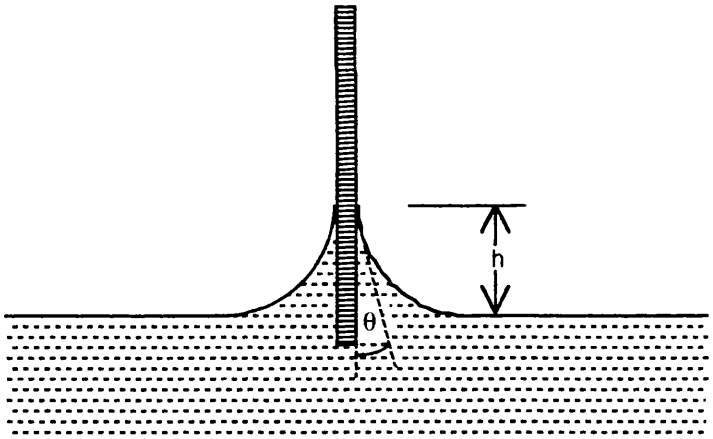

Figure 1.5.3 Neumann's method for contact angle measurement.

For an infinitely wide plate, (which for practical purposes may be about 2cm wide, integration of the Laplace equation gives;

$$\sin\theta = 1 - \frac{\Delta\rho.g.h^2}{2.\gamma_{lv}} \qquad \text{Eqn.1.5.4}$$

This method has been successfully used to monitor the temperature dependence of contact angles (Adamson, 1982)

1.5.1.5. Reflection method (Langmuir-Schaeffer Method).

The Langmuir-Schaeffer method (Adamson, 1982) employs the specular reflection from a drop to measure the contact angle. A light source, mounted on a viewing arm, is pivoted on an axis until an angle is found whereby the reflected beam from the edge of the meniscus on a vertical plate or capillary tube returns along the line of the incident beam (Padday, 1978). The accuracy of this method is reputedly equivalent to that of other methods.

1.5.2. Irregular Particles, (powders).

Obviously, those methods requiring a flat surface for the direct measurement of θ are not applicable to powders which comprise small, irregularly shaped particles. Indirect methods of estimating θ therefore have to be employed which, in the main, consider the flow of liquid through capillaries formed in a loosely compressed bed of the powder.

1.5.2.1. Rate of capillary penetration techniques.

The simplest equation to model the rate of capillary penetration into a porous medium is attributed to Washburn (1921). The model assumes the packed powder bed to be a bundle of uniform capillary tubes, and the

driving force for penetration is assumed to be the capillary pressure. Then, according to Pouseuille's law, the rate at which a liquid penetrates a small cylindrical capillary of radius, **r**, is;

$$\frac{dl}{dt} = \frac{\Delta P \, . \, r^2}{8.\eta.l} \qquad \text{Eqn.1.5.5}$$

where **P** is the driving pressure, **l** is the length of the column of liquid at the time, **t**, and η is the viscosity of the liquid.

Integration of equation 1.5.5 yields;

$$l^2 = \frac{\gamma_{lv}.Cos\theta}{2\eta} .r \ .t \qquad \text{Eqn.1.5.6}$$

which is applicable to a liquid flowing under its own capillary pressure in horizontal capillaries, or any capillaries with a sufficiently small surface.

According to the Washburn equation (eqn.1.5.6), l^2 is directly proportional to t. Hence, a plot of l^2 as a function of t should yield a straight line.

Although the model of a bundle of parallel capillaries is simplistic, it is generally accepted and has been widely used, e.g. Fisher and Lark (1979), Buckton (1985a, 1986), Crawford (1987). However, reservations do exist regarding the use of the Washburn equation, most notably those expressed by Yang et al.

(1986,1988) and Carli and Simioni (1979). These will be discussed in Chapter 2, section 2.8.3.3.

1.6. The wetting process.

Much of the work contained in this thesis is concerned (directly or indirectly) with the wetting of a solid by a liquid, a process that has been studied in depth due to its importance in a wide range of fields such as froth flotation, detergency and pigment dispersion.

Three distinct types of wetting have been identified to describe the wetting of a powder by a liquid to form a solid/liquid interface. These have been termed adhesional, spreading and immersional wetting (Parfitt, 1973, Osterhof and Bartell, 1930).

In order to fully disperse a powder such that complete wetting occurs, a combination of the three wetting processes is often required (Heertjes & Witvoet, 1969,1970).

A useful model to describe the three process of dispersion has been given by Patton (1966) and Parfitt (1973). The model assumes the solid to be in equilibrium with the vapour and that the density of the solid is equal to that of the liquid. The solid is assumed to be a cube of one metre dimensions, and each stage in the process is considered individually. The model is illustrated in figure 1.6.1.

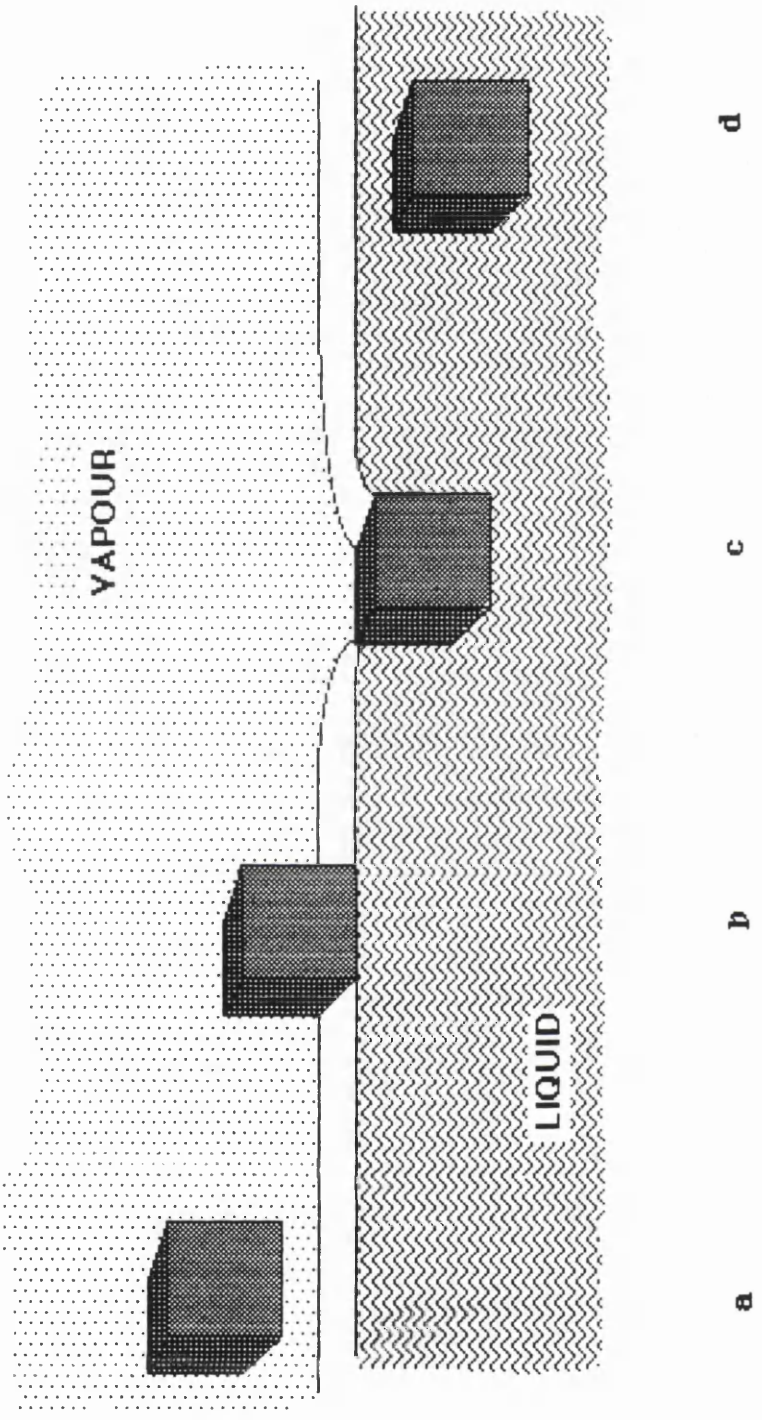

Figure 1.6.1 The stages in the wetting process.
a - b = adhesional wetting,
b - c = immersional wetting,
and c - d = spreading wetting.
(after Parfitt, 1973).

1.6.1. Adhesional wetting.

Adhesional wetting can be described as the replacement of $1m^2$ of plane liquid surface by $1m^2$ solid/liquid interface. In this case the work required, W_a, is given by;

$$W_a = \gamma_{sl} - (\gamma_{sv} + \gamma_{lv}) = -\gamma_{lv}.(\text{Cos } \theta + 1)$$

Eqn.1.6.1

1.6.2. Immersional wetting.

The immersion of a solid in a liquid involves the replacement of the solid/vapour interface with a solid/liquid interface. In the case of a cube with each face having an area of $1m^2$;

$$W_i = 4.\gamma_{sl} - 4.\gamma_{sv} = -4.\gamma_{lv}.\text{Cos } \theta$$

Eqn.1.6.2

1.6.3. Spreading wetting.

As the liquid spreads over the solid surface, solid surface area is replaced in equal amounts by liquid surface and solid/liquid interface. Hence the work of spreading wetting is given by;

$$W_S = (\gamma_{sl} + \gamma_{lv}) - \gamma_{sv} = -\gamma_{lv}.(\text{Cos } \theta - 1)$$

Eqn.1.6.3

1.6.4. Conditions for spontaneous wetting.

By considering the changes in free energy, it can be deduced that each phase will occur spontaneously if the following conditions are met;

Adhesion: $\gamma_{lv}.(1-\text{Cos }\theta) > 0$

Immersion: $\gamma_{lv}.\text{Cos }\theta > 0$

Spreading: $\gamma_{lv}.(-1 + \text{Cos }\theta) > 0$

Since γ_{lv} is always positive, the value of Cos θ will determine whether each condition is satisfied.

Therefore adhesional wetting will occur for all values of Cos θ greater than -1. i.e. in all cases except when θ=180. Similarly, immersional wetting will be spontaneous if Cos θ > 0 (0 <= θ <= 90). The condition for spontaneous spreading wetting, Cos θ > 1, can never be satisfied although, in practice, extra influences such as density can facilitate spontaneous spreading wetting.

Consideration of the total process (a-d, Fig.1.6.1) yields the following relationship;

$$W_t = W_a + W_i + W_s = 6.\gamma_{sl} - 6.\gamma_{sv} = -6.\gamma_{lv}.\text{Cos }\theta$$

Eqn.1.6.4

From this it could be inferred that the entire process will be spontaneous when Cos θ > 0. This conclusion must however be false as it has already been shown that the

condition for spontaneous spreading wetting can never be satisfied. It is apparent that the process of complete wetting should be considered in terms of the composite stages of wetting along with various extra influences (e.g. density), rather than as a single transition.

1.7. Pharmaceutical applications of wetting.

The phenomena of wetting, spreading and adhesion have a wide range of application, from the dispersion of pigments in paints to froth floatation. One field where the application of a knowledge of these phenomena has perhaps been underexploited, however, is in the rationalisation of pharmaceutical formulation.

By definition, any formulation consists of two or more ingredients. Excipients in a formulation have the potential to interact at the interfacial level, and it is these interactions which should, in theory, be predictable from a knowledge of the surface free energy of the individual excipients. Interfacial interactions between the excipients and container in which they are packaged should also be predictable.

Recently, however, a growing amount of interest has been shown in the application of wetting phenomena to pharmaceutical formulation. Rowe (1990) attempted to correlate measured properties of paracetamol granules and tablets with estimations of the interfacial interactions between the binder and paracetamol. Rowe (1989) and Zajic and Buckton (1990) have also used

surface energy values to predict optimum binder selection for granulations.

The adhesion of polymer film coatings to tablets has been considered in terms of surface energies by Davies (1985) and Rowe (1988), and the stability of suspensions is well known to be dependent on interfacial interactions (Hiestand, 1966). Young and Buckton (1990) have investigated some of these interactions in suspensions of barbiturates.

1.8. Aims and Objectives.

The potential usefulness of solid surface energy values is emphasised by the extensive volume of work that has been, and continues to be, performed in the field.

Some pharmaceutical applications of wetting are listed in the previous section. With pharmaceutical formulations, however, the potential for the use of solid surface energies is virtually endless since most excipients and pack components have the ability to interact interfacially.

The application of surface energy values is pointless, however, if the values estimated are not accurate or representative of the actual surface energies. Since the first stage in the calculation of solid surface energy generally requires the measurement of a contact angle, it is vital that the contact angle is measured accurately and reproducibly.

In Chapter 2 of this work, three techniques commonly used to measure contact angle will be assessed and compared. Two of the techniques (the sessile drop and Wilhelmy plate techniques) employ a compressed plate of the test powder, and the third technique (liquid penetration) uses the uncompressed powder.

In order to minimise differences occurring between the techniques due to powder processing (i.e. compression) model surfaces will be used. The usefulness and range of applicability of each technique will be assessed, and differences between them discussed.

The treatment of contact angle data will be assessed in Chapter 3, by applying several well used theoretical models for surface energy determination to the contact angle data obtained in Chapter 2.

Finally, in Chapter 4, surface energy values will be calculated for several model powders. The calculated surface energy values will be correlated with various interfacial events occurring in nonaqueous, nonpolar suspensions with the aim of assessing the applicability of surface energy values to this purpose. The strengths and weaknesses of applying surface energy values to interfacial events in nonaqueous, nonpolar media will also be discussed.

Chapter 2

A comparison of three techniques used to measure contact angles.

2.1 Introduction.

Recently, considerable interest has been shown in the measurement of the surface energetics of pharmaceutical powders (Rowe 1990, Young and Buckton 1990, Zajic & Buckton 1990), the aim being to predict the outcome of various interfacial phenomena. For example, Young and Buckton (1990) attempted to describe the physical stability of suspensions of various barbiturates in terms of surface and interfacial free energies. Similarly, Rowe (1990) and Zajic and Buckton (1990) used surface energy values and spreading coefficients to predict the optimum choice of binder for granulation.

As discussed in the previous chapter, in order to estimate solid surface energy it is first necessary to measure the contact angle of various liquids on the solid in question. It is crucial therefore that the contact angle is measured accurately and reliably, to ensure that the best estimate of solid surface energy is obtained.

Samples of interest pharmaceutically, however, often exist as powders, and the decision has to be made whether or not to compress the powder to form a compact suitable for use in, for example, the sessile drop technique, or to use the powder as received and employ a penetration technique. The decision is not straightforward since compression of the powder may alter the surface characteristics of the sample (Buckton, 1985, Buckton & Newton, 1986c). Crawford et

al. (1987) also claimed that compression of particles into a compact creates problems such as variations in porosity, liquid absorption and surface roughness. On the other hand, the use of a penetration technique has been criticised theoretically (Yang and Zografi, 1986, Levine and Neale, 1974) and may present problems such as nonpenetration of the liquid.

There is an abundance of techniques by which contact angles may be measured on a wide range of different solid systems (see Ch.1, section 1.5) which has inevitably lead to a wealth of contact angle data being published (Liao & Zatz, 1979b, Lerk, 1977, Zografi & Tam, 1976). However, different techniques often yield different and sometimes conflicting results (see Buckton, 1985, Hansford et al., 1980a). Despite the apparent discrepancies between techniques, only a very limited amount of work has been performed specifically to compare the techniques. Neumann and Good (1979) for example have described many techniques and highlighted their various merits and drawbacks in terms of practicality. Davies (1985) performed a detailed comparison of three methods of contact angle measurement, namely the Wilhelmy plate technique, the direct goniometric technique and the capillary rise technique, with particular regard to the precision and accuracy of each method. Each of the three techniques reviewed by Davies (1985), however, utilise a flat plate and are well suited to the polymer systems studied.

While methods utilising a flat plate are of

interest pharmaceutically and are extensively used (Young & Buckton, 1990, Zajic & Buckton, 1990), most pharmaceuticals exist as powders and the means by which flat plates are produced from powders may have serious implications for the surface energy of the sample (Buckton, 1985; Hansford, 1980a).

Perhaps surprisingly, a comparison of contact angles obtained from techniques utilising a flat plate with those obtained using the untreated powder, in which the surface energy of the plates and particles was known to be the same, has not to date been performed, and yet would provide a valuable and interesting insight into the differences between the techniques. The following work therefore attempts to perform such a comparison.

For the purposes of this study, particles and plates with identical surface energies have been created by coating glass beads and glass microscope cover slips with two polymers (hydroxypropylmethylcellulose and polyvinylpyrollidone) and a silanising compound (chlorotrimethylsilane).

A controlled, empirical comparison of three techniques widely used to measure contact angle has then been performed. The sessile drop technique (e.g. Odidi, 1991, Zografi and Tam, 1986, and Lerk, 1976) and the Wilhelmy-gravitational technique (e.g. Zajic & Buckton, 1990 and Young & Buckton, 1990), both of which utilise the sample in the form of a flat plate, will be compared with each other and with the liquid penetration technique, as modified by Studebaker and Snow (1955),

which utilises the untreated powder. The coated plates and particles have been used to model powder particles and powder compacts, such that the techniques themselves are compared, and possible effects from powder processing (such as compaction) are eliminated.

The sources of error associated with each technique will be investigated and discussed, along with the relative value, ease of performance and range of application of the three methods.

2.2. Preparation of model powders and plates.

Spherical glass beads were chosen as model particles since they allowed the surface energy of the system to be varied without altering the packing geometry of the particles. Similar systems have been used by Yang and Zografi (1986) and Crawford et al. (1987). The glass beads were monodisperse ballotini (Jencons scientific, size 18) containing less than 20% irregular shaped particles, with a volume median diameter of approximately 66 microns. The particle size of the ballotini was determined using a Malvern instruments particle sizer, series 2600c. The ballotini were suspended in Arcton 113 (ICI, Macclesfield, England), a model chlorofluorocarbon propellant, for the purposes of particle size analysis.

Glass microscope cover slips were used to model flat plates.

Particles with three surface energies were obtained by coating the ballotini with hydroxypropyl methylcellulose (HPMC) (Sigma, viscosity of 2% aqueous solution at 25C ~100cP), polyvinylpyrollidone (PVP) (BDH, viscosity of a 5% aqueous solution at 25C ~2.4cP, molecular weight ~44,000) and Chlorotrimethylsilane (CTMS) (Aldrich).

2.2.1. Preparation of coating solutions.

2.2.1.1. Polymer solutions.

Aqueous solutions of HPMC were prepared by the hydration method used by Davies (1985) in his investigation into the properties of aqueous polymer film coatings. The required weight of polymer was gradually added to double distilled deionised cold water and allowed to hydrate for 48 hours in a refrigerator at 5°C, before being mixed to ensure dispersion of the microgel structure and therefore the homogeneity of the solution.

A solution of PVP was prepared by adding the defined weight of polymer to double distilled deionised water, mixing, and making up to volume with further double distilled deionised water.

The polymer solutions were made to a concentration of 1% w/v, the concentration being limited by the viscosity of the final solution and its ability to be sprayed (see section 2.2.2.1.).

2.2.1.2. Chlorotrimethylsilane solution

Chlorotrimethylsilane (CTMS) solution was prepared by serially diluting CTMS in cyclohexane. All glassware used was rinsed with concentrated CTMS before use to prevent reaction occurring between the CTMS solution and the glassware during the dilution steps and coating procedure with the possible depletion of CTMS molecules.

2.2.2. Coating procedure.

2.2.2.1. Polymer coating.

Both cover slips and ballotini were coated in a laboratory scale Aeromatic fluidised bed coater. Coated particles were produced by fluidising 150g batches of ballotini from below with air at 70°C while spraying the polymer solution from below. A spray of the polymer solution was produced by feeding the solution to an atomising nozzle using a peristaltic pump, where an aerosol of the solution was generated by a jet of compressed air.

The cover slips were coated under identical conditions, while suspended from a wire frame within the fluidised bed coater.

A temperature of 70°C was found to be adequate to evaporate water during coating. The coating procedure was continued for 30 minutes with the polymer solution being fed in at a rate of 9 ml/minute, after which the supply of polymer to the atomising nozzle was stopped.

Buckton (1985) found that the moisture content of the packed powder bed had a significant effect on the

rate at which liquids penetrated. In this study the polymer coated beads and plates were dried as part of the coating procedure by continued exposure to fluidising hot air at 70°C for 10 minutes after coating had been completed. Coated ballotini and cover slips were examined microscopically to ensure that a complete, even polymer coating had been applied.

The ballotini were weighed before and after coating and the amount of PVP and HPMC coated on the ballotini was found to be approximately 1.6% w/w and 1.65% w/w respectively.

2.2.2.2. Chlorotrimethylsilane coating.

Chlorotrimethylsilane reacts with the silanol groups on glass surfaces according to the following reaction;

$$\text{-SiOH} + (CH_3)_3SiCl \rightarrow \text{-Si-O-Si}(CH_3)_3 + HCl$$

hence the surface chemical nature of the glass can be modified. Blake and Ralston (1985) exploited this reaction to produce quartz particles with varying surface coverages of methyl groups (methylation). At high enough concentrations of CTMS, full methylation (i.e. saturation of the silanol sites) can be achieved. In this study, full methylation (as opposed to partial methylation) was desired, since the production of beads and plates with identical surfaces was an overriding

necessity and is far more reliably achieved with full methylation.

The use of concentrated CTMS however is reputedly associated with the formation of multilayer films, whereby layers of the silane compound build up on the initial layer (Netzer & Sagiv, 1983). This uncontrolled build up of layer upon layer has the potential to alter the chemical nature of the surface. In this study, therefore, methylation was achieved by soaking the plates and ballotini in a large volume of CTMS in cyclohexane at a concentration of 7.88×10^{-2}M. This concentration was found to be dilute enough for complete silanisation to be slow and controllable, but not so dilute that the concentration changed drastically over the coating time period. The extent of coating achievable was investigated by coating clean glass slides with various concentrations of CTMS and measuring the contact angle formed between water and the plates. The results are displayed in figure 2.2.1. The kinetics of coating with the chosen concentration (7.88×10^{-2}M) was investigated similarly, by changing the time of coating (see figure 2.2.2.). A coating time of 60 minutes was eventually settled on to produce full silanisation and thus ensure that the surfaces of the ballotini and silanised plates were comparable.

Small batches (5g) of ballotini were soaked in 500ml of 7.88×10^{-2}M CTMS with gentle stirring for 60 minutes, along with several clean glass cover slips which were immersed in the liquid. The consistency of

the coating ability of the CTMS solution was ensured by coating one clean glass cover slip 10 minutes before coating the ballotini and one clean glass cover slip after coating the ballotini and checking that the contact angle formed between the plates and water (as measured on the dynamic contact angle analyser (DCAA), see section 1.5.1.3.) was the same in both cases.

The chlorotrimethylsilane coated beads were dried for 15 minutes at 75°C in a hot air oven before use.

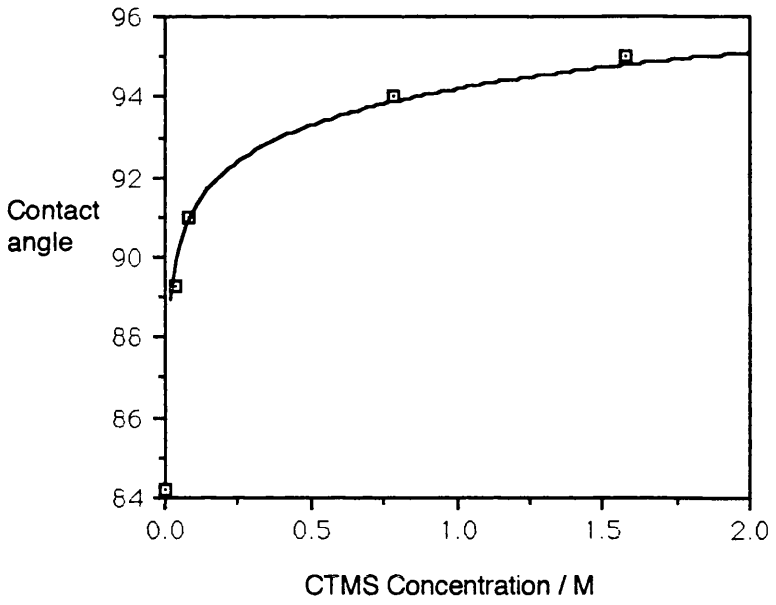

Figure 2.2.1 The change in contact angle between water and a glass cover slip coated in various concentrations of CTMS.

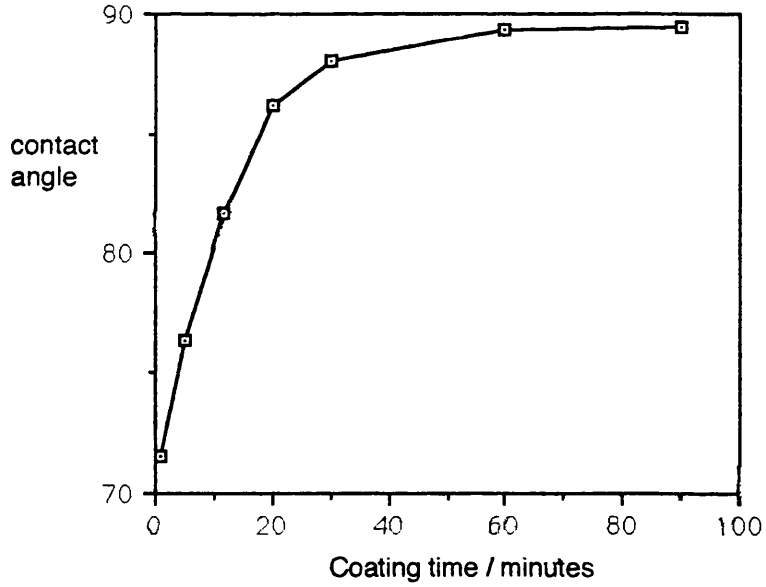

Figure 2.2.2 The change in contact angle between water and a glass cover slip coated for various lengths of time in 7.88×10^{-2}M CTMS.

2.3. Liquid penetration.

2.3.1. Introduction.

The liquid penetration method of contact angle determination is based on the Washburn (1921) equation;

$$l^2 = \frac{\gamma_{lv} \cos\theta r t}{2\eta} \qquad \text{Eqn.2.3.1}$$

which combines Pouseuille's equation for viscous flow through a capillary, and Young's equation for the determination of surface tension in a capillary. The Washburn equation assumes that when a powder is packed into a tube, the resulting plug acts like a bundle of capillaries of radius r.

Studebaker and Snow (1955) reasoned that the radius of the capillary tube, r, will be equal in different identically prepared tubes, if the packing is reproducible. If a liquid is found for which $\theta = 0$ (i.e. a *perfectly wetting liquid*), then;

$$l^2 = \frac{\gamma'_{lv} r t'}{2\eta'} \qquad \text{Eqn.2.3.2}$$

In the case of a nonperfectly wetting liquid with a finite contact angle;

$$l^2 = \frac{\gamma'' \cos\theta'' r t''}{2\eta''} \qquad \text{Eqn.2.3.3}$$

Dividing 2.3.2 by 2.3.3 gives;

$$\cos\theta = \frac{\gamma' \eta'' t'}{\gamma'' \eta' t''} \qquad \text{Eqn.2.3.4}$$

and since the gradient of l^2 as a function of t is inversely proportional to t, then;

$$\text{Cos}\theta = \frac{\gamma'\eta''\text{gradient}''}{\gamma''\eta'\text{gradient}'} \qquad \text{Eqn.2.3.5}$$

Equation 2.3.5 was used in this form to determine values of Cos θ, using the method outlined in section 2.3.2.

2.3.1.1. Effect of temperature.

Fluctuations in ambient temperature on the rate of penetration of the probe liquids were found by Buckton (1985) to have a negligible effect. An explanation for this can be found by considering equation 2.3.5. The surface tension and viscosity of the liquid will tend to decrease as temperature increases and as a quotient of these two physical values of the liquid is used in equation 2.3.5., the changes will cancel each other out to some extent. It is also possible that the rate of penetration is insensitive to changes in temperature.

2.3.1.2. Perfectly wetting liquid.

When using the equation of Studebaker and Snow (1955) it is necessary to compare the penetration rate of the imperfectly wetting liquid with that of a "perfectly wetting" liquid. Studebaker and Snow (1955) suggested that if a value of 1 for Cos θ is obtained when the data for any two liquids is substituted into equation 2.3.5, then they should both be assumed to be

perfectly wetting, since this is more likely than both liquids wetting the powder to the same extent.

In practice it is often found that no two liquids produce a value of Cos $\theta = 1$ (Buckton 1985a). In these circumstances the best wetting liquid is normally taken to be that which produces the highest values of Cos θ when substituted into equation 2.3.5. For this study, however, the choice of perfectly wetting liquid has been investigated as a potential source of error and for this reason all of the liquids chosen as potentially perfectly wetting were assumed to be so.

2.3.2. Experimental procedure.

2.3.2.1. Preparation of tubes.

Constant bore, graduated tubes of 10cm length with a uniform internal diameter (0.5cm) were coated on the inner surface with dimethyldichlorosilane, to render them hydrophobic and thus prevent preferential wetting of the glass and hence the powder nearest the tube wall. Coating was performed after first cleaning the tubes in an ultrasonic bath containing a 2% solution of Micro cleaning fluid (International products corporation; Chislehurst, Kent) for 2 minutes, rinsing thoroughly in double distilled deionised purified water before drying in a hot air oven at 75°C. Dried tubes were then dipped into the solution of dimethyldichlorosilane, rinsed in ethanol and allowed to dry.

A rubber bung was inserted into the base of the sample tube and a close fitting piece of filter paper

was inserted into the tube using a glass rod, such that it sat on the rubber bung. A known weight of coated glass beads was then poured into the tube. Uniform packing was achieved by repeatedly dropping a glass rod (of diameter just less than the internal diameter of the tube) from a height of 2cm onto the surface of the powder. One hundred repetitions was found to be sufficient to achieve uniform packing and form a stable powder bed, supported by the filter paper. The bung was then removed and the sample was ready for investigation.

2.3.2.2. Measurement of liquid flow

Studebaker and Snow's method (1955) has been used to obtain values of cos θ for the various liquids on the model powders. The experimental procedure was carried out as described by Buckton and Newton (1985).

The prepared tube was supported vertically and illuminated from the sides by a nonheating variable-intensity fibre-optic cold light source in order to prevent uneven flow of the penetrating liquid due to heating. The test liquid was added from a burette and the distance, l, travelled by the liquid front was observed visually. The time, t, taken by the liquid front to travel various predetermined distances was measured using a stopwatch. If the liquid passage was not uniform, poor packing was suspected and the result was rejected. A minimum of six replicates were performed for each liquid on each powder.

An important consideration during liquid penetration experiments is the problem of dissolution of the solid in the penetrating liquid. For this reason it is conventional to use saturated solutions. With HPMC and PVP, it is obvious that saturated solutions are not acceptable due to extreme viscosity. In this work, penetration rates were extremely rapid (compared to normal powder systems), perhaps due to the comparatively large size and uniform packing of the ballotini, and the plots of distance of penetration squared as a function of time were very straight (correlation coefficients tending to unity), thus it was assumed that the polymers did not dissolve to any significant extent, and that no significant changes occurred in either surface tension or viscosity at the wetting front (as these could be expected to result in deviation from a linear plot (Hansford et al, 1980b)).

2.4. The sessile drop technique.

2.4.1. Introduction.

The classic image of a drop of liquid incident on a flat solid surface (Fig. 1.3.2) forms the basis for this approach. The measurement of the contact angle is normally undertaken using the methods of Kossen and Heertjes (1965) or Zografi and Tam (1976).

The Zografi and Tam approach requires the direct measurement of the contact angle using either a protractor eye-piece or from a photograph of the drop.

The method of Heertjes and Kossen (1967) and Kossen and Heertjes (1965) is slightly more complicated. They proposed that the maximum attainable height of a drop on a presaturated powder bed, (ht), can be related to the contact angle, θ_e, by equations 2.4.1 and 2.4.2. Equation 2.4.1 (Kossen and Heertjes, 1965) is applied for values of θ_e between 0° and 90°, and equation 2.4.2 is used when θ_e is greater than 90° (Heertjes and Kossen, 1967).

$$\text{Cos}\theta_e = 1 - \sqrt{\frac{B(ht)^2}{3(1 - Z_v)\left(1 - B(ht)^2/2\right)}} \qquad \text{Eqn 2.4.1.}$$

$$\text{Cos}\theta_e = -1 + \sqrt{\frac{2}{3(1 - Z_v)}\left(\frac{2}{B(ht)^2} - 1\right)} \qquad \text{Eqn.2.4.2.}$$

Where B is a constant, equivalent to $\frac{\rho_l g}{2\gamma_{lv}}$, and Z_v is a volume porosity term.

Lerk et al. (1977) have used this approach extensively to study contact angles on pharmaceutical powders.

Fell and Efentakis (1979) compared the approaches of Heertjes and Kossen (1967) and Zografi and Tam (1976) and found a reasonable degree of agreement despite the fact that the method of Zografi and Tam (1976) does not take into account bed porosity.

In this study, the method of Zografi and Tam (1976) has been used throughout, since it is simpler and

generates results comparable to those obtained from the Kossen and Heertjes (1965) approach.

2.4.2. Experimental procedure.

The apparatus represented diagrammatically in figure 2.4.1. was used to measure the contact angle of drops of pure liquids on the polymer surface.

The polymer coated cover slip was supported on a horizontal stage attached to a micromanipulator. The slide was encased within a cell consisting of a solid base plate with a detachable sample cover. The base plate had a raised sample stage and two shallow wells into which a quantity of the probe liquid could be added to allow saturation of the vapour immediately around the sample prior to contact angle measurement. Two sides of the sample cover were made of optical quality glass (Jencons Scientific Ltd., Hemel Hempstead), and three holes were drilled in the top through which the agla needle could be introduced. The liquid drop was added from an agla syringe (fitted with a micrometer dispenser) via an agla needle. The syringe was cleaned according to the glassware cleaning procedure used for the liquid penetration tubes in section 2.3.2.1.

The polymer coated glass cover slip was placed on the sample stage and left to equilibrate with the vapour of the probe liquid. A 20µl droplet of the probe liquid was formed at the tip of the needle which was firmly clamped in position to minimise vibration. The sample stage was raised slowly by means of a screwthread until

contact was made with the drop. The drop was then illuminated using a nonheating fibre optic light source and viewed using a microscope fitted with a camera. Photographs were taken of five separate drops of each liquid on each surface, within three seconds of solid/liquid contact. Contact angle measurements were repeated three times on each photograph and then averaged. The average measurements from the five separate photographs for each liquid on each solid were again averaged to generate the values for the contact angles given in table 2.8.5.

A camera was used in preference to an eyepiece protractor for several reasons. Firstly, dynamic effects are eliminated as a photograph can be taken instantly and the angle measured at leisure. With an eyepiece protractor, difficulties arise if the angle is slowly changing.

Secondly, a permanent record is obtained using a camera, and thirdly an enlarged print of the drop improves the accuracy with which the angle can be measured.

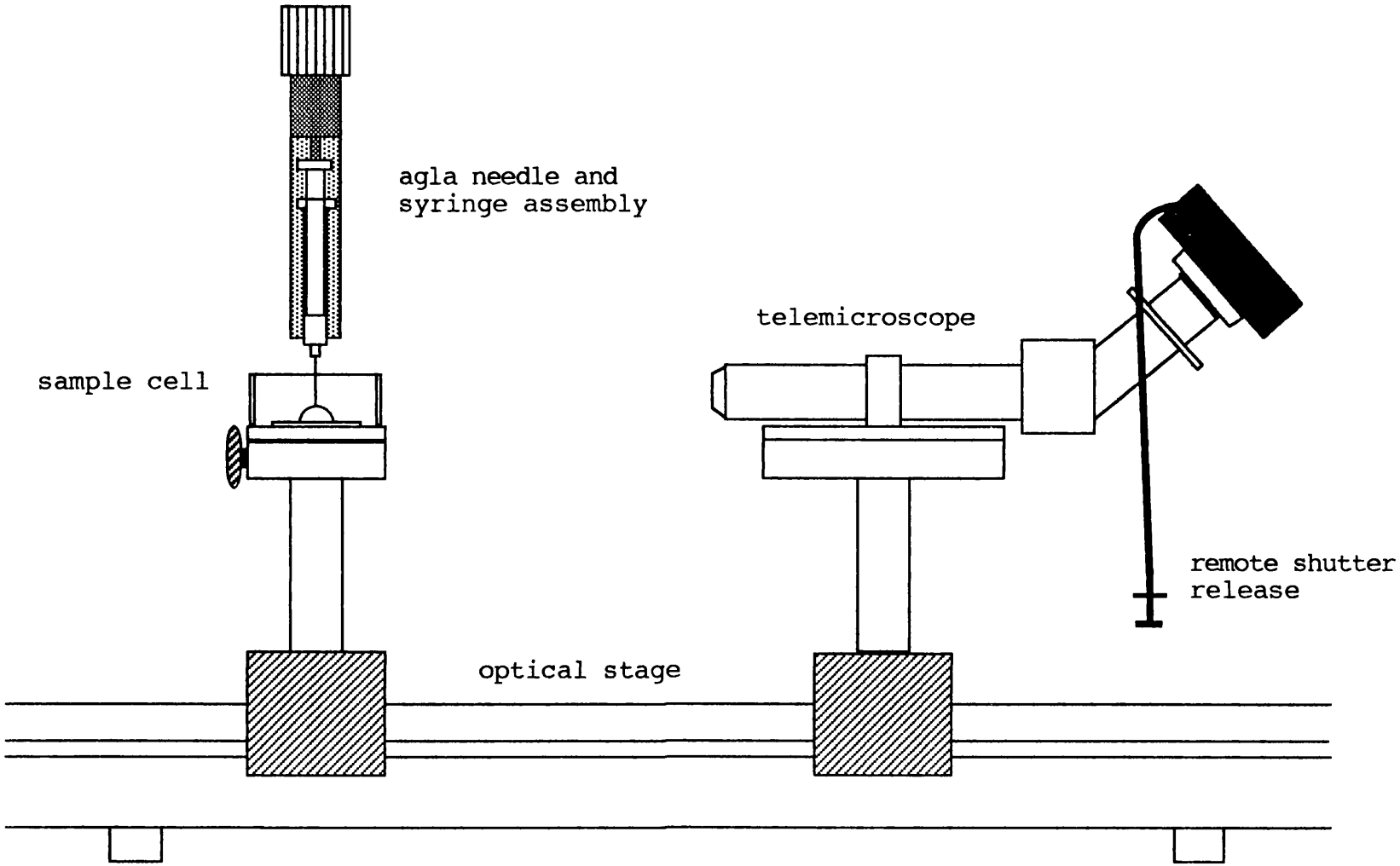

Figure 2.4.1 A diagrammatic representation of the apparatus used for the direct measurement of contact angles. (Sessile drop technique).

2.4.2.1. The effect of the needle in the drop.

Neumann and Good (1979) reported that if the needle through which the liquid is added remains in the upper surface of the drop, even though some capillary rise of the liquid up the needle occurs, the liquid region in contact with the solid is not affected. This effect was attributed to the total reliance of the contact angle on the interfacial free energies of the solid/liquid, solid/vapour and liquid/vapour interfaces.

2.4.2.2. The effect of drop size.

The effect of drop size has been investigated by Neumann and Good (1979) and Buckton (1985). Neumann and Good tentatively suggested that the variation in contact angle with drop size was related to the extent of hysteresis, stating that if hysteresis is small, then the effect of drop size is negligible. For larger hysteresis (in the region of 20°) θ increases with increasing drop size. Neumann and Good (1979) proposed that this could be a cause of discrepancy between experimenters.

Buckton (1985), however, found very little change in contact angle with drops varying in size from 10µl to 40µl.

In the present study, drops with an approximate volume of 20µl were used throughout.

2.5. The Wilhelmy plate technique.

2.5.1. Introduction.

The use of the Wilhelmy gravitational approach to determine surface tension has been discussed previously (section 1.5.1.3.). This technique has been widely used to measure the contact angle of liquids on fibres, polymers (Davies, 1985) and compacts of pharmaceutical powders (Zajic and Buckton, 1989, Rowe, 1988, Young, 1990).

Equation 2.5.1 is used to determine cos θ. Therefore the perimeter of the plate, p, and the surface tension of the test liquid must be known. The development of microbalances enables an accurate determination of the force, f, acting on the plate to be made, and consequently a simple calculation yields cos θ;

$$f = p\gamma_{lv}\cos\theta \qquad \text{Eqn.2.5.1.}$$

2.5.2. Experimental procedure.

Contact angles were measured using a Cahn Dynamic Contact Angle Analyzer (DCAA), which consists of a microbalance interfaced with a personal computer. The sample and probe liquid are enclosed in a chamber containing a motorised platform.

The coated plates are suspended lengthways from the balance arm by means of a microcrocodile clip (RS components) with a hook soldered to it. The test liquid, in a clean beaker (see section 2.3.2.1. for cleaning procedure) is positioned below the sample in an

enclosed, draught-free chamber on the motorised platform of adjustable speed (20-264μm/second, available in 0.1μm/second intervals). The platform has a 39.0mm travelling range. The procedure from this point onwards is microprocessor controlled. Sample details (such as plate perimeter) are input along with operational instructions for platform speed and distance of platform travel. The plate perimeter was measured using calipers equipped with a vernier scale.

The computer records the force reading from the microbalance every 1 second (up to a maximum of 600 data points). A typical plot of force with time (platform position) is shown in Figure 2.5.1. The motorised platform raises the liquid up to and beyond the first point of contact with the solid (A-D in figure 2.5.1). Point B is known as the zero depth of immersion position (Z.D.O.I.). At this point, there are no buoyancy effects. The gradual reduction in force (C-D, figure 2.5.1) due to buoyancy as the plate slowly immerses in the liquid is eliminated by extrapolating the buoyancy slope (C-D) back to the point of zero depth of immersion, where there is no buoyancy effect. The force acting on the plate at this point is used in the calculation of Cos θ from equation 2.5.1. and is a measure of the advancing angle.

The portion of the plot D-E, corresponds to the reversal of direction of the platform and the transformation of the contact angle from an advancing angle to a receding angle. The subsequent portion of the

plot, E-F, is analogous to the C-D section for the receding angle. An extrapolation of the line E-F to the line of zero depth of immersion (Z.D.O.I.) yields the receding angle, when the corresponding force value at the intersection of line E-F with the line of Z.D.O.I. is used in equation 2.5.1.

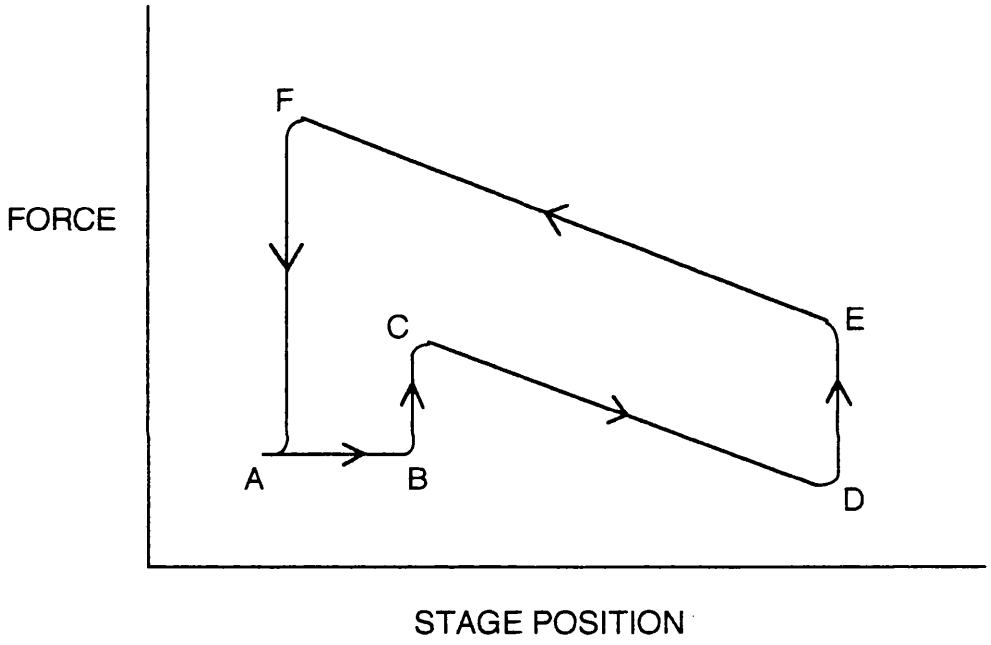

Figure 2.5.1 A typical plot of force against stage position from the Wilhelmy plate technique.

2.5.2.1. The effect of platform speed.

The platform speed and hence the rate at which the solid entered the liquid, was found to influence the contact angle. The effect was marked for systems where the contact angle was high ($\theta > 70^\circ$) and when the liquid was notably viscous. In cases where the liquid "wet" the solid well, the platform speed had no effect on the

contact angle. The advancing angle, θ_a, was always affected to a greater extent than the receding angle, θ_r. In the present study, an intermediate platform speed was used (100μm/second) except in special cases where, for example, a highly hydrophobic solid (P.T.F.E, Parafilm M) or viscous liquid was used. In these situations, a slow platform speed (20μm/sec.) was used.

2.6. Choice of liquid media.

A series of glycols were used as probe liquids, namely glycerol, ethanediol and propanediol, giving a range of surface tensions and polarities. Diiodomethane was used as a nonpolar probe liquid.

Octane, toluene and cyclohexane and ethanol were used as "perfectly wetting" liquids.

Dimethylchlorosilane in carbon tetrachloride (Hopkin and Williams Ltd.) was used to coat the inner surface of the penetration tubes (section 2.3.2.1.). A similar silane compound, chlorotrimethylsilane (CTMS), was used to coat the ballotini.

Details of the liquids are given in table 2.6.1.

2.6.1. Liquid characterisation.

Where necessary, the viscosities of the test liquids were measured with a U-tube viscometer (Gallenkamp size B, British Standard 188) in a thermostated water bath at 20°C.

Density measurements were made using a specific gravity bottle at 20°C.

Table 2.6.1 Details of probe liquids.

Liquid	Source	Grade	Batch
Octane	Koch-light Ltd.	HiPure	02671F
Toluene	BDH	AnalaR	2852770L
Arcton 113	ICI	----------	17010
Glycerol	Sigma	Sigma grade	30H0793
Ethanediol	Sigma	Spectroscopic	03009BW
Propanediol	Sigma	----------	129F0123
Diiodomethane	Aldrich	99%	34969

2.6.2. Surface tension measurements.

Many methods of surface tension determination are possible (Padday, 1969). In this study, the Wilhelmy plate method has been used throughout (section 1.5.1.3.). Instead of the test solid, a thin, flat, rectangular plate of glass is suspended form the microbalance. If the glass is perfectly wetted by the test liquid, $\cos \theta = 1$, and equation 2.5.1. becomes;

$$f = \gamma_{LV}.p \qquad \text{Eqn.2.6.1.}$$

from which γ_{LV} can be determined.

A thin rectangular piece of filter paper was used instead of the glass slide to determine the surface tension of the nonpolar liquids, which did not wet the glass slide (see Gaines, 1977). This method enables fast, simple and accurate determinations of surface tension to be made.

2.7. Results

The surface tensions and viscosities of the test liquids are presented in tables 2.7.1 and 2.7.2, along with the standard deviations and the standard deviations expressed as a percentage of the mean (referred to in this study as the *percent error*). The reproducibility of both the surface tension and viscosity measurements was very good, with the percent error not exceeding 0.35 and 0.15 respectively.

The penetration data for each liquid into each powder bed is presented in tables 2.7.3, 2.7.4 and 2.7.5. The plots of distance of penetration (l) squared as a function of time all produced a good fit line, with a correlation coefficient close to unity in all cases. Yang and Zografi (1986) and Carli and Simioni (1979) have, however, warned against using this as a vindication of the technique and the Washburn equation itself. The percent error of the penetration rates for liquids into packed beds of HPMC, PVP and CTMS coated ballotini ranges from 1.33 to 2.75.

Table 2.7.1 Surface tensions of various liquids at 20°C.

Liquid	Surface tension (mN/m)	Percent error
Octane	21.25 ± 0.05	0.24
Cyclohexane	23.81 ± 0.06	0.25
Ethanol	21.76 ± 0.07	0.32
Toluene	28.50 ± 0.05	0.18
Glycerol	60.22 ± 0.21	0.35
Ethanediol	48.38 ± 0.10	0.21
Propanediol	35.53 ± 0.11	0.31
Diiodomethane	50.05 ± 0.11	0.22
Water	72.60 ± 0.20	0.28

Table 2.7.2 Viscosities of various liquids at 20°C.

Liquid	Viscosity (cp)	Percent error
Octane	0.567 ± 0.0002	0.04
Cyclohexane	1.02 ± 0.0002	0.02
Ethanol	1.018 ± 0.0005	0.05
Toluene	0.590 ± 0.0002	0.03
Glycerol	1,222†	
Ethanediol	19.90 ± 0.01	0.05
Propanediol	58.10 ± 0.09	0.15
Diiodomethane	2.820 ± 0.001	0.04
Water	1.002 ± 0.0001	0.01

† literature value (rubber company manual)

Table 2.7.3 gradients of (penetration distance) ^{2} plotted as a function of time for various liquids through packed beds of HPMC coated ballotini.

Liquid	l^2 / t	standard deviation	correlation coefficient	percent error
octane	8.37×10^{-2}	1.6×10^{-3}	0.996	1.91
cyclohexane	5.73×10^{-2}	1.0×10^{-3}	0.998	1.75
toluene	0.1181	2.3×10^{-3}	0.996	1.95
ethanol	5.24×10^{-2}	8.4×10^{-4}	0.996	1.98
glycerol	9.18×10^{-6}	1.9×10^{-7}	0.995	2.07
ethanediol	2.48×10^{-3}	3.3×10^{-5}	0.997	1.33
propanediol	8.37×10^{-4}	1.4×10^{-5}	0.997	1.67
diiodomethane	2.64×10^{-2}	6.6×10^{-4}	0.993	2.50

Table 2.7.4 gradients of (penetration distance) ^{2} plotted as a function of time for various liquids through packed beds of PVP coated ballotini.

Liquid	l^2 / t	standard deviation	correlation coefficient	percent error
octane	9.19×10^{-2}	1.7×10^{-3}	0.997	1.85
cyclohexane	6.20×10^{-2}	1.7×10^{-3}	0.991	2.75
toluene	0.1137	3.1×10^{-3}	0.993	2.73
ethanol	5.15×10^{-2}	6.9×10^{-4}	0.996	1.76
glycerol	3.64×10^{-5}	9.2×10^{-7}	0.998	1.40
ethanediol	2.85×10^{-3}	4.6×10^{-5}	0.998	1.61
propanediol	7.73×10^{-4}	1.6×10^{-5}	0.996	2.07
diiodomethane	3.49×10^{-2}	6.6×10^{-4}	0.997	1.89

Table 2.7.5 gradients of (penetration distance) ^{2} plotted as a function of time for various liquids through packed beds of CTMS coated ballotini.

Liquid	l^2 / t	standard deviation	correlation coefficient	percent error
octane	0.1617	3.2×10^{-3}	0.996	1.98
cyclohexane	0.1077	2.2×10^{-3}	0.996	2.04
toluene	0.2301	4.9×10^{-3}	0.996	2.13
ethanol	8.61×10^{-2}	1.6×10^{-3}	0.997	1.86
glycerol	D.N.P.	---------	-----	----
ethanediol	1.88×10^{-3}	2.8×10^{-5}	0.998	1.49
propanediol	1.42×10^{-3}	2.5×10^{-5}	0.997	1.76
diiodomethane	7.86×10^{-3}	1.6×10^{-4}	0.995	2.04

D.N.P. = did not penetrate

The values of Cos θ and θ have been calculated as described in section 2.3., using octane, cyclohexane, ethanol and toluene as the "perfectly wetting" liquid and are presented in tables 2.8.1 to 2.8.3.

The contact angles measured using both the Wilhelmy plate and sessile drop technique are presented in tables 2.8.4 to 2.8.5. The values obtained from the two techniques are in remarkably good agreement, the difference not exceeding 1.9° in the worst case (glycerol on PVP). The reproducibility of the techniques is also excellent, being of the order of 2° for the direct measurement from a sessile drop, and 1° for the Wilhelmy plate technique.

2.8. Discussion.

2.8.1. The extent of the errors associated with contact angles obtained from liquid penetration experiments.

Compared to the other techniques studied, the calculation of contact angles from the liquid penetration technique is complex, requiring a knowledge of the viscosities and surface tensions of two liquids along with a measure of their penetration rate into a uniformly packed powder bed.

Since the techniques used to measure these physical properties of viscosity and surface tension to the degree of accuracy achieved in this study (see tables 2.7.1 and 2.7.2) are widely available and established, it is likely that any error associated with contact

angles derived from liquid penetration experiments will be derived from the measurement of penetration rates and the choice of "perfectly wetting" liquid.

In order to assess the extent of the errors associated with liquid penetration experiments, the standard deviations for surface tension, viscosity and gradients of penetration distance squared as a function of time have been selectively added to or subtracted from the mean value for each parameter of each test liquid and "perfectly wetting" liquid in order to determine the "maximum" and "minimum" possible values for cos θ and θ that are consistent with the range of experimental error. These values are presented in tables 2.8.1 to 2.8.3, along with the mean results.

2.8.1.1. Choice of perfectly wetting liquid for liquid penetration experiments.

The choice of a "perfectly wetting" liquid is never straightforward in liquid penetration experiments (see Buckton and Newton, 1986), and the extent to which an inappropriate choice will influence results is not known. The procedure described by Studebaker and Snow (1955), whereby two liquids are found which wet the liquid to the same extent (the rationale that it is more likely that both are perfectly wetting than for both liquids to partially wet the solid to the same extent can then be applied) is not always practically possible. In a case such as this, the implications of using a

liquid with a finite contact angle (albeit small) as "perfectly wetting" has not been fully evaluated.

A comparison of the data in tables 2.8.1, 2.8.2 and 2.8.3, reveals that no one liquid can be assigned as "perfectly wetting" for either PVP or CTMS. This cannot, of course, be taken to imply that none of the liquids is in fact "perfectly wetting". All that can be reported with confidence, though, is that one of the liquids employed as "perfectly wetting" has a lower contact angle than the other two. In the case of PVP, cyclohexane exhibits the lowest contact angle, and for CTMS coated ballotini, toluene is the best wetting liquid. In the case of HPMC coated ballotini, cyclohexane, ethanol and toluene exhibit the same degree of wetting. Following the reasoning of Studebaker and Snow (1955), it is more likely that all three liquids are perfectly wetting than for all three to wet HPMC to the same finite extent.

Taking each substrate in turn, the absolute extent of the error, in terms of contact angle, that would be introduced by using octane as the perfectly wetting liquid for HPMC (rather than cyclohexane, ethanol or toluene, which are perfectly wetting liquids) is dependent upon the extent of wetting achieved by the test liquid. If the contact angle for the test liquid is intrinsically high (e.g. glycerol) then the choice of "perfectly wetting" liquid is almost inconsequential (0.4°, see table 2.8.1). However, if the test liquid has a low intrinsic contact angle (e.g.diiodomethane) then

the error is more significant (4.5°, see table 2.8.1). This principle also holds true for the PVP and CTMS coated ballotini (see tables 2.8.2 and 2.8.3). For example, the difference in contact angle for glycerol on PVP that may be produced by using two different "perfectly wetting" liquids is 2.2° but for the probe liquid with the lowest contact angle (diiodomethane) it is 8.8°. Similarly for CTMS , the greatest difference in the calculated contact angle with diiodomethane produced by using different perfectly wetting liquids is 1°. In the case of propanediol, the difference is 6°.

It is apparent from the results presented in tables 2.8.1 to 2.8.3 that the choice of perfectly wetting liquid against which the penetration characteristics of the probe liquid are to be compared in liquid penetration experiments is of vital importance, particularly when the contact angle being measured is small.

Table 2.8.1. Mean and worst cases of cos θ and θ for various probe liquids on HPMC using octane, ethanol, cyclohexane and toluene as 'perfectly' wetting liquids.

Probe liquid	'Perfectly' wetting liquid	Cos θ mean	Cos θ maximum	Cos θ minimum	Error (±%)
Glycerol	Octane	0.0834 (85.2°)	0.0878 (85.0°)	0.0791 (85.5°)	5.2
	Ethanol	0.0760 (85.6°)	0.0799 (85.4°)	0.0722 (85.9°)	5.1
	Cyclohexane	0.0759 (85.6°)	0.0798 (85.4°)	0.0721 (85.9°)	5.1
	Toluene	0.0762 (85.6°)	0.0802 (85.4°)	0.0723 (85.9°)	5.2
Ethanediol	Octane	0.4568 (62.8°)	0.4740 (61.7°)	0.4401 (63.9°)	3.8
	Ethanol	0.4161 (65.4°)	0.4312 (64.5°)	0.4017 (66.3°)	3.6
	Cyclohexane	0.4156 (65.4°)	0.4306 (64.5°)	0.4010 (66.4°)	3.6
	Toluene	0.4172 (65.3°)	0.4328 (64.4°)	0.4021 (66.3°)	3.7
Propanediol	Octane	0.6129 (52.2°)	0.6395 (50.2°)	0.5875 (54.0°)	4.3
	Ethanol	0.5583 (56.1°)	0.5817 (54.4°)	0.5363 (57.6°)	4.2
	Cyclohexane	0.5576 (56.1°)	0.5809 (54.5°)	0.5353 (57.6°)	4.2
	Toluene	0.5598 (56.0°)	0.5838 (54.3°)	0.5368 (57.5°)	4.3
Diiodo-methane	Octane	0.6661 (48.2°)	0.6992 (45.6°)	0.6347 (50.6°)	5.0
	Ethanol	0.6067 (52.6°)	0.6360 (50.5°)	0.5794 (54.6°)	4.8
	Cyclohexane	0.6060 (52.7°)	0.6351 (50.6°)	0.5784 (54.7°)	4.8
	Toluene	0.6084 (52.5°)	0.6383 (50.3°)	0.5800 (54.5°)	4.9

Table 2.8.2. Mean and worst cases of cos θ and θ for various probe liquids on PVP using octane, ethanol, cyclohexane and toluene as 'perfectly' wetting liquids.

Probe liquid	'Perfectly' wetting liquid	Cos θ mean	Cos θ maximum	Cos θ minimum	Error (±%)
Glycerol	Octane	0.3012 (72.5°)	0.3184 (71.4°)	0.2846 (73.5°)	5.7
	Ethanol	0.3066 (72.1°)	0.3230 (71.2°)	0.2908 (73.1°)	5.3
	Cyclohexane	0.2781 (73.9°)	0.2964 (72.8°)	0.2605 (74.9°)	6.6
	Toluene	0.3138 (71.7°)	0.3342 (70.5°)	0.2942 (72.9°)	6.5
Ethanediol	Octane	0.4781 (61.4°)	0.4972 (60.2°)	0.4597 (62.6°)	4.0
	Ethanol	0.4866 (60.9°)	0.5042 (59.7°)	0.4697 (62.0°)	3.6
	Cyclohexane	0.4414 (63.8°)	0.4628 (62.4°)	0.4207 (65.1°)	4.8
	Toluene	0.4980 (60.1°)	0.5218 (58.5°)	0.4751 (61.6°)	4.8
Propanediol	Octane	0.5155 (59.0°)	0.5396 (57.3°)	0.4925 (60.5°)	4.7
	Ethanol	0.5247 (58.4°)	0.5472 (56.8°)	0.5033 (59.8°)	4.3
	Cyclohexane	0.4759 (61.6°)	0.5023 (59.8°)	0.4508 (63.2°)	5.5
	Toluene	0.5370 (57.5°)	0.5663 (55.5°)	0.5091 (59.4°)	5.5
Diiodo-methane	Octane	0.8020 (36.6°)	0.8363 (33.2°)	0.7691 (39.7°)	4.3
	Ethanol	0.8163 (35.3°)	0.8481 (32.0°)	0.7858 (38.2°)	3.9
	Cyclohexane	0.7404 (42.2°)	0.7784 (39.9°)	0.7040 (45.3°)	5.1
	Toluene	0.8349 (33.4°)	0.8777 (28.6°)	0.7949 (37.4°)	5.1

Table 2.8.3. Mean and worst cases of cos θ and θ for various probe liquids on CTMS using octane, ethanol, cyclohexane and toluene as 'perfectly' wetting liquids.

Probe liquid	'Perfectly' wetting liquid	Cos θ mean	Cos θ maximum	Cos θ minimum	Error (±%)
Glycerol	Octane	DNP	DNP	DNP	----
	Ethanol	DNP	DNP	DNP	----
	Cyclohexane	DNP	DNP	DNP	----
	Toluene	DNP	DNP	DNP	----
Ethanediol	Octane	0.1792 (79.7°)	0.1864 (79.3°)	0.1723 (80.1°)	4.0
	Ethanol	0.1920 (78.9°)	0.1977 (78.5°)	0.1846 (79.4°)	3.0
	Cyclohexane	0.1676 (80.4°)	0.1744 (79.9°)	0.1610 (80.7°)	4.1
	Toluene	0.1623 (80.7°)	0.1689 (80.3°)	0.1558 (81.0°)	4.1
Propanediol	Octane	0.5382 (57.4°)	0.5624 (55.8°)	0.5148 (59.0°)	4.5
	Ethanol	0.5765 (54.8°)	0.6026 (52.9°)	0.5513 (56.5°)	4.5
	Cyclohexane	0.5031 (59.8°)	0.5261 (58.3°)	0.4809 (61.3°)	4.6
	Toluene	0.4873 (60.8°)	0.5097 (59.4°)	0.4657 (62.2°)	4.6
Diiodo-methane	Octane	0.1027 (84.1°)	0.1073 (83.8°)	0.0982 (84.4°)	4.5
	Ethanol	0.1099 (83.7°)	0.1150 (83.4°)	0.1052 (83.9°)	4.6
	Cyclohexane	0.0960 (84.5°)	0.1004 (84.2°)	0.0917 (84.7°)	4.6
	Toluene	0.0930 (84.7°)	0.0973 (84.4°)	0.0888 (84.9°)	4.6

DNP - did not penetrate.

2.8.1.2. Sensitivity of liquid penetration experiments to error.

If the errors that may be introduced from other sources (i.e. surface tension measurements etc.) are also taken into account to produce theoretical maximum and minimum values within experimental error (tables 2.8.1 - 2.8.3), then the problem is magnified.

From table 2.8.2 it can be seen that, in the worst case (i.e. the difference between the highest "maximum" and lowest "minimum" values), the error in cos θ can be as high as 0.1737 (diiodomethane on PVP) which is equivalent to a 16.8° variation in the contact angle.

Again, the implications of introducing errors are more serious when the contact angle is small.

2.8.1.3. Errors associated with quoting values as contact angles.

From tables 2.8.1 - 2.8.3, it is clear that as the value of cos θ tends towards unity, the size of the error, in absolute terms, increases. Taking the HPMC results to illustrate this, the error (which has been calculated by halving the difference between the maximum and minimum values) in cos θ for glycerol is approximately ±0.004 around a mean of approximately 0.08 (from table 2.8.1) but for diiodomethane, the error is in the order of 0.04 around a mean of approximately 0.65 (the ultimate values vary depending upon the choice of perfectly wetting liquid). In other words, the error is an order of magnitude greater for the diiodomethane (in

absolute terms). This observation holds true for the contact angle values also; when the contact angle is high, for example glycerol on HPMC, the result is good to ±0.2°, but for diiodomethane, which has a low contact angle on HPMC, the error is ±2.2°. Although the magnitude of these errors is acceptably low (which may, in part, be due to the idealised system of perfect spheres as opposed to less regular powders) the trend is consistent; in all cases the error increases in absolute terms as cos θ tends to unity (and θ tends to 0). It is interesting, however, to investigate any trends in the errors in relative, rather than absolute, terms.

The percentage spread in cos θ is presented in tables 2.8.1 - 2.8.3. It is apparent that, although the errors that are observed in cos θ increase in absolute terms as the value approaches unity, the percentage error in cos θ does not follow this trend, as all results are in the approximate range of 2-5% error (irrespective of the magnitude in cos θ).

Although the percentage error in cos θ is directly related to the percentage errors of the relevant penetration values, this is not true for the error in θ. The overriding factor in determining the error in the contact angle is not the experimental error, but the magnitude of the angle. The following example illustrates this point; for diiodomethane on PVP (using ethanol as the perfectly wetting liquid, table 2.8.2) the percentage error in cos θ is 4.2, but the error in the contact angle is almost 22% (this figure has been

calculated as the difference between the maximum and minimum values divided by two to give the error and then expressing this value as a percentage of the mean), whilst for ethanediol the percentage error in cos θ is almost identical (4.1) but the error in the contact angle is only 2.5%. This is simply due to the cosine function, which results in an identical change in cos θ producing different changes in θ, depending upon the gradient of the cosine curve at that point.

Consequently, to quote a value for a contact angle, and state that it is accurate to ± a number of degrees, does not necessarily reflect the accuracy of the experiment, but rather the magnitude of the angle. It is, therefore, perhaps more appropriate to work with the more useful cos θ values (rather than θ) and to quote the accuracy of such.

2.8.2. The extent of the errors associated with the Sessile drop and Wilhelmy plate techniques.

As in the case of the liquid penetration experiments, it is evident that as the size of the contact angle decreases, the reproducibility of both the Wilhelmy plate and sessile drop techniques deteriorates.

Davies (1985) attributed the poorer reproducibility of the Wilhelmy plate technique to "a low sensitivity to the measurement of contact angles less than 20° particularly for those liquids which possess a low surface tension". This seems unlikely, particularly when the advent of sensitive microbalances is taken into

account. It is more likely that the reason given for the lower reproducibility of the liquid penetration experiments, namely the shape of the cosine curve, is also responsible for the poorer reproducibility of the Wilhelmy plate technique at lower contact angles, since errors in measuring the plate perimeter, the liquid surface tension and fluctuations in the microbalance readings, no matter how small, will be magnified at lower values of θ.

With sessile drop experiments, the angle itself is being measured directly and the cosine function has no bearing on the results. A similar drop-off in reproducibility is still seen however, requiring an alternative explanation.

Poor reproducibility at low values of θ is well documented by Neumann and Good (1979). Although the use of a photographic approach eliminates problems associated with alignment of the eyepiece crosshair to the tangent of the contact angle in the goniometric technique (Davies, 1985), the construction of a tangent on a photograph at the three phase boundary becomes increasingly difficult at lower values of θ, resulting in a reduction in the reproducibility of the technique.

Table 2.8.4. θ and cos θ from the *Wilhelmy plate* technique

Liquid	Surface	Cos θ	% error	θ	% error
Glycerol	HPMC	0.2672 ± 0.0048	1.8	74.5° ± 0.3°	0.4
	PVP	0.3891 ± 0.0082	2.1	67.1° ± 0.5°	0.8
	CTMS	0.1461 ± 0.0022	1.5	81.6° ± 0.1°	0.2
Ethane-diol	HPMC	0.4617 ± 0.0042	0.9	62.5° ± 0.3°	0.4
	PVP	0.5592 ± 0.0106	1.9	56.0° ± 0.7°	1.3
	CTMS	0.3173 ± 0.0048	1.5	71.5° ± 0.3°	0.4
Propane diol	HPMC	0.6972 ± 0.0112	1.6	45.8° ± 0.9°	2.0
	PVP	0.7254 ± 0.0131	1.8	43.5° ± 1.1°	2.5
	CTMS	0.5962 ± 0.0119	2.0	53.4° ± 0.8°	1.6
Diiodo-methane	HPMC	0.6468 ± 0.0110	1.7	49.7° ± 0.8°	1.7
	PVP	0.7649 ± 0.0145	1.9	40.1° ± 1.3°	3.2
	CTMS	0.1650 ± 0.0026	1.6	80.5° ± 0.2°	0.2

Table 2.8.5 θ and cos θ from the *sessile drop* technique.

Liquid	Surface	Cos θ	% error	θ	% error
Glycerol	HPMC	0.2907 ± 0.0216	7.4	73.1° ± 1.3°	1.8
	PVP	0.4195 ± 0.0205	4.8	65.2° ± 1.3°	2.0
	CTMS	0.1719 ± 0.0155	9.0	80.1° ± 0.9°	1.1
Ethane-diol	HPMC	0.4726 ± 0.0275	5.9	61.8° ± 1.8°	2.9
	PVP	0.5736 ± 0.0240	4.2	55.0° ± 1.8°	3.1
	CTMS	0.3173 ± 0.0197	6.2	71.5° ± 1.2°	1.7
Propane diol	HPMC	0.7193 ± 0.0203	2.8	44.0° ± 1.7°	3.9
	PVP	0.7420 ± 0.0207	2.8	42.1° ± 1.8°	4.3
	CTMS	0.6060 ± 0.0207	3.4	52.7° ± 1.5°	2.8
Diiodo-methane	HPMC	0.6574 ± 0.0221	3.4	48.9° ± 1.7°	3.5
	PVP	0.7660 ± 0.0209	2.7	40.0° ± 1.9°	4.8
	CTMS	0.1633 ± 0.0109	11.6	80.6° ± 1.1°	1.4

Table 2.8.6 θ and cos θ from the *liquid penetration* technique.

Liquid	Surface	Cos θ	θ
Glycerol	HPMC	0.0767	85.6°
	PVP	0.2773	73.9°
	CTMS	DNP	DNP
Ethane-diol	HPMC	0.4163	65.4°
	PVP	0.4415	63.8°
	CTMS	0.1925	78.9°
Propane-diol	HPMC	0.5577	56.1°
	PVP	0.4756	61.6°
	CTMS	0.5764	54.8°
Diiodomethane	HPMC	0.6060	52.7°
	PVP	0.7408	42.2°
	CTMS	0.1097	83.7°

DNP - Did not penetrate

2.8.3. A comparison of the results obtained using the three techniques

The contact angle values obtained from the liquid penetration experiments are presented in table 2.8.6, along with the results from the sessile drop and Wilhelmy plate techniques in tables 2.8.4 and 2.8.5.

It is striking that the liquid penetration technique, whilst maintaining the same rank order of θ for the contact angles, produces significantly higher contact angle values than the two 'plate' techniques, without exception. This is consistent with the findings of Buckton (1985) and Hansford et al. (1980) who attributed the differences to surface roughness, an effect of compression and the potential differences between the advancing contact angle obtained by the liquid penetration technique and the static contact angle obtained from a sessile drop technique.

2.8.3.1. Influence of advancing angle.

While it is reasonable to expect an advancing angle to be different to an equilibrium angle, differences have still been seen in this study between the contact angle values generated by the Wilhelmy plate and sessile drop methods and those generated by the liquid penetration technique, despite the fact that all the angles measured are advancing.

It is clear then that a difference in contact angle mode (advancing or equilibrium) does not account for the

higher values of θ generated by liquid penetration experiments in this study.

2.8.3.2. Effect of surface heterogeneity

It is unlikely that surface heterogeneity is the reason for the differences seen between the liquid penetration technique results and the results from the two techniques based on plates.

Although previous work (Buckton, 1985a and Hansford et al, 1980a) has suggested that differences may, at least in part, be due to the the possible change in surface nature of the powder due to compression, similar differences in contact angle have been seen in the current work despite the use of identical model surfaces.

2.8.3.3. Effect of pore geometry.

Despite the fact that liquid penetration experiments generate contact angles which are higher than those on plates, the experiments do rank the wettability of the surfaces in an order which is in excellent agreement with the other techniques. This is illustrated in figure 2.8.1, in which the dynamic contact angle data from the Wilhelmy experiments (table 2.8.4) has been plotted against those from the liquid penetration technique (table 2.8.6). The equation for the line in figure 2.8.1 is:

$$\theta_w = 0.889\ \theta_{LP} + 1.78 \qquad \text{Eqn.2.8.9.}$$

where θ_w is the contact angle from the Wilhelmy experiments and θ_{LP} is the contact angle from the liquid penetration technique. The correlation coefficient is 0.95. Thus, for the model systems used in this study, the liquid penetration results are well correlated with the advancing dynamic contact angle results.

The line intercepts the Y-axis at an angle of 1.78 degrees, which is within experimental error of the origin, suggesting that the results from the two techniques will deviate more significantly as the contact angle increases. From equation 2.8.1., the value at which a liquid would not penetrate (i.e. θ_{LP}) is equivalent to an angle measured by the Wilhelmy method (θ_W) of 81.8°. From the data in table 2.8.6, it can be seen that glycerol would not penetrate into a bed of CTMS coated beads. The corresponding Wilhelmy angle (θ_W) is 81.6°, which is totally consistent with the prediction from the linear plot in figure 2.8.1.

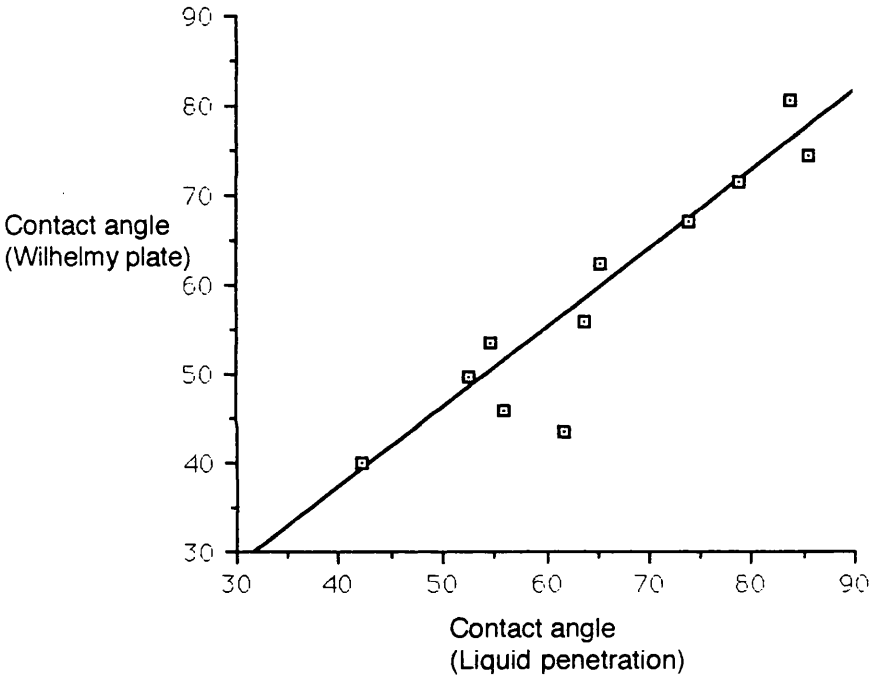

Figure. 2.8.1 correlation between θ_w (obtained from the Wilhelmy method) and θ_{lp} (obtained from the liquid penetration method).

Yang et al. (1988) use the descriptors of similar media and similar states, where similar media have identical geometry, which is a necessary, but incomplete, requirement for similar states. Similar states must have identical reduced film curvature and the contact angle at each point in one medium must also match the contact angle at the equivalent point in the other medium. The materials used in the current study have different surface energies and therefore meet the requirement for similar media, and one of the requirements for similar states. The linearity of figure 2.8.1. is due in part to the fact that the model systems constitute similar media. Yang et al. (1988) state that for dissimilar states there is no justification for estimating contact angles from the derivations of the Washburn equation, such as that of Studebaker and Snow (1955), however the linearity of the line in figure 2.8.1. would suggest that such approaches are capable of detecting the wettability of the solid for similar media in dissimilar states. The significance of the gradient of equation 2.8.1, however, is not clear.

It is obvious that the use of the Washburn model is continually overestimating the contact angle values for these model surfaces (albeit in a predictable manner). The Washburn equation uses as a model of the packed bed, a bundle of capillary tubes, being cylindrical along their length and uniform in diameter. Dullien (1979) describes the danger of using the simplistic model of a bundle of capillary tubes, warning that its simplicity

leads to its popularity, which in turn may result in the belief that it is a close approximation to reality.

The model powder systems used in this study were comprised of essentially spherical ballotini and as such will have a consistent, regular packing geometry. The densest regular pack will be rhombohedral, with a coordination number (which can be related to the percolation probability of the lattice geometry) of 12 and a bulk mean porosity of 0.2595 (Dullien, 1979). A probable reason for the differences in the results between the liquid penetration and other experiments is the effect of pore geometry on the penetration rate. In fact, numerous workers (e.g. Yang et al., 1988, Marmur, 1992, Dullien, 1979) have shown that penetration into capillaries can be limited in systems in which the pores have changes in their capillary radius, such that meniscus curvature has a significant effect on pressure, which will have a retardant effect on penetration.

However, a relationship between contact angles on plates and particles has not previously been reported.

Marmur (1992) has reviewed the penetration of liquids into porous media and has concluded that the penetration and displacement of small liquid reservoirs in porous media is dependent upon the curvature of the pores, rather than being totally dependent upon contact angle. Yang et al (1988) have also considered the fact that liquid penetration into porous beds can be explained by phenomena other than just a contact angle dependence. It is likely, therefore, that the liquid

penetration results reported in table 2.8.6 are composed of a contribution from contact angle, and another from bed geometry. In general terms, (within the rapid timescale of the experiment), it is likely that the bed geometry will be the same for each of the packed beds used, irrespective of surface coating. On longer exposure, however, liquid may be expected to partition into the smaller capillaries of the coat itself in certain circumstances. Thus, the liquid penetration contact angle results, which can be expected to consist of a geometry factor and a wetting factor, would be expected to rank the surfaces in the same order as other contact angle techniques.

In addition to the discussion above, it is likely that the linearity in figure 2.8.1 is a consequence of the identical pore geometry, and in particular that the film curvature is identical during the penetration through the pores of the column, for each packed bed. The existence of one linear plot for four different liquids on three different surfaces (with a range of in contact angle from 40° to 80°) demonstrates the applicability of the Washburn equation to liquids in dissimilar states. Furthermore, the considerations of surface tension and viscosity in the Studebaker and Snow (1955) equation (cf the Washburn equation) are adequate to eliminate these parameters from further influence in the penetration process. Although we have no data for such systems, it is likely that changes in the pore geometry will result in changes in the gradient of

figure 2.8.1. In other words, if the experiment were repeated for the same surface energy particles of different, but consistent geometry, a straight line would be produced, which would have a different gradient to that in figure 2.8.1. It follows that the gradient of figure 2.8.1. is a function of pore geometry. Thus, for different model systems, it would be possible to construct a plot such as that in figure 2.8.1, where the gradient relates to pore geometry, and in each case the intercept with $\theta_{LP} = 90°$ would be different, such that the true contact angle at which penetration would no longer occur spontaneously would be different. This is in keeping with the penetration into porous beds being driven by a function of contact angle, but limited by a function of the radius of curvature of the liquid entering the pores. This also explains why different workers report different values of contact angle as being the point where spontaneous penetration will no longer occur e.g. 80.5° in this study, and ca. 73° reported by Yang et al. (1988).

The negative view of the use of the Washburn equation in the assessment of contact angle, for systems in dissimilar states, given by Yang et al. (1988) may not be entirely justified, since in cases of consistent pore geometry, it is possible to correct data from penetration studies. For example, if materials were available in spheres of the geometry used in this study, which were not readily available as a flat smooth surface, their apparent contact angle could be measured

by penetration, and the true contact angle determined from figure 2.8.1. Such an application would obviously be rare. However, the views expressed by Yang et al. (1988) (for similar media, dissimilar states) are totally justifiable if applied to the case of dissimilar media, as there will be no way to correct the apparent contact angle measured by penetration to the true contact angle, as inevitably the pore geometry will be unknown. Consequently for real powdered systems, there would be serious problems in obtaining true contact angle data from liquid penetration experiments, as the influence of pore geometry will be unknown.

2.8.9. Range of application of the three techniques.

The apparent unreliability of the results from the liquid penetration technique would preclude its use for the routine measurement of contact angles, despite the fact that it is the only approach that allows contact angles to be measured on a powder. The liquid penetration approach, however, does have undoubted value if used as a qualitative assessment of wettability. The workable range for the liquid penetration technique is from around 30° (below which errors become too big) to approximately 80° (above which penetration does not occur at a fast enough rate for useful measurements to be made).

The direct measurement of contact angles from sessile drops produces values comparable to those produced by the Wilhelmy plate technique, although its

applicability at low values of θ is suspect. It is of most value when samples exist in a form unsuitable for use with the Wilhelmy plate technique. For example, samples of small surface area, or irregular shaped samples (so long as a flat portion exists). It can also provide an extremely quick visual impression of the contact angle and therefore give an indication of the wettability of the solid.

The Wilhelmy plate technique is a viable method over a vast range of contact angles. It is fair to say that the Wilhelmy plate technique could be applied over the full range of possible contact angles, from 0° (hence its use to determine γ) to 180°.

From a practical point of view, the Wilhelmy plate technique is easier to perform than either a direct measurement or the liquid penetration technique, and less prone to error/variability introduced through operator inexperience.

2.9. Conclusions.

For the three model surfaces studied, and with the liquids used, the Wilhelmy plate and sessile drop methods of contact angle determination produce results that are in good agreement.

The results generated from liquid penetration experiments are consistently higher than the contact angle values obtained using either the Wilhelmy plate or sessile drop techniques, suggesting that the Washburn model of a bundle of parallel capillaries is inadequate.

A strong relationship appears to exist, however, between the contact angle values obtained from the Wilhelmy plate technique and the liquid penetration technique, which depends on the contact angle and some function of pore geometry.

The choice of "perfectly wetting" liquid is an important factor in liquid penetration experiments. At low values of Cos θ, (high values of θ), the implications of using a nonperfectly wetting liquid as "perfectly wetting" are inconsequential. At high values of Cos θ, (low values of θ), however, the wrong choice of perfectly wetting liquid may introduce large errors into the calculated values of θ, due to the shape of the cosine curve.

The inaccuracy in the determination of θ at low contact angles is compounded when errors from other sources (e.g. viscosity and surface tension measurements) are taken into account. This also applies to data obtained from the Wilhelmy plate technique in which cos θ and θ are obtained indirectly.

It is therefore more useful to work with values of cos θ, rather than θ, and quote the accuracy of such.

Chapter 3

The estimation of solid surface energy from contact angle measurements.

3.1. Solid Surface Energy.

A knowledge of solid surface energies theoretically allows the outcome of any interfacial interaction involving a solid to be determined, if the surface energy of the second phase is known.

As discussed in chapter 1 (section 1.2.1.2), however, it is not possible to directly measure solid surface energy and most attempts to quantify solid surface energy involve measuring the contact angle formed between a liquid of known surface energy and the solid surface being studied.

In this chapter, the historical development of various methods of contact angle treatment will be considered, and a selection of the methods available will then be applied to the contact angle results obtained for the model surfaces in the previous chapter.

3.1.1. Critical surface tension for wetting, γ_c.

A significant breakthrough in the treatment of contact angle data was made by Fox and Zisman (1950, 1952a, 1952b).

By performing many contact angle measurements on low energy solids, they observed that Cos θ is usually a linear function of γ_{LV} for a homologous series of liquids, of the form;

$$\text{Cos } \theta = a - b.\gamma_{LV} \qquad \text{Eqn.3.1.1}$$

The extrapolation of the line to Cos $\theta = 1$ yields a similar value of γ_{LV} for various homologous series. Zisman proposed that this value of γ_{LV} was characteristic for a particular solid and referred to it as the *critical surface tension for wetting*, γ_c, since γ_{LV} is the surface tension of a hypothetical liquid which would just spread (spontaneously) on a particular solid. γ_c may be defined as;

$$\gamma_c = \lim_{\theta \to 0} \gamma_{LV} \qquad \text{Eqn.3.1.2}$$

It is important to note early on that γ_c is not equivalent to γ_S (Aveyard & Heydon, 1973 and Kinloch, 1980). Zisman (1964) described γ_c as a "useful empirical parameter whose relative values act as one would expect of γ_s of the solid".

Equation 3.1.1 may also be written;

$$\text{Cos } \theta = 1 - \beta.(\gamma_{LV} - \gamma_c) \qquad \text{Eqn.3.1.3}$$

The empirically determined value of β is usually about 0.03 to 0.04 (Adamson, 1990). This allows the contact angle for various systems to be estimated.

Following Fox and Zismans early work, other workers have attempted to obtain γ_c using nonhomologous liquid series. Dann (1970a) used a series of polar and hydrogen bonding liquids and liquid mixtures to measure γ_c for a range of polymeric materials. Liao and Zatz (1979) and Bernett and Zisman (1959) used aqueous solutions of

surfactants to determine the critical surface tension for Teflon and polyethylene. Values obtained using the surfactants and liquid mixtures are invariably lower than those obtained when a homologous series is used (Good, 1977). Dann (1970a) attributed this effect to the presence of polar forces at the interface. Another explanation, proposed by Good (1977) and supported by Pyter (1982) is that solute adsorption is occurring at the solid/vapour and solid/liquid interfaces. However, certain circumstances necessitate the use of liquid mixtures (for example the problem of nonpenetration of water into a packed powder bed). Hansford et al. (1980a & b) and Buckton (1985b) used alcohol/water mixtures to assess the wettability of pharmaceutical powders.

It has since been suggested by Zisman (1975) that γ_c may not be characteristic of the surface alone but may be a function of the type of liquid used. This theory was supported by Dann (1970a) who demonstrated that γ_c for poly(ethylene terephthalate) varies from 27-46mNm^{-1} depending on the choice of homologous series. Fox and Zisman (1950, 1952a, 1952b) saw similar effects with paraffin and hexatriacontane.

In 1977, Good suggested that some of the discrepancies in the derived values of γ_c may be due to the long extrapolations which are sometimes necessary. Good (1979) refined this theory to predict that if the lowest value of γ_L for the liquid series is greater than $1.25\gamma_c$, then linear extrapolation will be erroneous, giving a value of γ_c approximately 10% too low. Good

proposed that γ_c be determined by plotting Cos θ against $(\gamma_{LV})^{1/2}$. Using this method, Good (1977) was able to obtain a single value of γ_c for polystyrene using both hydrogen bonding liquids and nonhydrogen bonding liquids.

Occasionally the Good approach still produces differing values for γ_c. In these cases, a plot of $(\gamma_{LV}.(1 + \text{Cos } \theta)^2)/4$ against γ_{LV} can be used to obtain values of γ_c (Good, 1979).

Kitazaki and Hata (1972) came to the conclusion that γ_c should be obtained by using several liquid series and taking the highest value of γ_c, as this would represent the minimum interfacial free energy between the liquid and solid.

Therefore, because of the empirical nature of γ_c, as many approaches as possible should be used to provide a spectrum of values from which the experimenter can determine a typical value. The value obtained should then provide a convenient and useful measure of the wettability of the solid surface.

3.1.2. Good and Girifalco interaction parameter.

Another major advance in the study of interfacial energies was made by Good and Girifalco (1957). By treating the free energies of adhesion and cohesion for two phases as analogous to the Berthelot (1898) relation for the attractive constants between like molecules and unlike molecules, the following relationship was

derived;

$$\gamma_{ab} = \gamma_a + \gamma_b - 2.\Phi.(\gamma_a\gamma_b)^{1/2} \qquad \text{Eqn.3.1.4.}$$

Φ is a constant, characteristic for a particular system and represents a ratio involving the free energies of adhesion and cohesion, which compensates for deviations from the geometric mean rule of molecular interactions. The value of Φ may be estimated from a knowledge of the molecular polarisability, the dipole moment and the ionisation energy of the molecules interacting across the interface.

Good (1964) expanded the relationship to deal with the solid/liquid interface by combining equation 3.1.4 with Young's equation (Equation 1.3.1) to give;

$$\text{Cos}\theta = 2.\Phi.\left(\frac{\gamma_s}{\gamma_l}\right) - 1 - \frac{\pi_e}{\gamma_l} \qquad \text{Eqn.3.1.5.}$$

In situations where a finite contact angle exists, π_e is considered to be negligible, giving;

$$\text{Cos}\theta = 2.\Phi.\left(\frac{\gamma_s}{\gamma_l}\right)^{\frac{1}{2}} - 1 \qquad \text{Eqn.3.1.6.}$$

Good (1979) calculated Φ for a variety of solid/liquid pairs and, in combination with experimentally determined contact angles, calculated the surface free energies of the solids, using equation 3.1.6. The values of γ_S obtained were very similar to the critical surface tension values measured by the

method of Zisman (1950). Hence, if Cos θ, γ_{LV} and Φ are known, then the value of γ_S can be calculated from a single value of Cos θ.

By definition Φ takes the value unity for "regular interfaces" i.e. interfaces between phases in which the dominant cohesive and adhesive forces are the same. In most cases Φ has a value between 0.5 and 1, depending on the relative nature of the phases. A value close to unity is obtained when the phases possess similar intermolecular interactions. As the disparity between the phases increases, so Φ decreases. For example, Good and Girifalco (1957) found Φ to have a value of ~1 for the water/alcohol interface, but a value of ~0.7 for the water/aromatic hydrocarbon interface. Becher (1977) noted that Φ deviated from unity most markedly for those liquids composed of small, highly dipolar molecules (e.g. water, glycerol, diiodomethane), but is close to unity for interactions involving most other liquids.

This implies that γ_s of most solids may be determined from a single contact angle measurement, provided the liquid has predominantly nonpolar intermolecular forces, by employing equation 3.1.6 and assuming $\Phi = 1$.

In 1965, Driedger et al. derived an empirical equation to cater for the situation where Φ is not known. A value for Φ can be estimated if γ_{LV} is known using;

$$\Phi = -0.0075.\gamma_{LV} + 1 \qquad \text{Eqn.3.1.7}$$

3.2. Theory of surface tension components.

Fowkes (1962, 1963) stated that interactions across an interface only occur between forces of similar types, common to both phases. For example, no interaction due to permanent dipoles can take place across an interface between a nonpolar phase and a polar phase.

As a continuation of this theory, Fowkes (1964) proposed that the surface tension of a phase could be decomposed into components, such that;

$$\gamma_{tot} = \gamma^d + \gamma^h + \gamma^i + ... \qquad \text{Eqn.3.2.1}$$

where γ^d, γ^h and γ^i etc are considered to be physical properties of a material, representing dispersion forces (van der Waals forces) hydrogen-bonding forces, induction forces and so on.

The forces are commonly divided into just two groups; dispersion forces and polar forces (Zografi and Tam, 1986 and Wu, 1973) so that;

$$\gamma_{tot} = \gamma^d + \gamma^p \qquad \text{Eqn.3.2.2}$$

Much of Fowkes work was performed with saturated hydrocarbons (which involve only dispersion forces) enabling the magnitude of γ^d contributions to be determined in more complex liquids and solids. Fowkes (1964) used an approach based on the Berthelot relationship (cf. Good-Girifalco approach) to derive a relationship between the interfacial tensions of two phases. According to Fowkes (1964), the decrease in

surface tension of one phase (phase 1) resulting from the presence of a second phase (phase 2) is given by;

$$\Delta\gamma_{1(2)} = \sqrt{\gamma_1^d \cdot \gamma_2^d} \qquad \text{Eqn.3.2.3}$$

the resulting tension in the interfacial monolayer of phase 1, (γ_1^{IM}), is then;

$$\gamma_1^{IM} = \gamma_1 - \sqrt{\gamma_1^d \cdot \gamma_2^d} \qquad \text{Eqn.3.2.4}$$

similarly for phase 2;

$$\gamma_2^{IM} = \gamma_2 - \sqrt{\gamma_1^d \cdot \gamma_2^d} \qquad \text{Eqn.3.2.5}$$

in combination, eqns 3.2.4 and 3.2.5 give;

$$\gamma_{12} = \gamma_1 + \gamma_2 - 2.\sqrt{\gamma_1^d \cdot \gamma_2^d} \qquad \text{Eqn.3.2.6}$$

(The Fowkes equation is very similar to the Good-Girifalco equation, except that the Good-Girifalco equation includes an interaction parameter in the last term ($- 2.\Phi.(\gamma_a\gamma_b)^{1/2}$) and uses the total surface tension term). Equation 3.2.6 is only applicable when at least one of the phases is completely dispersive.

For interactions between a solid and hydrocarbon, Fowkes (1964) combined equation 3.2.6 with Youngs' equation (eqn. 1.3.1) to cancel γ_S;

$$\gamma_L.\cos\theta = -\gamma_L + 2.\sqrt{\gamma_L^d \cdot \gamma_s^d} - \pi_e \qquad \text{Eqn.3.2.7}$$

which can be rearranged to give;

$$\text{Cos}\theta = -1 + \frac{2\sqrt{\gamma_L^d \cdot \gamma_s^d}}{\gamma_L} - \pi_e \qquad \text{Eqn.3.2.8}$$

Equation 3.2.8 provides a means of estimating γ_s^d, since a plot of Cos θ as a function of $\frac{\sqrt{\gamma_L^d}}{\gamma_L}$ yields a straight line of slope $2\sqrt{\gamma_s^d}$, provided $\gamma_L = \gamma_L^d$ and π_e is negligible.

3.2.1. Methods for determining polar components.

Fowkes' (1964) approach for determining the dispersion component of solid surface tension is well accepted. However, a knowledge of the dispersion component of surface tension does not enable the investigator to estimate the total solid surface tension, since the magnitude of the "polar" interactions is unknown.

The polar component of surface tension is a much more difficult value to ascertain as polar interactions may be divided into many subgroups, and no liquids exist which consist of purely polar intermolecular forces.

This has not deterred several workers from tackling the problem of determining polar components of surface tension.

3.2.1.1. The "extended Fowkes'" equation.

Owens and Wendt (1969) were the first to attempt to solve the problem of polar components of surface energy. Their method is based on the equation for work of adhesion given by Fowkes (1964);

$$W_{SL}^{d} = \gamma_L(1 + \cos\theta) = 2.\left(\gamma_L^{d}\gamma_s^{d}\right)^{\frac{1}{2}} \qquad \text{Eqn.3.2.9}$$

W_{SL}^{d} is the proportion of the work of adhesion due to van der Waals forces. By using liquids which have only van der Waals interactions with the substrate, Owens and Wendt were able to determine W_{SL}^{d}. By subsequently using polar test liquids whose dispersion component γ_s^{d} of surface tension is known, such that the work of adhesion due to van der Waals forces can be calculated, the excess work of adhesion, $(W_{SL} - W_{SL}^{d})$ could then be attributed to the polar components of the surface tension of the liquid and solid surface;

$$W_{sL}^{p} = 2.\left(\gamma_L^{p}\gamma_s^{p}\right)^{\frac{1}{2}} \qquad \text{Eqn.3.2.10}$$

The interfacial tension between phases 1 and 2 is then given by;

$$\gamma_{12} = \gamma_1 + \gamma_2 - 2.\left(\gamma_1^{d}.\gamma_2^{d}\right)^{\frac{1}{2}} - 2.\left(\gamma_1^{p}.\gamma_2^{p}\right)^{\frac{1}{2}} \qquad \text{Eqn.3.2.11}$$

Kaeble (1969, 1971) also employed the work of adhesion

in an approach which is effectively equivalent to that of Owens and Wendt. Using two liquids (i and j) with surface tension γ_{Li} and γ_{Lj} and contact angle θ_i and θ_j on the same solid respectively, the following simultaneous equations can be set up;

$$\gamma_{Li}(1 + \cos\theta) = \left(\gamma_{Li}^{d}.\gamma_{s}^{d}\right)^{\frac{1}{2}} + .\left(\gamma_{Li}^{p}.\gamma_{s}^{p}\right)^{\frac{1}{2}} \qquad \text{Eqn.3.2.12}$$

$$\gamma_{Lj}(1 + \cos\theta) = \left(\gamma_{Lj}^{d}.\gamma_{s}^{d}\right)^{\frac{1}{2}} + .\left(\gamma_{Lj}^{p}.\gamma_{s}^{p}\right)^{\frac{1}{2}} \qquad \text{Eqn.3.2.13}$$

Kaeble solved these equations using a determinant method;

$$\Delta = \begin{vmatrix} \left(\sqrt{\gamma_{Li}^{d}}\right)\left(\sqrt{\gamma_{Li}^{p}}\right) \\ \left(\sqrt{\gamma_{Lj}^{d}}\right)\left(\sqrt{\gamma_{Lj}^{p}}\right) \end{vmatrix} \qquad \text{Eqn.3.2.14}$$

$$\gamma_{s}^{d} = \frac{\begin{vmatrix} (1 + \cos\theta_i)\left(\sqrt{\gamma_{Li}^{p}}\right) \\ (1 + \cos\theta_j)\left(\sqrt{\gamma_{Lj}^{p}}\right) \end{vmatrix}^2}{\Delta^2} \qquad \text{Eqn.3.2.15}$$

$$\gamma_{s}^{p} = \frac{\begin{vmatrix} \left(\sqrt{\gamma_{Li}^{d}}\right)(1 + \cos\theta_i) \\ \left(\sqrt{\gamma_{Lj}^{d}}\right)(1 + \cos\theta_j) \end{vmatrix}^2}{\Delta^2} \qquad \text{Eqn.3.2.16}$$

3.2.1.2. Wu's harmonic mean approach.

Wu (1971) used a similar approach to Owens and Wendt (1969) and Kaeble (1969, 1971), except that he averaged the interaction energies using a harmonic mean (equation 3.2.17), as opposed to the geometric mean (equation 3.2.10) used by Owens and Wendt.

Wu (1971) demonstrated empirically that a harmonic mean of intermolecular forces is more appropriate for low energy solids such as polymers and the liquid polar-polar systems he studied. Wu (1973) also reported that for high energy solids such as mercury, glass, graphite etc a hybrid equation is best. Equation 3.2.11 is said to be unsatisfactory in general.

$$W_{SL} = W_{SL}^{d} + W_{SL}^{p} = 4\left\{\frac{\gamma_s^{d}\cdot\gamma_L^{d}}{\left(\gamma_s^{d} + \gamma_L^{d}\right)}\right\} + 4\left\{\frac{\gamma_s^{p}\cdot\gamma_L^{p}}{\left(\gamma_s^{p} + \gamma_L^{p}\right)}\right\}$$

Eqn.3.2.17

The interfacial free energy between any two phases, γ_{12}, can be estimated from a knowledge of the individual surface free energies γ_1 and γ_2, and the energies associated with the interactions taking place across the interface (Fowkes, 1964), which, in general terms (Wu, 1971), may be expressed as;

$$\gamma_{12} = \gamma_1 + \gamma_2 - 2\phi^{d} - 2\phi^{p} \qquad \text{Eqn.3.2.18}$$

where ϕ^{d} and ϕ^{p} represent nonpolar and polar interactions respectively.

Applying the harmonic mean rule of Wu (1971)

therefore gives;

$$\phi^d = \frac{2\gamma_1^d\gamma_2^d}{\gamma_1^d + \gamma_2^d} \qquad \text{Eqn.3.2.19}$$

and

$$\phi^p = \frac{2\gamma_1^p\gamma_2^p}{\gamma_1^p + \gamma_2^p} \qquad \text{Eqn.3.2.20}$$

Substituting equations 3.2.19 and 3.2.20 into equation 3.2.18 gives;

$$\gamma_{12} = \gamma_1 + \gamma_2 - \frac{4\gamma_1^d\gamma_2^d}{\gamma_1^d + \gamma_2^d} - \frac{4\gamma_1^p\gamma_2^p}{\gamma_1^p + \gamma_2^p} \qquad \text{Eqn.3.2.21}$$

Combining equation 3.2.21 with the Young equation (equation 1.3.1) to eliminate γ_{12} gives (for a solid and liquid);

$$(b + c - a)\gamma_s^d\gamma_s^p + c(b - a)\gamma_s^d + b(c - a)\gamma_s^p - abc = 0 \qquad \text{Eqn.3.2.22}$$

where; $c = \gamma_1^p$, $b = \gamma_1^d$ and $a = \frac{\left(\frac{\gamma_1}{4}\right)}{(1 + \cos\theta)}$.

There are two unknowns in equation 3.2.22; γ_s^d and γ_s^p. Therefore it is necessary to obtain contact angle data for two different liquids of known γ_1^d and γ_1^p on each particular solid. An iterative computer program can be used to determine best fit values of γ_s^d and γ_s^p for the contact angle data obtained.

3.2.2. Theory of nonadditive surface tension components.

The approaches to solid surface tension estimation discussed so far in which the surface tension is divided into components, assume that the parameters which comprise the components are essentially additive. Van Oss et al (1987) have treated the theory of surface tension components in a slightly different way. The parameters of the component of surface tension produced by apolar forces are still considered to be additive, however, the surface tension parameters comprising the overall polar force are considered nonadditive.

Van Oss et al (1988) also employ different notation for apolar and polar forces. The apolar forces are referred to as Lifshitz-van der Waals (LW) interactions and comprise induction (Debye), dispersion (London) and orientation (Keesom) interactions. The significant polar forces are the hydrogen-bonding type and are designated by van Oss et al. as (Lewis) acid-base (AB) or electron-acceptor/electron-donor interactions. Since Lewis acid-base interactions are intrinsically asymmetrical (Jenson, 1980), van Oss et al. (1988) reason that they are therefore nonadditive.

3.2.2.1. Apolar or LW interactions.

Van Oss et al (1989) distinguish between the polar nature of hydrogen bonds and attractions due to permanent dipoles/induced dipoles as described by Debye, since this type of interaction blurs the boundary

between polar and apolar forces. Van Oss (1987) proposes that the components of surface tension arising from the three electrodynamic interactions (i.e. London, Keesom and Debye forces) should be combined into one term, namely "LW", for Lifshitz-van der Waals.

The interfacial tension due to Lifshitz-van der Waals (LW) forces between two phases i and j is expressed according to the Good-Girifalco (1957) combining rule in a similar way to previously discussed surface tension component theories;

$$\gamma_{ij}^{LW} = \left(\sqrt{\gamma_i^{LW}} - \sqrt{\gamma_j^{LW}}\right)^2 \qquad \text{Eqn.3.2.23}$$

which can be rewritten;

$$\gamma_{ij}^{LW} = \gamma_i^{LW} + \gamma_j^{LW} - 2\left(\gamma_i^{LW}\gamma_j^{LW}\right)^{\frac{1}{2}} \qquad \text{Eqn.3.2.24}$$

combining with the Young equation;

$$1 + \text{Cos}\theta = 2\left(\frac{\gamma_i^{LW}}{\gamma_j^{LW}}\right)^{\frac{1}{2}} \qquad \text{Eqn.3.2.25}$$

As with the Fowkes approach to surface tension components (see section 3.2.1.2.), the apolar (LW) component of solid surface tension is directly obtainable from contact angle measurements with purely apolar liquids, using;

$$1 + \text{Cos}\theta = 2\left(\frac{\gamma_i^{LW}}{\gamma_j}\right)^{\frac{1}{2}} \qquad \text{Eqn.3.2.26}$$

or;

$$4\gamma_i^{LW} = \gamma_j(1 + \cos\theta)^2 \qquad \text{Eqn.3.2.27}$$

A value for γ^{lw} is easily measurable (as it equates to the surface tension of an apolar liquid) and the values of γ^{lw} for many LW liquids have been published (Jasper, 1972).

3.2.2.2. Polar or AB interactions.

By comparison to LW interactions, the attraction associated with polar substances (in particular hydrogen bonds) is short range, decaying to zero within 0.3 to 0.4nm in vaccuo (van Oss et al , 1986). LW interactions are relatively long range in nature, decaying to zero over 10 to 20nm, depending on the nature of the van der Waals forces (Tabor and Winterton, 1968). However, this is not to say that short range interactions (i.e. AB interactions) are negligible. On the contrary, their influence may be marked and indeed can lead to negative interfacial tensions as will be shown.

As little or no interaction can occur between H-bonds and LW forces, no cross term can exist. Hence;

$$\gamma^{TOT} = \gamma^{LW} + \gamma^{AB} \qquad \text{Eqn.3.2.28}$$

Therefore, for two polar substances, i and j, the free energy of adhesion is given by;

$$\Delta G_{ij}^{adh} = \Delta G_{ij}^{adhLW} + \Delta G_{ij}^{adhAB} \qquad \text{Eqn.3.2.29}$$

It is at this point that the treatment of γ^{LW} and γ^{AB} differs in the van Oss approach. Contrary to the resolution of γ^{LW} into parameters which are simply added together to produce γ^{LW}, γ^{AB} may be resolved into two parameters;

$$\gamma_i^{AB} = 2\sqrt{\gamma_i^+ \gamma_i^-} \qquad \text{Eqn.3.2.30}$$

In this case, γ_i^+ represents the electron acceptor (Lewis acid) component of compound i, and γ_i^- its electron donor (Lewis base) component. It should be stressed that γ_i^+ and γ_i^- may not be equal and should not be assumed to be so. Equation 3.2.31 describes the free energy of adhesion between compounds i and j, since both substances i and j may have electron donor and electron acceptor capabilities. Therefore according to van Oss (1987);

$$\Delta G_{ij}^{aAB} = -2\sqrt{\gamma_i^+ \gamma_j^-} - 2\sqrt{\gamma_i^- \gamma_j^+} \qquad \text{Eqn.3.2.31}$$

The free energy of AB adhesion between compound i and j can also be represented using the Dupré equation;

$$\Delta G_{ij}^{aAB} = \gamma_{ij}^{AB} - \gamma_i^{AB} - \gamma_j^{AB} \qquad \text{Eqn.3.2.32}$$

rearranging gives;

$$\gamma_{ij}^{AB} = \Delta G_{ij}^{aAB} + \gamma_i^{AB} + \gamma_j^{AB} \qquad \text{Eqn.3.2.33}$$

and combining equations 3.2.31, and 3.2.33, produces the

following relationship;

$$\gamma_{ij}^{AB} = 2\left(\sqrt{\gamma_i^+\gamma_i^-} + \sqrt{\gamma_j^+\gamma_j^-} - \sqrt{\gamma_i^+\gamma_j^-} - \sqrt{\gamma_i^-\gamma_j^+}\right)$$

Eqn.3.2.34

The Young equation can now be written in terms of LW and AB interactions by combining the Young-Dupré equation;

$$\Delta G_{SL} = -\gamma_L(1 + \cos\theta) \qquad \text{Eqn.3.2.35}$$

(where the subscripts s and l refer to solid and liquid respectively), with equation 3.2.29. to give;

$$1 + \cos\theta = \frac{-1}{\gamma_L^{TOT}}\left(\Delta G_{sL}^{LW} + \Delta G_{sL}^{AB}\right)$$

Eqn.3.2.36

or;

$$1 + \cos\theta = \frac{2}{\gamma_L^{tot}}\left(\sqrt{\gamma_s^{LW}\cdot\gamma_L^{LW}} + \sqrt{\gamma_s^+\cdot\gamma_L^-} + \sqrt{\gamma_s^-\cdot\gamma_L^+}\right)$$

Eqn.3.2.37

It is now possible for γ^+ and γ^- for any polar surface of known γ^{LW} to be calculated from contact angle measurements with liquids of which all three parameters are known, i.e. γ_1^{LW}, γ_1^+ and γ_1^-.

It is clear from equation 3.2.28 that the apolar (LW) and polar (AB) components of surface tension are *additive*. It is equally clear from equation 3.2.30 that the constituent electron-acceptor (γ^+) and electron donor (γ^+) parameters of the AB component of surface tension

are *not* additive.

Van Oss et al (1987) have demonstrated that for most liquids, $\gamma_i^+ \neq \gamma_i^-$. In some cases, polar solids and liquids were found which were strong electron donors but had little or no electron acceptor capacity. Less common are polar liquids and solids that are electron acceptors but not electron donors (van Oss, 1987b). These compounds were termed *monopoles* (van Oss et al, 1987), i.e. compounds with either a strong γ^+ or γ^- parameter. For monopolar compounds, there is no contribution to the work of cohesion of these compounds by the polar component of surface tension because of the absence of a parameter (γ^+ or γ^-) of the opposite sign.

The surface tension of monopolar compounds, therefore, is equal to the apolar (LW) contribution. However, the capacity for the AB parameter (γ^+ or γ^-) to interact with the AB parameter of the opposite sign in bipolar compounds or a monopolar compounds of opposite nature is still present. From equation 3.2.27, then, one of the terms on the right hand side remains even if one of the compounds is monopolar.

3.2.2.3. Classification of binary systems.

The description of solids and liquids as apolar, monopolar or bipolar by van Oss and co-workers (1988), logically leads to the separation of binary systems consisting of phases 1 and 2, into seven distinct classes (see table 3.2.1).

Table 3.2.1 Classification of binary systems according to van Oss et al. (1988).

CLASS	PHASE	
	1	2
I	apolar	apolar
II	apolar	monopolar
III	apolar	bipolar
IV	monopolar	monopolar*
V	monopolar	monopolar**
VI	monopolar	bipolar
VII	bipolar	bipolar

* same sense
** opposite sense

In the case of a liquid drop on a solid, there are nine permutations in all (allowing for certain asymmetrical cases), which are represented in figure 3.2.1 (from van Oss et al, 1988). Cohesive interactions are indicated by horizontal lines, adhesive interactions by vertical lines. Class I interactions involve only apolar phases and therefore do not involve polar forces. Interfacial polar forces are also absent in classes II, III and IV. In the case of classes II and III-A, this is because the polar solid has no influence on the apolar solid. For class III-B the polar portion of the surface tension cannot interact with the apolar solid, and the case whereby monopoles of the same polarity do not interact is demonstrated by class IV. In mathematical terms, equation 3.2.37, for classes I, II, IIIA, and IV

reduces to;

$$1 + \text{Cos}\theta = 2\sqrt{\frac{\gamma_s^{LW}}{\gamma_L^{LW}}} \qquad \text{Eqn.3.2.38.}$$

In the case of class III-B, equation 3.2.37 reduces to;

$$(1 + \text{Cos}\theta)\gamma_L^{TOT} = 2\sqrt{\frac{\gamma_s^{LW}}{\gamma_L^{LW}}} \qquad \text{Eqn.3.2.39.}$$

demonstrating that a value for γ_S^{LW} (i.e. γ_S^{TOT}) for an apolar solid is obtainable using a bipolar liquid, since the polarity of the liquid influences only its cohesion and not the adhesion between the liquid and solid. Equation 3.2.37 can be applied to classes V and VI-A, although, in these cases $\gamma_L^{LW} = \gamma_L^{TOT}$. For class VI-B, one of the polar terms in equation 3.2.37 reduces to zero. An unadulterated form of equation 3.2.37 can be used for class VII.

Fig.3.2.1. Schematic classification of the interaction between a liquid drop and a solid surface (according to van Oss et al, 1988).

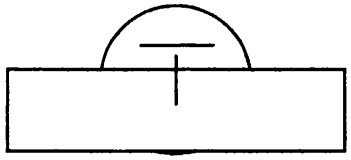

I. APOLAR L / APOLAR S

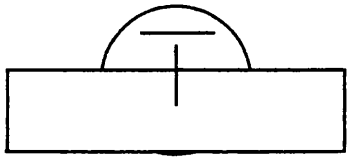

II. APOLAR L / MONOPOLAR S (AND VICE VERSA)

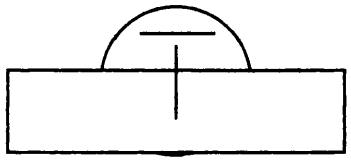

III-A. APOLAR L / BIPOLAR S

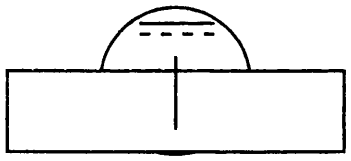

III-B. BIPOLAR L / APOLAR S

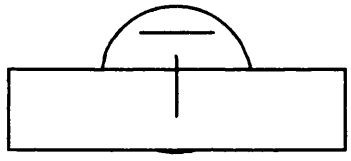

IV. MONOPOLAR L / MONOPOLAR S (SAME SENSE)

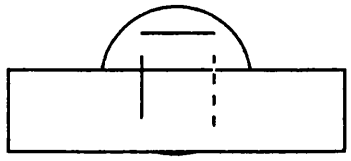

V. MONOPOLAR L / MONOPOLAR S (OPPOSITE SENSE)

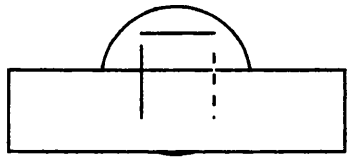

VI-A. MONOPOLAR L / BIPOLAR S

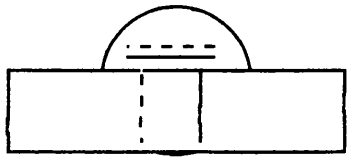

VI-B. BIPOLAR L / MONOPOLAR S

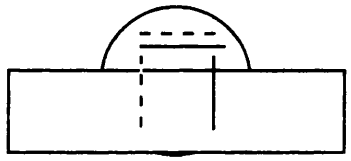

VII. BIPOLAR L / BIPOLAR S

----- AB interaction ——— LW interaction

3.2.2.4. Negative interfacial interactions.

The Dupré equation as it applies to polar interactions may be written as follows;

$$\Delta G_{ij}^{AB} = \gamma_{ij}^{AB} - \gamma_i^{AB} - \gamma_j^{AB} \qquad \text{Eqn 3.2.40.}$$

combining equation 3.2.31 with equation 3.2.40 to eliminate ΔG_{ij}^{AB} gives;

$$\gamma_{ij}^{AB} = \gamma_i^{AB} + \gamma_j^{AB} - 2\sqrt{\gamma_i^+\gamma_j^-} - 2\sqrt{\gamma_i^-\gamma_j^+} \qquad \text{Eqn 3.2.41.}$$

From equation 3.2.41, the cohesive energy due to polar interactions of a given material, i (ΔG_{ii}^{AB}), is given by;

$$\Delta G_{ii}^{AB} = -2\sqrt{\gamma_i^+\gamma_i^-} - 2\sqrt{\gamma_i^-\gamma_i^+} = -4\sqrt{\gamma_i^-\gamma_i^+} \qquad \text{Eqn 3.2.42.}$$

and since $\Delta G_{ii}^{coh} = -2\gamma_i$, it follows that;

$$\gamma_i^{AB} = 2\left(\sqrt{\gamma_i^+\gamma_i^-}\right) \qquad \text{Eqn 3.2.43.}$$

Substituting equation 3.2.43 into equation 3.2.41 gives;

$$\gamma_{ij}^{AB} = 2\left(\sqrt{\gamma_i^+\gamma_i^-} + \sqrt{\gamma_j^+\gamma_j^-} - \sqrt{\gamma_i^+\gamma_j^-} - \sqrt{\gamma_i^-\gamma_j^+}\right) \qquad \text{Eqn 3.2.44.}$$

It becomes apparent, therefore, that contrary to γ_{ij}^{LW}, γ_{ij}^{AB} can become *negative*. Rearranging equation 3.2.44;

$$\gamma_{12}^{AB} = 2\left\{\left(\sqrt{\gamma_1^+} - \sqrt{\gamma_2^+}\right)\left(\sqrt{\gamma_1^-} - \sqrt{\gamma_2^-}\right)\right\} \qquad \text{Eqn 3.2.45.}$$

shows that the AB component of surface tension will be negative if $\gamma_i^+ < \gamma_j^+$ and $\gamma_i^- > \gamma_j^-$, or $\gamma_i^+ > \gamma_i^-$ and $\gamma_i^- < \gamma_j^-$. Indeed, if equations 3.2.44 and 3.2.23 are combined to produce;

$$\gamma_{ij}^{TOT} = \left(\sqrt{\gamma_i^{LW}} - \sqrt{\gamma_j^{LW}}\right)^2 + 2\left(\sqrt{\gamma_i^+\gamma_i^-} + \sqrt{\gamma_j^+\gamma_j^-} - \sqrt{\gamma_i^+\gamma_j^-} - \sqrt{\gamma_i^-\gamma_j^+}\right)$$

Eqn 3.2.46.

it is evident that γ_{ij}^{TOT} can be negative in the case of polar compounds.

3.2.2.5. The concept of fractional polarities.

Unfortunately, it is not possible to obtain absolute values of γ^+ and γ^-, since absolute values are not known for the test liquids. van Oss et al. (1987) have therefore introduced the concept of fractional polarities to allow ΔG_{ij}^{adhAB} and γ_{ij}^{AB} to be calculated.

In order to do this, however, it is necessary to make an arbitrary estimate of the ratio of γ^+ and γ^- for a reference compound. For convenience, van Oss et al (1987) chose water and assumed that $\gamma_{H_2O}^+ = \gamma_{H_2O}^- = 25.5$ mJ/m^2. This value is derived from the value for the apolar component of water surface tension ($\gamma^{AB} = 51$ mJ/m^2) and the fact that $\gamma^{AB} = 2(\gamma^+\gamma^-)^{1/2}$. Polarity values for another compound, 1, can then be calculated relative to water (W).

Therefore, polarity ratios can be defined as;

$$\delta_{1W}^{+} = \sqrt{\frac{\gamma_1^{+}}{\gamma_W^{+}}} \qquad \text{Eqn.3.2.47.}$$

and;

$$\delta_{1W}^{-} = \sqrt{\frac{\gamma_1^{-}}{\gamma_W^{-}}} \qquad \text{Eqn.3.2.48.}$$

Rearranging equations 3.2.47 and 3.2.48 gives;

$$\sqrt{\gamma_W^{+}} = \frac{25.5}{\sqrt{\gamma_W^{-}}} \qquad \text{Eqn.3.2.49a.}$$

and;

$$\sqrt{\gamma_W^{-}} = \frac{25.5}{\sqrt{\gamma_W^{+}}} \qquad \text{Eqn.3.2.49b.}$$

which can be substituted into equation 3.2.37, to give;

$$\gamma_W(1 + \text{Cos}\theta) = 2\left(\sqrt{\gamma_1^{LW}\gamma_W^{LW}} + 25.5\sqrt{\frac{\gamma_1^{+}}{\gamma_W^{+}}} + 25.5\sqrt{\frac{\gamma_1^{-}}{\gamma_W^{-}}}\right)$$

Eqn.3.2.50.

therefore;

$$\gamma_W(1 + \text{Cos}\theta) = 2\sqrt{\gamma_1^{LW}\gamma_W^{LW}} + 51\delta_{1W}^{+} + 51\delta_{1W}^{-}$$

Eqn.3.2.51.

A similar equation has been developed for glycerol (G). The polar component of the surface tension of glycerol is 30 mN/m^2 (van Oss et al 1987) and, therefore;

$$\sqrt{\gamma_G^{-}} = \frac{15}{\sqrt{\gamma_G^{+}}} \qquad \text{Eqn.3.2.52a.}$$

and

$$\sqrt{\gamma_G^+} = \frac{15}{\sqrt{\gamma_G^-}} \qquad \text{Eqn.3.2.52b.}$$

Equation 3.2.50 for the case with glycerol then becomes;

$$\gamma_G(1 + \cos\theta_G) = 2\left(\sqrt{\gamma_1^{LW}\gamma_G^{LW}} + 15\sqrt{\frac{\gamma_1^-}{\gamma_G^-}} + 15\sqrt{\frac{\gamma_1^+}{\gamma_G^+}}\right)$$

Eqn.3.2.53.

van Oss et al (1989), by measuring contact angles on monopolar surfaces with water and glycerol were able to estimate values for δ_{GW}^- and δ_{GW}^+. The values reported were;

$$\delta_{GW}^- = 1.500 \qquad \text{and} \qquad \delta_{GW}^+ = 0.392$$

The values of γ_G^+ and γ_G^- in equation 3.2.53 do not then need to be known, and equation 3.2.51 can be written in the form;

$$\gamma_G(1 + \cos\theta_G) = 2\sqrt{\gamma_1^{LW}\gamma_G^{LW}} + 76.5\delta_{1W}^+ + 20\delta_{1W}^-$$

Eqn.3.2.54.

Values for δ_{1W}^+ and δ_{1W}^- can now be determined by solving equations 3.2.54 and 3.2.51 simultaneously.

The AB component of surface tension can then be derived from ;

$$\gamma_1^{AB} = 51.\delta_{1W}^+.\delta_{1W}^- \qquad \text{Eqn.3.2.55.}$$

Finally, the determination of LW surface tension of solid 1 can be derived from contact angle measurements with an apolar (LW) liquid (2) using;

$$4\gamma_1^{LW} = \gamma_2(1 + \text{Cos } \theta)^2 \qquad \text{Eqn.3.2.56.}$$

3.2.3. Equation of state approach.

Ward and Neumann (1974) have attempted to show that interfacial free energy can be described by an equation of state of the form;

$$\gamma_{SL} = f(\gamma_{SV}, \gamma_{LV}) \qquad \text{Eqn.3.2.57.}$$

When used in combination with Young's equation (eqn.1.3.1) the two unknown quantities, γ_{sl} and γ_{sv}, can be obtained by measuring the contact angle formed by a liquid of known surface tension on the solid of interest.

Ward and Neumann (1974) have attempted to prove the existence of an equation of state in the following way; based on the Gibbs-Duhem equations for a three phase interfacial system comprising a pure liquid in equilibrium with its vapour, and a rigid insoluble solid on which there is no liquid or vapour adsorption,

$$d\gamma_{sv} = -S_{(1)}^{sv}dT - \Gamma_{2(1)}^{sv}d\mu_2 \qquad \text{Eqn.3.2.58.}$$

$$d\gamma_{sL} = -S_{(1)}^{sL}dT - \Gamma_{2(1)}^{sL}d\mu_2 \qquad \text{Eqn.3.2.59.}$$

$$d\gamma_{LV} = -S^{LV}dT - \Gamma_2^{LV}d\mu_2 \qquad \text{Eqn.3.2.60.}$$

where the subscript 2 refers to the liquid component and the subscript 1 refers to the "definition of the Gibbs dividing surface chosen to eliminate adsorption of the solid component at the particular interface".

$S_{(1)}^{sv}$	=	surface entropy of the solid/vapour interface
T	=	absolute temperature
$\Gamma_{2(1)}^{sv}$	=	is the surface excess of component 2 (the liquid) at the solid/vapour interface.
μ_2	=	chemical potential of the liquid component

Equations 3.2.58 - 3.2.60 imply that each of the surface tensions is a function of T and μ_2 such that;

$$\gamma_{sv} = \gamma_{sv}\ (T,\mu_2) \qquad \text{Eqn.3.2.61.}$$

$$\gamma_{sl} = \gamma_{sl}\ (T,\mu_2) \qquad \text{Eqn.3.2.62.}$$

$$\gamma_{sv} = \gamma_{sv}\ (T,\mu_2) \qquad \text{Eqn.3.2.63.}$$

It can then be reasoned that since three equations exist in terms of two variables T and μ_2, any one of the three equations 3.2.61 - 3.2.63 may be expressed as a linear combination of the other two. This is taken to imply that an equation of the form of equation 3.2.57 must exist, i.e. an equation of state for interfacial tensions.

In 1979 Wu also proposed an equation of state analysis for the determination of solid surface tension.

The rationale behind Wu's approach being that the Fox and Zisman (1950) γ_c approach yields different values for γ_c depending on the liquid series used, but can be generalised to enable surface tension to be determined reliably.

γ_c may be defined as;

$$\gamma_c = \lim_{\theta \to 0} \gamma_{LV} \qquad \text{Eqn.3.2.64.}$$

combining equation 3.2.64 with equation 3.1.5 gives;

$$\gamma_c = \phi_{\gamma_s}^{\ 2} - \pi_e + \left(\frac{\pi_e^{\ 2}}{4\phi\gamma_s} \right) + \ldots\ldots \qquad \text{Eqn.3.2.65.}$$

Equation 3.2.65 rapidly converges and may therefore be abbreviated to;

$$\gamma_c = \Phi^2.\gamma_s - \pi_e \qquad \text{Eqn.3.2.66.}$$

substituting equation 3.2.66 back into equation 3.1.5 gives;

$$\text{Cos}\theta = 2\left(\frac{\gamma_c}{\gamma_{LV}} \right)^{\frac{1}{2}} - 1 \qquad \text{Eqn.3.2.67.}$$

or;

$$\gamma_c = \frac{1}{4}(1 + \text{Cos}\theta)^2 \gamma_{LV} \qquad \text{Eqn.3.2.68.}$$

which Wu termed the equation of state.

Equation 3.2.68 allows γ_c to be calculated from a single contact angle measurement with a liquid of known surface tension. A range of critical surface tensions can be determined if a series of liquids are used.

When the range of values of γ_c is plotted against

γ_{lv} of the testing liquids, a scatter of points is obtained which fall into a rough curve. If a curve is then drawn to just encompass all the data points, the maxima of the curve is equivalent to γ_s. (The following reasoning is used; the maximum value Φ can take is 1, which occurs when the intermolecular forces of the two phases are identical and π_e is small (Good, 1967, Wu, 1973). Then, if $\theta >> 0$, equation 3.2.66 becomes; $\gamma_c = \gamma_s - \pi_e = \gamma_s$).

3.3. Results.

Surface energy values for the three model surfaces used in chapter 2 have been calculated from the contact angles measured with various liquids on the model surfaces, using the Wilhelmy plate technique.

Both the geometric mean and harmonic mean approaches have been used, along with the Neumann equation of state approach. Values for surface energy from the equation of state approach have been calculated by use of a simple computer program described by Taylor, 1984.

The van Oss theory of nonadditive surface tension parameters has also been applied. The results are presented in tables 3.3.3 to 3.3.12.

Table 3.3.1 Surface tension components and % polarity for various liquids.

Liquid	γ_l	γ_l^p	γ_l^d	% Polarity
Water	72.8	45.8	27.0	63
Glycerol	60.2	29.2	31.0	51
Ethanediol	48.8	20.3	28.5	42
Propanediol	35.5	5.9	29.6	17
Diiodomethane	50.1	0	50.1	0

Table 3.3.2 θ and cos θ from the *Wilhelmy plate* technique

Liquid	Surface	Cos θ	θ
Glycerol	HPMC	0.2672 ± 0.0048	74.5° ± 0.3°
	PVP	0.3891 ± 0.0082	67.1° ± 0.5°
	CTMS	0.1461 ± 0.0022	81.6° ± 0.1°
Ethanediol	HPMC	0.4617 ± 0.0042	62.5° ± 0.3°
	PVP	0.5592 ± 0.0106	56.0° ± 0.7°
	CTMS	0.3173 ± 0.0048	71.5° ± 0.3°
Propanediol	HPMC	0.6972 ± 0.0112	45.8° ± 0.9°
	PVP	0.7254 ± 0.0131	43.5° ± 1.1°
	CTMS	0.5962 ± 0.0119	53.4° ± 0.8°
Diiodomethane	HPMC	0.6468 ± 0.0110	49.7° ± 0.8°
	PVP	0.7649 ± 0.0145	40.1° ± 1.3°
	CTMS	0.1650 ± 0.0026	80.5° ± 0.2°
Water	HPMC	0.0326 ± 0.0055	88.1° ± 0.3°
	PVP	****	****
	CTMS	0.0467 ± 0.0083	87.3° ± 0.5°

**** not determined due to excessive solubility

Table 3.3.3 Solid Surface energy for **HPMC** derived using the **Harmonic mean** Equation with 4 liquids.

Liquid pair	Surface energy (mNm^{-1})		
	γ_s	γ_s^p	γ_s^d
Water/Diiodomethane	38.86	3.83	35.03
Glycerol/Diiodomethane	37.92	2.89	35.03
Ethanediol/Diiodomethane	37.40	2.37	35.03
Propanediol/Diiodomethane	30.70	0.0	30.70
Water/Glycerol	30.14	7.62	22.52
Water/Ethanediol	28.72	8.70	20.02
Water/Propanediol	28.05	9.32	18.73
Glycerol/Ethanediol	28.17	11.36	16.81
Glycerol/Propanediol	28.76	9.66	19.09
Ethanediol/Propanediol	27.88	8.32	19.57

Table 3.3.4 Solid Surface energy for **HPMC** derived using the **Geometric mean** Equation with 4 liquids.

Liquid pair	Surface energy (mNm^{-1})		
	γ_s	γ_s^p	γ_s^d
Glycerol/Diiodomethane	35.05	1.12	33.93
Ethanediol/Diiodomethane	34.18	0.25	33.93
Propanediol/Diiodomethane	34.69	0.76	33.93
Glycerol/Ethanediol	26.16	5.83	20.33
Glycerol/Propanediol	25.94	6.11	19.83
Ethanediol/Propanediol	26.02	6.41	19.61

Table 3.3.5 Solid Surface energy for **PVP** derived using the **Harmonic mean** Equation with 4 liquids.

Liquid pair	Surface energy (mNm^{-1})		
	γ_s	γ_s^p	γ_s^d
Glycerol/Diiodomethane	43.55	4.02	39.52
Ethanediol/Diiodomethane	42.32	2.80	39.52
Propanediol/Diiodomethane	31.76	0.00	31.76
Glycerol/Ethanediol	32.05	14.98	17.07
Glycerol/Propanediol	32.25	13.45	18.80
Ethanediol/Propanediol	31.13	12.03	19.11

Table 3.3.6 Solid Surface energy for **PVP** derived using the **Geometric mean** Equation with 4 liquids.

Liquid pair	Surface energy (mNm^{-1})		
	γ_s	γ_s^p	γ_s^d
Glycerol/Diiodomethane	40.68	1.71	38.97
Ethanediol/Diiodomethane	39.21	0.24	38.97
Propanediol/Diiodomethane	41.76	2.79	38.97
Glycerol/Ethanediol	29.47	10.82	18.65
Glycerol/Propanediol	29.19	12.15	17.04
Ethanediol/Propanediol	19.96	13.59	16.34

Table 3.3.7 Solid Surface energy for **CTMS** derived using the **Harmonic mean** Equation with 4 liquids.

Liquid pair	Surface energy (mNm^{-1})		
	γ_s	γ_s^p	γ_s^d
Water/Diiodomethane	29.41	8.84	20.57
Glycerol/Diiodomethane	26.44	5.87	20.57
Ethanediol/Diiodomethane	24.73	4.17	20.57
Propanediol/Diiodomethane	23.61	3.04	20.57
Water/Glycerol	26.10	19.20	6.90
Water/Ethanediol	25.79	16.76	9.03
Water/Propanediol	27.11	11.30	15.81
Glycerol/Ethanediol	24.24	10.64	13.60
Glycerol/Propanediol	25.16	7.65	17.51
Ethanediol/Propanediol	27.03	10.41	16.62

Table 3.3.8 Solid Surface energy for **CTMS** derived using the **Geometric mean** Equation with 4 liquids.

Liquid pair	Surface energy (mNm^{-1})		
	γ_s	γ_s^p	γ_s^d
Glycerol/Diiodomethane	21.55	4.58	16.98
Ethanediol/Diiodomethane	21.36	4.38	16.98
Propanediol/Diiodomethane	23.18	6.20	16.98
Glycerol/Ethanediol	21.16	5.08	16.08
Glycerol/Propanediol	22.64	3.54	19.09
Ethanediol/Propanediol	22.74	2.26	20.47

Table 3.3.9 Solid surface energy for **HPMC** derived using the **Neumann equation of state.**

Liquid	Surface energy data (mNm^{-1})	
	γ_{sv}	γ_{sl}
Glycerol	29.4	13.3
Ethanediol	27.9	5.6
Propanediol	26.0	1.3
Diiodomethane	35.3	2.9

Table 3.3.10 Solid surface energy for **CTMS** derived using the **Neumann equation of state.**

Liquid	Surface energy data (mNm^{-1})	
	γ_{sv}	γ_{sl}
Glycerol	25.6	16.8
Ethanediol	23.7	8.3
Propanediol	23.3	2.1
Diiodomethane	20.4	12.2

Table 3.3.11 Solid surface energy for **PVP** derived using the **Neumann equation of state.**

Liquid	Surface energy data (mNm^{-1})	
	γ_{sv}	γ_{sl}
Glycerol	33.4	10.0
Ethanediol	31.0	4.0
Propanediol	26.8	1.0
Diiodomethane	39.7	1.4

Table 3.3.12 Components of surface energy for HPMC, PVP and CTMS, calculated by the van Oss theory of nonadditive surface tension components approach, (mN/m).

Solid	γ^{LW}	γ_s^+	γ_s^-	γ^{AB}	γ_s
HPMC	33.9	0.1	3.0	1.2	35.1
CTMS	17.0	0.7	5.8	4.0	21.0
PVP	39.0	0.0	12.0	0.4	39.4

3.4. Discussion.

The extensive array of methods by which surface energy values may be calculated from contact angles demonstrates both the lack of absolute knowledge associated with interfacial interactions and the avid interest in the subject.

An accurate understanding of interfacial interactions, coupled with a quantitative measure of their extent, would facilitate the prediction of the outcome of interfacial events in a multitude of applications.

Among these, pharmaceutical formulation is an ideal candidate for the application of quantified surface energies, because of the limitless potential for interfacial interactions in pharmaceutical formulations.

A rationalisation of the formulation process, through an appreciation of the possible extent of interfacial interactions, has the potential to save both time and money.

Debate still rages, however, as to the most accurate method of surface energy determination, with many questions recurring; what is the range of application of each technique?; is the choice of liquid pair important?; is a value of solid surface energy truly meaningful/applicable?

The methods investigated in this section cover the spectrum of those available, the case for each convincingly argued by their respective creators. It is

clear from tables 3.3.3 - 3.3.12, however, that significant differences do exist.

The results generated by the geometric mean and harmonic mean approaches are generally in good agreement (tables 3.3.3 - 3.3.8). Both approaches require the use of a liquid pair, the influence of which is illustrated in tables 3.3.3 - 3.3.8, for the three model surfaces studied. Although the values generated by both methods for γ_s and γ_s^d are in reasonable agreement, there appears to be a large discrepancy between the values of γ_s^p generated.

3.4.1. Choice of liquid pair.

Theoretically, any liquid pair should yield the same surface energy values for any particular solid surface, provided the solid surface energy does not change and the surface energies of the liquids are well characterised.

Tables 3.3.3 - 3.3.8 suggest that this does not happen despite the fact that the solid surfaces are identical and the liquids used are historically well characterised and established. The results generated for the CTMS surface are far more consistent through the range of liquid pairs than are the results for the two polymer systems. This may suggest that some degree of rearrangement of the polymers on the solid surfaces is occuring in response to each particular liquid system. i.e. the nature of the surface is changing and is therefore not necessarily identical for different

liquids.

Another possibility is that localised reorientation of the liquid molecules is occuring at the interface to produce a configuration of minimum surface energy for the system. This would imply that the liquid surface energy is variable and hence the ratio of the components of surface energy for a particular liquid may differ for different solid materials. In the case of a low energy solid such as CTMS, the induction of a change in molecular ordering of the liquid molecules would be expected to be less, explaining the more consistent surface energy values generated.

If the results for the CTMS surface are considered (which are relatively consistent) and specifically those results from the liquid pairs which include diiodomethane, the dispersion term generated by the harmonic mean equation is identical, as it is when using the geometric mean equation. The polar term, however, is variable.

The size of the polar term is directly related to the polarity of the probe liquid; as the polarity of the probe liquid increases, so does the calculated polarity of the CTMS. For example, from table 3.3.7, the liquid pair water/diiodomethane predicts a solid surface polarity of 8.84 mN/m, in contrast to the figure of 3.04 mN/m predicted by the liquid pair propanediol/diiodomethane. Water and propanediol have polar components of surface energy of 45.8 and 5.9 mN/m respectively (see table 3.3.1).

The same is also true for the values obtained for HPMC and PVP using liquid pairs including diiodomethane. The use of liquid pairs not including diiodomethane leads to a reduction in the predicted value of the dispersion component of solid surface energy, and a corresponding increase in the polar component.

An explanation for this can be derived by considering the equations used to produce a harmonic or geometric mean. The harmonic mean for two values A and B is given by;

$$\frac{2AB}{A+B}$$

the corresponding geometric mean for A and B is given by;

$$(AB)^{\frac{1}{2}}$$

Both equations, although producing different values (unless A=B), weight the mean towards the lowest component (be it A or B).

The implications of this are that if a liquid pair involving diiodomethane is used, which essentially 'pins down' the value of γ_s^d (since polar terms are eliminated) then the estimated value of γ_s^p is entirely reliant on the polar component of the liquid surface energy. If the polar component of the liquid surface energy is low and not similar to the polar component of the solid surface energy, then the mean term (either harmonic or geometric) will be weighted towards this and potentially

produce artificially low values of γ_s^p.

If, however, the polar component of the liquid surface energy is higher than the polar component of the solid surface energy (which, of course, will not be known when choosing the probe liquid) then the mean term will be closer to the value of solid surface energy component improving the chances of an accurate estimation of this value. When using diiodomethane, therefore, it would be prudent to select an appropriate polar liquid with the highest possible polar component of surface energy. In the case of this study, that liquid would be water.

Of course, the above argument holds just as well for the determination of the dispersion component of solid surface tension. i.e. the use of a liquid with a high dispersion component of surface energy maximises the chances of encompassing the full extent of the solid dispersion component contribution to the interfacial interaction. Diiodomethane obviously fits this description better than any other liquid and has the added advantage of being apolar, which simplifies calculations.

Ideally, the liquid used to probe the dispersion component of the solid surface energy would have a similar dispersion component of surface energy to the solid; similarly for the polar probe. In reality this is not possible since the solid components of surface energy are the very values to be determined. A compromise would therefore be to estimate solid surface

energy with two liquids, one with a high polar component of surface energy and one with a high dispersion component of surface energy, but continue re-estimating with further liquid pairs whose surface energy components were matched to the previously calculated solid surface energy components until the values did not change. i.e. perform a practical iteration with a series of liquid pairs. Obviously this would require an extensive library of appropriate liquids which is not, at least presently, possible.

In the meantime therefore, the most appropriate approach is to use the two most suitable complementary liquids, one having the highest possible dispersion component and the other the highest possible polar component of surface energy.

3.4.2. The equation of state approach

The equation of state values (tables 3.3.9 - 3.3.11) for γ_s are, at first glance, of the same order of magnitude as the corresponding values generated by the geometric and harmonic mean approaches. Large differences exist, however, between results generated using different liquids, particularly those generated using diiodomethane. Again the values of solid surface energy produced for CTMS are in better agreement than those for PVP and HPMC.

The existence of an equation of state would imply, through thermodynamic arguments, that solid/liquid interfacial tension is only a function of the total

solid and liquid surface tensions. This directly opposes the Fowkes (1964) approach which is based on the premise that the solid/liquid interfacial tension involves the types and relative magnitudes of the intermolecular forces present in each phase.

As such, less variation should be expected between the results from the equation of state method than from the other approaches. Unless the differences seen are due to liquid molecule reorientation at the interface and three phase boundary, resulting in a change in the liquid surface tension, or rearrangement of the long-chain HPMC or PVP molecules on the solid surface, then the equation of state approach appears to fail.

The larger values of γ_s produced from diiodomethane data, a purely nonpolar liquid, also suggest that the equation of state is inappropriate, and unable to cope with extreme situations.

However, Spelt et al.(1986), Spelt (1990) and Moy and Neumann (1990) have performed various empirical tests of both approaches and reported that the equation of state approach described their findings most satisfactorily. The theory of surface tension components was concluded to have "a basic deficiency" (Spelt et al., 1986).

The theory of surface tension components has also been criticised by Good (1979), since anomalies arise in the Owens and Wendt and Kaeble approaches (Good, 1979), in that polarities can be detected which are theoretically too low to be detected using contact angle

based methods. Good (1979) suggested that this may be due not only to errors in measuring θ, but also the division of the total surface tension terms into only two components, γ_s^d and γ_s^p. The polar component, γ_s^p, often envelops a multitude of different interactions, which are greatly simplified when combined in a single term.

Fowkes (1990) went even further to say that the premise that interfacial polar interactions are a function of the individual internal polar interactions of each phase is entirely erroneous. Instead, Fowkes now supports the van Oss (1987) approach which treats all polar interactions as acid-base in nature. Consequently, interactions only occur between acidic and basic sites, and Fowkes (1990) concluded that the use of a geometric or harmonic mean approach in an attempt to determine polar interactions is, in fact, futile.

Fowkes et al. (1990) have rigorously tested Neumann's equation of state approach and the theories of Owens and Wendt (1969) and Kaeble (1969, 1971) and Wu (1971) empirically, using model liquid/liquid interfaces and reported the failure of every approach when used to attempt to predict interfacial interactions.

3.4.3. The van Oss approach.

Van Oss has extensively tested his theories of surface tension with real systems such as the solubility of polymers and biopolymers (1989) and adhesion of biopolymers to low energy surfaces (1985), with a

reasonable degree of success. Such an empirical approach is ultimately inexact but inevitably provides the best insight into the range of applicability of a particular technique.

The van Oss approach of Bronsted-Lewis acid-base concepts requires data from three different liquids, one nonpolar, in order to calculate surface energy components. At present only enough information is known about diiodomethane, water and glycerol to allow surface energy components to be determined with these three liquids. The effect therefore of using different combinations of liquids is unknown.

It is also not possible to characterise interfacial interactions between solids and liquids (other than water and glycerol) at present.

The basis of the van Oss approach is that the polar component of surface tension can be further divided into electron donor (γ_s^-, Lewis base) and electron acceptor (γ_s^+, Lewis acid) contributions, which are asymmetrical and therefore nonadditive. i.e.;

$$\gamma^P = 2.(\gamma^{P+} \gamma^{P-})^{1/2}$$

This leads to some interesting situations. For example, PVP has a strong γ^{P-} influence but a negligible γ^{P+} influence. Overall therefore, the polar component of the surface energy of PVP is almost zero. However, PVP is potentially capable of a stronger 'polar' interaction

(with a material of high γ^{P+}) than either HPMC or CTMS.

Using this approach, some materials generally accepted as nonpolar have been shown by Odidi (1990) to have a finite degree of polarity. Examples are magnesium stearate, stearic acid and calcium stearate. Similarly, van Oss et al (1987) detected trace polar interactions from diiodomethane, α-bromonaphthalene and dimethylsulphoxide.

3.5 Conclusions

The values for solid surface energy, γ_s, generated by the four methods studied for the three model surfaces are in reasonably good agreement.

The decomposition of the solid surface energy into components when applying the harmonic mean and geometric mean approaches, however, produces variable results both inter- and intra-method.

The value obtained for γ_s^p is dependent upon the polarity of the probe liquid with which the contact angle is measured. The size of the polar term determined for the solid surface increases as the magnitude of the polar component of the probe liquid increases.

When determining components of solid surface energy by the geometric mean or harmonic mean approach, therefore, it is advisable to use a nonpolar liquid of high surface tension along with a polar liquid of high surface tension as the probe liquid pair.

The values generated by the equation of state approach are not consistent for a range of liquids, and the equation of state therefore appears to be inadequate.

The van Oss theory of nonadditive surface tension components requires further development in order that a wider range of liquids than presently available can be applied. Interesting situations do however arise when applying this theory, such as the existence of monopolar compounds.

In the next chapter, the harmonic mean approach and the van Oss approach have been employed to estimate the surface energy of some pharmaceutical powders. The ability of each technique to predict the outcome of various interfacial phenomena has then been investigated.

Chapter 4

The stability of pharmaceutical nonaqueous, nonpolar suspensions.

4.1. Suspensions

By definition, a suspension consists of an insoluble solid or liquid suspended in a solid, liquid or gas. The most prevalent type of suspension consists of a solid in a liquid, and such systems are classified according to the mean diameter of the suspended particles. Three classes of suspension have been defined in this way (Weiser, 1949), namely molecular dispersions, colloidal dispersions and coarse dispersions. The limiting sizes for each class are necessarily arbitrary and overlap can readily occur. Commonly used values are; less than 1 nanometer (nm) for a molecular dispersion, between 1nm and 0.5μm for a colloidal dispersion and greater than 0.5μm in the case of a coarse dispersion (Martin et al, 1983).

Pharmaceutical suspensions generally fall into the third class i.e. coarse dispersions, and despite the problems associated with liquid products (e.g. bulkiness, susceptibility to microbial contamination), can offer a number of advantages as a dosage form. A suspension provides a means by which drugs that are insoluble in all acceptable solvents may be administered. A liquid dose is easier to swallow than a solid dose which may be a consideration for young or elderly patients, as may the taste masking properties of a suspension. Improved bioavailability is usually seen with a suspension of drug (compared to a tablet formulation), although the prolonged release of a drug administered in suspension can be achieved when

administered intra-muscularly (e.g. zinc insulin).

Nevertheless, suspensions are a rarely formulated dosage form, posing many problems for the formulator (Zatz, 1985). A case in which there is often no alternative to the use of a suspension of drug, however, is that of the metered dose inhaler. Metered dose inhalers consist of a suspension of drug particles in a chlorofluorocarbon (CFC) propellant and, as with all suspensions, are a challenge to formulate, since the drug and propellant have the potential to interact. This process, which creates both formulation and stability problems is not clearly understood. In this chapter, various interactions present in nonaqueous, nonpolar suspensions will be considered in terms of surface and interfacial energies, with the aim of identifying some of the factors responsible for the stability of these suspensions.

4.2. Metered dose inhalers.

The use of aerosols as pharmaceutical delivery systems began in the 1950's, with the development of oral and topical products. Since then, a wide variety of uses for aerosols as pharmaceutical delivery systems have been developed. Examples include intra-nasal devices, foam systems of various kinds, solution and suspension systems and the continuing use of oral and topical products. One of the most successful uses of aerosol systems pharmaceutically has been the metered dose inhaler, designed to deliver drug directly to the

lungs. Inhalation aerosols provide a valuable method of introducing a drug substance to the lung for disease states such as asthma by offering several advantages over other routes of administration (Lieberman et al., 1989), including;

1. rapid onset of therapeutic action,
2. protection of the drug from degradation in the GI tract,
3. avoidance of first pass metabolism,
4. minimises side effects for potent drugs.

Other pharmaceutically important advantages offered by MDI's include the ability to remove a dose without risk of contaminating the remaining material and the enhanced stability for substances adversely affected by oxygen and/or moisture.

4.2.1. Particle size of suspended solids.

The size of the suspended solids in metered dose inhalers is a major formulation consideration.

The site of deposition of particles within the respiratory tract depends upon the size, shape and density of the aerosol particles. A term known as the aerodynamic diameter (D_A) of the aerosol particles encompasses all three variables. The aerodynamic diameter is defined as the diameter of a sphere of unit density (1 kg dm^{-3}) which has the same terminal settling

velocity as the particle in question.

As a rule of thumb, however, in order for particles to penetrate the lower airways of the lungs, it is necessary for the particles to be less than 5μm in diameter. Larger particles impact on the upper respiratory tract and throat. Particles less than approximately 2μm, however, are exhaled, dictating that the particle size distribution of the suspended solids must be tightly controlled.

Obviously, therefore, any increase in particle size after manufacture, through crystal growth or aggregation, can seriously compromise dose uniformity.

Kanig and Cohn (1962) identified particle size as one of the most important factors determining the stability of metered dose inhaler formulations, relating the reduction in particle size necessary for these formulations with a corresponding increase in surface area and consequently surface free energy.

Later in this chapter, the surface energy of various solids will be related to their stability in a nonaqueous, nonpolar environment.

4.3. Aerosol propellants.

The metered dose inhaler generally consists of a suspension of fine drug particles in chlorofluorocarbon (CFC) propellants. At present, all aerosol products designed to deliver drug to the lung contain CFC's as the propellant. CFC's have been used as propellants in

aerosols since the second world war, prior to which they were used only in the refrigeration and air conditioning industries. Other propellants currently in use include compressed gasses such as nitrogen, carbon dioxide and nitrous oxide. Hydrocarbons such as butane, isobutane and propane can also be used as propellants, however, these are not used for pharmaceutical aerosols.

The most commonly used CFC's are trichlorofluoromethane, dichlorodifluoromethane and dichlorotetrafluoroethane. The "fluorocarbon" propellants are more commonly referred to by their tradename followed by a number. The numbering system for fluorinated compounds, developed by Du Pont, follows seven rules (Sanders, 1979);

RULE 1 The number of fluorine atoms in the compound is signified by the right hand digit.

RULE 2 The second digit from the right signifies the number of hydrogen atoms in the compound, plus 1.

RULE 3 The third digit from the right signifies the number of carbon atoms in the compound, minus 1. If this value is equal to zero, it is omitted.

RULE 4 The number of chlorine atoms in the compound can be derived by subtracting the sum of the fluorine and hydrogen atoms from the number of atoms that can be connected to carbon.

RULE 5 In the case of isomers, the degree of asymmetry is indicated by the suffixes a,b,c etc. in order of ascending asymmetry. The most symmetrical isomer is indicated by the number alone.

RULE 6 Cyclic compounds are identified by using the letter C followed by a dash before the compound number.

RULE 7 The number 1 is included in the identifying number, fourth from right, if the compound is unsaturated.

Hence trichlorofluoromethane (CCl_3F) is fluorocarbon number 11, dichlorodifluoromethane (CCl_2F_2) is fluorocarbon number 12 and dichlorotetrafluoroethane ($CClF_2CClF_2$) becomes fluorocarbon number 114.

4.4. Problems associated with nonaqueous suspensions.

One of the most common problems with this type of system is the physical instability of the system, which can cause formulation difficulties. Caking, agglomeration, particle-size growth, clogging of the valve and adhesion of the drug to the container wall are all potentially possible, and all may result in a loss of drug available to the patient.

The potential importance of solid surface energy was noted by Kanig and Cohn (1962) who identified several problems associated with the suspension of powders in chlorofluorocarbons (CFC's). The most

significant problem was the agglomeration of particles, since the agglomeration of particles can result in clogging of valves and crucially, loss of dose uniformity (Ranucci et al, 1990). The rate and extent of agglomeration was seen to be accelerated by storage at elevated temperatures.

Kanig and Cohn (1962) proposed that four major factors affect particulate stability; the initial particle size of the suspended solids, the moisture content of the system, the relative polarity of the powder and the suspending medium and the relative density of the suspended solid and propellant.

In this chapter, the physical stability of nonaqueous, nonpolar suspensions of a variety of solids of differing surface energy will be assessed and related to estimated surface and interfacial free energies.

Surface free energies for the solids used have been estimated from contact angle determinations with various liquids. Two approaches to surface energy determination from contact angle measurements have been employed for each of the solids.

4.5. Materials and methods.

4.5.1. Liquid media.

Glycerol, ethanediol and double distilled water from an all glass still were used to measure contact angles, giving a range of surface tensions and polarities. Diiodomethane was used as a nonpolar probe liquid.

Trichlorotrifluoroethane (Arcton 113), a model chlorofluorocarbon propellant was used as a suspending medium for the stability studies.

Details of the liquids are given in table 4.5.1.

Table 4.5.1 Details of probe liquids.

Liquid	Source	Grade	Batch
Arcton 113	ICI	----------	17010
Glycerol	Sigma	Sigma grade	30H0793
Diiodomethane	Aldrich	99%	34969
Ethanediol	Sigma	Spectroscopic	03009BW

4.5.1.1. Surface tension measurements.

Many methods of surface tension determination are possible (Padday, 1969). In this study, the Wilhelmy plate method has been used throughout (see Ch.1 section 1.5.1.3.). Instead of the test solid, a thin, flat, rectangular plate of glass is suspended from the microbalance. Since the glass is perfectly wetted by the

test liquids, cos $\theta = 1$, and equation 2.5.1 becomes;

$$f = \gamma_{lv}.p \qquad \text{Eqn.4.5.1}$$

from which γ can be determined.

A thin rectangular piece of filter paper was used instead of the glass slide to determine the surface tension of the nonpolar liquids, which did not wet the glass slide (see Gaines, 1977). This method enables fast, simple and accurate determinations of surface tension to be made. Details of the surface tensions of the liquids used are presented in Table 4.5.2.

Table 4.5.2. Surface tensions of various liquids at 20°C.

Liquid	Surface tension (mN/m)
Glycerol	60.22 ± 0.21
Diiodomethane	50.05 ± 0.11
Water	72.60 ± 0.20
Ethanediol	48.80 ± 0.31
Arcton 113	19.50 ± 0.24

4.5.1.2. Determination of liquid surface energetics.

The surface energies and polarities of the probe liquids and Arcton 113 were assessed by using two probes; a clean glass slide (exhibiting zero contact angle) to measure the surface tension, γ_1, and Parafilm M, a purely nonpolar surface which has been well defined (Zografi and Yalkowsky, 1974, Zografi and Tam, 1976) to enable the dispersion component, γ_1^p, of the surface tension to be calculated.

This is performed by considering the work of adhesion. It has been demonstrated by Fowkes (1964) that the work of adhesion between any two phases, one of which is nonpolar, is given by;

$$W_a^{12} = 2\sqrt{\gamma_1^d \gamma_2^d} \qquad \text{Eqn.4.5.2.}$$

which for a solid/liquid system becomes;

$$W_a^{sl} = 2\sqrt{\gamma_s^d \gamma_1^d} \qquad \text{Eqn.4.5.3.}$$

The work of adhesion between two phases, 1 and 2, may also be defined in terms of surface and interfacial tension (Adamson, 1982);

$$W_a^{12} = \gamma_1 + \gamma_2 - \gamma_{12} \qquad \text{Eqn.4.5.4.}$$

From the Young equation (equation 1.3.1);

$$\gamma_{sl} = \gamma_s - \gamma_1 \cos\theta \qquad \text{Eqn.4.5.5.}$$

which, combined with equation 4.5.4 for a solid/liquid system, produces;

$$W_a^{sl} = \gamma_1 + \gamma_1 \text{Cos}\theta \qquad \text{Eqn.4.5.6.}$$

Therefore by measuring the contact angle between a nonpolar solid of known surface energy and any liquid, the dispersion component of the liquid surface tension can be determined by solving equations 4.5.3 and 4.5.6 simultaneously.

The polarity of the surface can then be determined from equation 4.5.2.;

$$\gamma_1 = \gamma_1^p + \gamma_1^d \qquad \text{Eqn.4.5.2.}$$

For the purposes of this study, the value of γ_s^d for Parafilm M has been taken to be 25.5mN/m (Zografi and Tam, 1986).

The calculated liquid surface energy values are presented in Table 4.5.3.

Table 4.5.3. Surface energy values for various liquids (mNm^{-1})

Liquid	γ_s^p	γ_s^p	γ_s^d
Water	72.6	48.6	24.0
Diiodomethane	50.1	0.0	50.4
Glycerol	60.2	29.2	31.0
Ethanediol	48.8	23.3	25.5
Arcton 113	19.50	0.0	19.50

4.5.2. Solid media

Five powders were chosen to cover a range of surface energies and surface polarities. Although the surface energies and polarities were measured in this study, literature values were used as the basis for choosing the powders (e.g. Lerk et al, 1977, Zografi & Tam, 1976). Four widely used pharmaceutical powders (aspirin, indomethacin, beclomethasone and isoprenaline) were chosen to give a range of polarities from 0 to ~ 50%, along with polytetrafluoroethylene (PTFE) powder which has an extremely low surface energy. Details of the solids are presented in table 4.5.4.

In order to model the formulation of a pharmaceutical metered dose inhaler later in the study as closely as possible, it was necessary for the powder particles to be in the sub-10 micron range (see section 4.2.1). Where necessary, particle size reduction was performed using an air jet mill.

4.5.2.1. Particle size analysis.

The size distributions of the powders were determined using a Malvern instruments particle sizer, series 2600c. All powders were suspended in Arcton 113. Details of the particle size distributions are given in table 4.5.5.

Table 4.5.4. Details of solids.

Solid	Source	Batch
Aspirin crystal	Monsanto	4F624
Indomethacin	Becpharm	890012-750
Isoprenaline	Lilly research	89F01A
Beclomethasone	---------	3401/M1
PTFE	Goodfellow	---------

Table 4.5.5. Initial (primary) particle size for various powders (means of 10 determinations)

Solid	50% undersize (μm)	90% undersize (μm)
Indomethacin	4.67 ± 0.5	7.12 ± 0.7
Isoprenaline	5.19 ± 0.4	10.99 ± 1.0
Aspirin	5.91 ± 0.3	12.01 ± 0.7
PTFE	6.71 ± 0.1	14.0 ± 0.2
Beclomethasone	3.58 ± 0.15	5.93 ± 0.26

4.5.2.2. Manufacture of powder compacts.

The powders were compacted into thin rectangular plates suitable for use as Wilhelmy plates using a custom designed punch and die, illustrated in Figure 4.5.1, of dimensions 7.07mm by 20.0mm.

For each powder, the quantity of powder necessary to produce plates less than 1mm in thickness was determined and consistently used. A compression force was applied such that the surface of the compact was smooth and shiny.

The die was manufactured such that it could be dismantled for ease of cleaning and regular polishing. Rigorous cleaning with 96% ethanol was performed between plate manufacture and those surfaces which came into contact with the powder were thoroughly dried.

4.5.3. Determination of solid surface energetics.

The surface energetics of the powders was assessed by two methods; the harmonic mean approach proposed by Wu (1971), and by applying the theory of nonadditive surface tension components proposed by van Oss (1987).

4.5.3.1. Harmonic mean approach.

The theory behind Wu's (1971) approach to surface energy determination has been presented in Chapter 3, section 3.2.1.2.

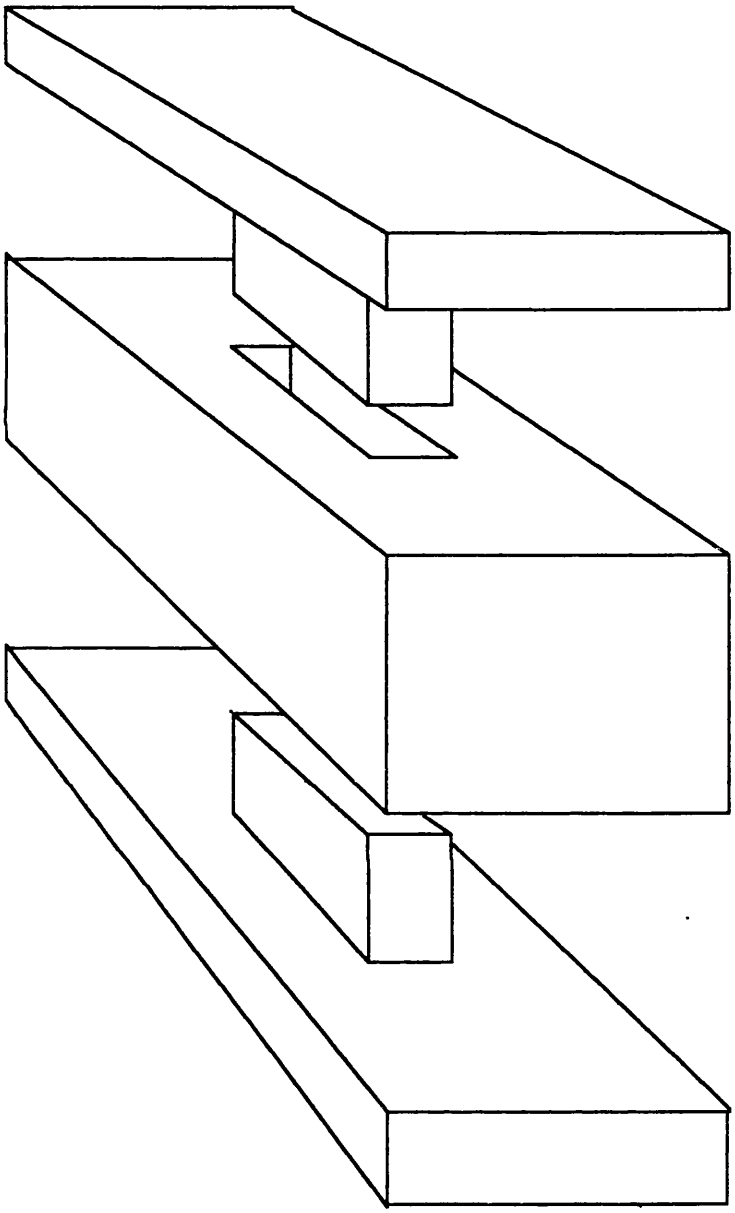

Figure 4.5.1 Diagram of the punch and die assembly used to prepare powder compacts.

In order to be able to determine solid surface energy by the harmonic mean approach, it is necessary to obtain contact angles on the solid of interest with two liquids of known γ_l^d and γ_l^p. The best fit of γ_s^d and γ_s^p can then be determined by computer analysis for the two sets of contact angle data.

4.5.3.2. The van Oss approach.

The van Oss method of surface tension component determination has been described previously, (chapter 3, section 3.2.2.).

In order to apply the theory of nonadditive surface tension components, it is necessary to obtain contact angle measurements with three liquids for a particular powder, one of which must be apolar. In this study, water and glycerol have been used, along with diiodomethane as an apolar probe.

The components of solid surface energy for each of the powders are presented in tables 4.7.1-4.7.6 and table 4.7.16.

4.5.3. Measurement of contact angles.

It was apparent from the results presented in chapter 2 that contact angles generated by the sessile drop and Wilhelmy gravitational technique are comparable, but invariably different from those generated by the liquid penetration technique.

It is also clear from the results presented in

chapter 2, that the three techniques used rank the surfaces studied in the same order of wettability. In the course of the following work, therefore, all contact angle data has been generated by the Wilhemy gravitational technique, despite the potential influence of compaction on the surface energetics of the solids, for the following reasons; firstly, the method is fast, reproducible and convenient in contrast to the two alternative methods. Secondly, the effects of solid solubility in the probe liquid are minimised as the contact time between the solid and liquid is relatively short. Solid solubility can be overcome by use of saturated solutions, however this itself can lead to poor reproducibility of results and inaccurate surface tension determinations.

The problem of solid solubility is most apparent for liquid penetration experiments where the long solid-liquid contact time occurring with real powders can render the method completely unworkable. (The idealised systems used in the previous chapter overcame this problem because of the relatively large size of the particles (diameter by volume ≈ 66μm) compared with the real powders (diameter by volume ≈ 4μm)).

The cosine of the contact angles measured for the various solids used in this study are presented in table 4.5.5., and are means of 10 measurements.

Table 4.5.5. Cosine (contact angle) for various solids with water, diiodomethane, glycerol and ethanediol.

Solid	Cosine θ			
	Water	Diiodo-methane	Glycerol	Ethane-diol
Indomethacin	0.0174	0.9974	0.2622	0.7930
Isoprenaline	0.9200	0.8198	0.6388	0.9397
Aspirin	0.3781	0.8725	0.4428	0.6717
PTFE	-0.5289	0.2990	-0.1924	0.1392
Beclomethasone	0.0181	0.8648	0.2840	0.8106

4.5.5. Application of surface energy data

Once the individual surface energy components of two phases, 1 and 2, are known, it is theoretically possible to predict various interfacial phenomena between phases 1 and 2. The results obtained from the harmonic mean approach require a different treatment to those obtained from van Oss' theory of nonadditive surface tension components.

4.5.5.1. Harmonic mean approach.

Not only can the work of cohesion (Wc) of each phase be determined from harmonic mean surface energy data, but also the work of adhesion between the two phases (Wa) and the spreading coefficients λ_{12} (phase 1 over phase 2) and λ_{21} (phase 2 over phase 1).

Therefore, we have;

$$W_{c_1} = 2\gamma_1 \qquad \text{Eqn.4.5.3.}$$

$$W_{c_2} = 2\gamma_2 \qquad \text{Eqn.4.5.4.}$$

$$W_a = 4\left(\frac{\gamma_1^d \gamma_2^d}{\gamma_1^d + \gamma_2^d} + \frac{\gamma_1^p \gamma_2^p}{\gamma_1^p + \gamma_2^p}\right) \qquad \text{Eqn.4.5.5.}$$

$$\lambda_{12} = W_a - W_{c_1} \qquad \text{Eqn.4.5.6.}$$

$$\lambda_{21} = W_a - W_{c_2} \qquad \text{Eqn.4.5.7.}$$

where γ^d and γ^p denote the nonpolar and polar contributions of the solid surface free energy.

4.5.5.2. Theory of nonadditive surface tension components approach.

The free energy of adhesion between substances 1 and 2 can be expressed in the form of the Dupré equation (1869) (section 3.2.3.2.);

$$W_a^{12} = \gamma_1 + \gamma_2 - \gamma_{12} \qquad \text{Eqn.4.5.8.}$$

The value for the total interfacial tension, γ_{12}, by the theory of nonadditive surface tension components (van Oss, 1987b) is given by;

$$\gamma_{12} = \left(\sqrt{\gamma_1^{LW}} - \sqrt{\gamma_2^{LW}}\right)^2 + 2\left(\sqrt{\gamma_1^{+}\gamma_1^{-}} + \sqrt{\gamma_2^{+}\gamma_2^{-}} - \sqrt{\gamma_1^{+}\gamma_2^{-}} - \sqrt{\gamma_1^{-}\gamma_2^{+}}\right)$$

Eqn.4.5.9.

Substitution of equation 4.5.9. into equation 4.5.8. allows the work of adhesion between substances 1 and 2 to be determined.

The work of cohesion for any substance, 1, is given by;

$$W_c^1 = 2\gamma_1 \qquad \text{Eqn.4.5.10.}$$

The above parameters from both the harmonic mean and theory of nonadditive surface tension components approach have been selectively calculated for various solids and liquids used in this study in an attempt to explain various aspects of the physical instability of nonpolar, nonaqueous suspensions.

4.6. Experimental procedures.

As stated previously, the major problems encountered with nonpolar nonaqueous suspensions are aggregation of particles and adhesion of drug to the container walls. These two parameters, along with the initial ease of dispersion of the powders were assessed in this study. Each of these will be considered in turn below.

4.6.1. General procedures.

All experiments were carried out using 20ml glass scintillation vials to mimic the size and shape of metered dose inhaler canisters. The scintillation vials were fitted with foil lined, plastic screw-cap lids. To minimise contact between the suspensions and the lid, the vials were stored in an upright position. Where storage was necessary as part of an experiment, an incubator set to 25°C was used. The suspensions were not exposed to light on storage.

All scintillation vials were cleaned according to the glassware cleaning procedure used for the liquid penetration tubes in chapter 2, described in section 2.3.2.1, prior to use.

4.6.2. Assessment of ease of dispersion.

In order to assess the ease of dispersion of the powders, suspensions of the powders were prepared in Arcton 113, and the particle size measured by laser light diffraction (Malvern Instruments, 2600c).

Different samples of the suspensions were then sonicated for defined times and then immediately sampled and sized by laser diffraction (Malvern 2600c). The minimum duration of sonication necessary to achieve a suspension of primary sized particles (i.e. the minimum size achievable through sonication) was taken as an indication of the ease of dispersibility of the powder.

4.6.3. Assessment of degree of aggregation.

The extent of particle aggregation was assessed by comparing the initial particle size of the suspended particles with the size measured after storage for three weeks.

A concentration of 10mg of drug in 15ml of Arcton 113 propellant was used. This was found to be a convenient concentration to enable samples of a suitable size to be taken from each vial for particle size analysis. The suspensions were prepared by weighing approximately 10mg of drug into a scintillation vial and adding 15ml of Arcton 113.

Primary sized particles were produced by sonicating the vial containing the suspension until no further change in particle size was detectable by laser light diffraction analysis using a Malvern 2600c apparatus. The possibility of erroneous particle size distributions being produced upon prolonged sonication due to the formation and detachment of slithers of glass was considered, however, the suspensions containing PTFE particles which dispersed spontaneously showed no change

in particle size distribution after prolonged sonication.

4.6.4. Assessment of extent of powder adhesion to container wall.

The extent of adhesion to the container wall was assessed by comparing the weight of the emptied scintillation vial with the weight of the scintillation vial before filling.

In order to evaluate the effect of different containers, container walls with three different surface energies were investigated. A simple cleaned glass surface (i.e. high surface energy), a cleaned glass surface coated with "Repelcoat" (a proprietary waterproofing compound) to impart medium hydrophobicity (i.e. medium surface energy), and a cleaned glass surface coated with octadecyltrichloromethylsilane (ODTCMS) to impart an extremely high degree of hydrophobicity (i.e. low surface energy).

The cleaned/coated scintillation vials were individually labelled and then dried in an oven at 70°C to constant weight. The weight of each vial was recorded before accurately weighing in 10mg of drug/powder and adding 15ml of Arcton 113. At least 10 vials were prepared for each powder system. The suspensions were sonicated for a period of time sufficient to disperse the particles (see section 4.7.1.1) and subsequently stored upright at 25°C for two weeks. After two weeks undisturbed storage, the vials were emptied, rinsed

three times with 10ml aliquots of Arcton 113 and dried to constant weight at 70°C.

The surface energies of the container substrates were measured by both the Wu (1971) harmonic mean approach and the van Oss (1987) nonadditive surface tension component approach.

Contact angles were measured using the Wilhelmy plate technique on glass cover slips treated in an identical manner to the container walls to allow surface energy calculations to be made on each of the substrates. The cosine of the contact angles measured with various liquids are presented in table 4.6.1.

Table 4.6.1. Cosine (contact angle) for various container wall coatings with water, diiodomethane and glycerol.

Solid	Cosine θ		
	Water	Diiodo-methane	Glycerol
Clean glass	1.0	0.7532	1.0
"Repelcoat"	0.5920	0.6205	0.7419
OTCMS	-0.6560	-0.3200	-0.3173

4.7. Results and Discussion.

The surface free energy values of the powders and container wall substrates have been calculated by both the harmonic mean approach outlined in section 4.5.3.1. and the van Oss approach described in section 4.5.3.2.

The harmonic mean results have subsequently been used to calculate the work of cohesion for the powders used and Arcton 113, the work of adhesion between the powders and Arcton 113 and the work of adhesion between the solids and various container wall substrates.

Spreading coefficients for Arcton 113 over each of the powder surfaces have also been calculated.

The data obtained by the van Oss approach have been used to calculate work of cohesion values for the powders, and work of adhesion values for the powders with the container wall.

Values of work of adhesion between the powders and Arcton 113 and spreading coefficients for Arcton 113 over the powders are unobtainable since the surface energy of Arcton 113 cannot be defined by this method.

4.7.1. Application of the Harmonic mean approach.

The results obtained through the harmonic mean approach using different liquid pairs are presented in tables 4.7.1.- 4.7.6. The values obtained are as diverse as seen previously for the model surfaces (Chapter 2). It is apparent from the results that unless one of the liquids is nonpolar, then the surface energy values for at least one of the powder or container wall systems studied are unsolvable. In particular, low energy surfaces appear to be particularly difficult to characterise using two polar liquids. For example, the surface energy values for PTFE and ODTMCS are unsolvable using the water/glycerol liquid pair. Surface energy parameters for PTFE are in fact unsolvable using any two of the polar liquids used in this study as the liquid pair.

In all cases where diiodomethane has been used as one of the liquids in the liquid pair, a value for surface energy has been obtained for all of the systems studied.

For the reasons given in section 3.4.1, the values of surface energy generated by the water/diiodomethane liquid pair have been used to calculate the various interfacial parameters (see section 4.5.6.1.) necessary to attempt to predict the behaviour of the solid in liquid systems being studied.

Table 4.7.1. Surface energy and % polarity for various powders by Harmonic mean calculation. Liquid pair: **Water / Diiodomethane.**

Solid	Surface energy (mN/m)			%Polarity
	γ_s	γ_s^p	γ_s^d	
Indomethacin	50.3	0.4	49.9	0.8
Isoprenaline	72.9	31.1	41.8	42.7
Aspirin	54.3	10.2	44.1	18.8
PTFE	13.3	0	13.3	0
Beclomethasone	45.6	1.9	43.7	4.2
Repelcoat	54.1	20.0	34.1	37.0
ODTMCS	10.2	0	10.2	0
Glass	75.0	36.9	39.1	49.2

Table 4.7.2 Surface energy and % polarity for various powders by Harmonic mean calculation. Liquid pair: **Glycerol / Diiodomethane.**

Solid	Surface energy (mN/m)			%Polarity
	γ_s	γ_s^p	γ_s^d	
Indomethacin	49.1	0	49.1	0
Isoprenaline	50.8	9.0	41.8	17.1
Aspirin	48.8	4.8	44.0	9.8
PTFE	20.0	0	20.0	0
Beclomethasone	45.0	1.3	43.7	2.9
Repelcoat	49.3	15.2	34.1	30.8
ODTMCS	13.1	2.8	10.3	21.4
Glass	61.9	22.9	39.0	37.0

Table 4.7.3 Surface energy and % polarity for various powders by Harmonic mean calculation. Liquid pair: **Water / Glycerol.**

Solid	Surface energy (mN/m)			%Polarity
	γ_s	γ_s^p	γ_s^d	
Indomethacin	37.8	2.8	35.0	7.4
Isoprenaline	138.2	137.6	0.56	99.6
Aspirin	40.1	31.9	8.2	79.6
PTFE	U N S O L V A B L E.			
Beclomethasone	34.5	4.9	29.6	14.2
Repelcoat	48.1	30.1	18.0	62.6
ODTMCS	U N S O L V A B L E.			
Glass	79.9	65.3	14.6	81.7

Table 4.7.4 Surface energy and % polarity for various powders by Harmonic mean calculation. Liquid pair: **Ethanediol/Diiodomethane**

Solid	Surface energy (mN/m)			%Polarity
	γ_s	γ_s^p	γ_s^d	
Indomethacin	54.5	4.6	49.9	8.4
Isoprenaline	51.8	10.0	41.8	19.3
Aspirin	47.7	3.6	44.1	7.5
PTFE	25.8	1.6	24.2	6.2
Beclomethasone	50.1	6.4	43.7	12.8

Table 4.7.5. Surface energy and % polarity for various powders by Harmonic mean calculation. Liquid pair: **Ethanediol / Glycerol.**

Solid	Surface energy (mN/m)			%Polarity
	γ_s	γ_s^p	γ_s^d	
Indomethacin	U N S O L V A B L E.			
Isoprenaline	U N S O L V A B L E.			
Aspirin	36.2	10.3	25.9	28.5
PTFE	U N S O L V A B L E.			
Beclomethasone	U N S O L V A B L E.			

Table 4.7.6 Surface energy and % polarity for various powders by Harmonic mean calculation. Liquid pair: **Water / Ethanediol.**

Solid	Surface energy (mN/m)			%Polarity
	γ_s	γ_s^p	γ_s^d	
Indomethacin	U N S O L V A B L E.			
Isoprenaline	76.6	65.1	11.5	85.0
Aspirin	38.3	24.5	13.8	64.0
PTFE	U N S O L V A B L E.			
Beclomethasone	U N S O L V A B L E.			

In tables 4.7.7., the surface energies and work of cohesion values for various powders are presented. The surface tension and work of cohesion of Arcton 113 is presented in table 4.7.8.

The estimated work of adhesion between the powders and Arcton 113 is presented in table 4.7.9, and the estimated work of adhesion between the various solids and the container wall substrates is presented in table 4.7.10.

In the following three sections of this work, three of the characteristic formulation problems associated with nonaqueous, nonpolar suspensions, (namely the ease of dispersion, degree of aggregation and extent of adhesion of drug to the container wall), will be assessed in terms of the interfacial events involved.

Table 4.7.7. Estimated Surface energy (γ_s) and Work of Cohesion (W_c) for various solids. (Harmonic mean data)

Solid	Surface energy (γ_s) mN/m	Work of Cohesion (W_c) mN/m
Indomethacin	50.3	100.6
Isoprenaline	72.9	145.8
Aspirin	54.3	108.6
PTFE	13.3	26.6
Beclomethasone	45.6	91.2

Table 4.7.8. Surface tension (γ_l) and Work of Cohesion (W_c) for Arcton 113. (Harmonic mean data)

Liquid	Surface tension (γ_l) mN/m	Work of Cohesion (W_c) mN/m
Arcton 113	19.50	39.0

Table 4.7.9. Estimated Work of Adhesion (W_a) between various solids and Arcton 113. (Harmonic mean data)

Solid	Work of Adhesion (W_a)
Indomethacin	56.1
Isoprenaline	53.2
Aspirin	54.1
PTFE	31.6
Beclomethasone	53.9

Table 4.7.10 Estimated Work of Adhesion (W_a) between various solids and container wall substrates.(Harmonic mean data)

Solid	Work of Adhesion (W_a) mN/m		
	Clean Glass	Repelcoat	ODTMCS
Indomethacin	89.3	82.6	34.2
Isoprenaline	148.4	123.8	33.1
Aspirin	114.9	103.9	33.4
PTFE	39.7	38.3	23.1
Beclomethasone	89.8	83.6	33.3

4.7.1.1. The ease of dispersion.

The minimum sonication time required to achieve the primary particle size for each powder is given in table 4.7.11.

In all cases, except PTFE, a reduction in particle size could be obtained by sonicating the suspension, indicating that dispersion was not instantaneous.

The primary size of the powders used are presented in Table 4.7.11., along with the minimum sonication time necessary to achieve these sizes.

Comparisons of the time required to achieve the primary particle size for the suspensions and the surface energy and polarity data revealed that a relationship exists between the work of cohesion of the solids and the sonication time (Figure 4.7.1). From Figure 4.7.1, it can be concluded that the greater the work of cohesion, the harder it will be to disperse the powder in the liquid; this is to be expected, however, and demonstrates that surface energies are of potential value in predicting the behaviour of nonpolar, nonaqueous suspensions.

The process of dispersion is a complex one, however, involving several stages (Bleier, 1983a, 1983b).

The first stage of the dispersion of a powder in a liquid phase is the wetting of the surface of the powder particles and the displacement of air from the interstices of powder clusters. The second stage of

Table 4.7.11 Initial (primary) particle size for various powders (means of 10 determinations), and minimum sonication time necessary to achieve them.

Solid	50% undersize (μm)	90% undersize (μm)	Minimum sonication time /secs
Indomethacin	4.67 ± 0.5	7.12 ± 0.7	75
Isoprenaline	5.19 ± 0.4	10.99 ± 1.0	210
Aspirin	5.91 ± 0.3	12.01 ± 0.7	120
PTFE	6.71 ± 0.1	14.0 ± 0.2	0
Beclomethasone	3.58 ± 0.15	5.93 ± 0.26	60

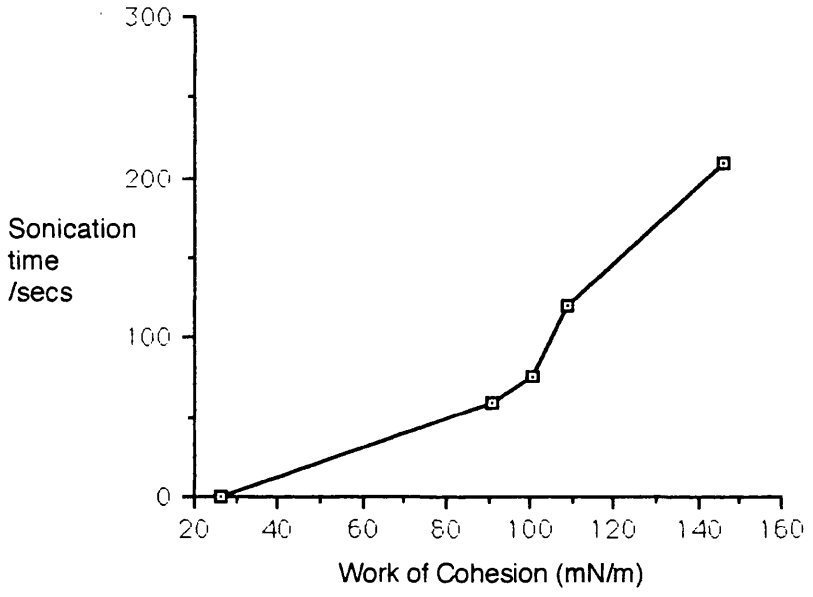

Figure 4.7.1. Sonication time required to disperse various powders as a function of the work of cohesion of the powders.

dispersion involves the breaking of clusters into smaller clusters or primary particles. Finally, it is necessary for the small clusters and primary particles to be dispersed throughout the dispersion medium (Bleier, 1983b).

The dispersibility of a powder is dependent more on the first two stages described above than the third stage, which is related to the powders stability (Bleier, 1983b).

In terms of surface energy parameters, when a liquid spreads over a solid, liquid/liquid interface is lost in favour of liquid/solid interface. Therefore, the "favourability" of a liquid spreading over a solid is given by the spreading coefficient of the liquid over the solid. However there is also a requirement for the individual solid particles to detach from one another, i.e. there is also a loss of work of cohesion in favour of the work of adhesion between the solid and the liquid.

Therefore the ease of dispersion should be related to the difference between the spreading coefficient of the liquid over the solid and the work of cohesion of the solid. i.e. the free energy associated with the dispersion of a solid in a liquid is given by; $W_{aSL}-W_{cL}-W_{cS}$.

It is clear from Figure 4.7.2., in which the sonication time has been plotted against $W_{aSL}-W_{cL}-W_{cS}$, that a clear relationship does exist between them.

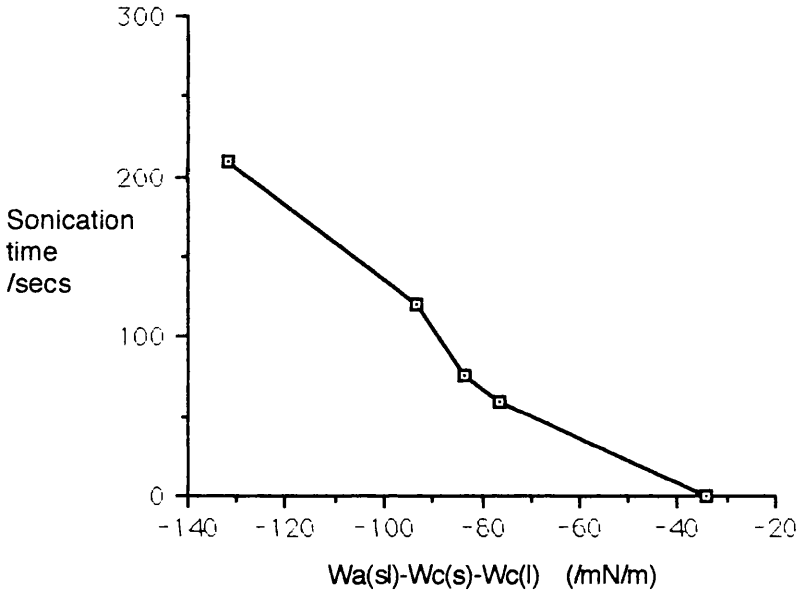

Figure 4.7.2. Sonication time required to disperse various powders as a function of Wa(sl)-Wc(s)-Wc(l)

4.7.1.2. Degree of aggregation.

The extent of aggregation has been assessed by monitoring changes in particle size, and recording the percent change in particle size over the initial, primary particle size after storage for varying lengths of time.

Initial investigations revealed that the increase in particle size reached a plateau after approximately one week. All suspensions were therefore stored for two weeks to ensure that aggregation was as complete as possible. The percentage increase in median particle size for the powders is presented in table 4.7.12.

Table 4.7.12 Initial median particle size for various powders (means of 10 determinations), and median particle size after 2 weeks storage.

Solid	50% undersize (μm). (Initial)	50% undersize (μm) (Final)	% increase in particle size.
Indomethacin	4.67 ± 0.5	5.98 ± 1.2	28
Isoprenaline	5.19 ± 0.4	10.12 ± 1.4	95
Aspirin	5.91 ± 0.3	10.87 ± 1.3	84
PTFE	6.71 ± 0.1	6.76 ± 0.2	0
Beclomethasone	3.58 ± 0.15	5.55 ± 0.8	55

No correlation is seen between either λ_{sl} (spreading coefficient for solid over liquid) or λ_{ls} (spreading

coefficient for liquid over solid) and the degree of aggregation. Neither can a relationship be seen with Wc or Wa.

The energy changes involved in the aggregation of solid particles suspended in a liquid are illustrated in figure 4.7.3.

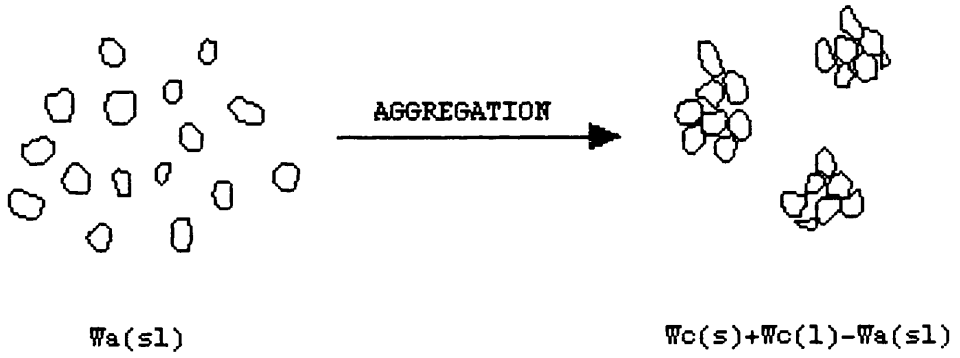

Figure 4.7.3 The process of aggregation of solid particles suspended in a liquid.

By considering the process of aggregation in terms of the changes in interfacial energies, it is expected that the extent of aggregation should be related to the difference between the sum of the work of cohesion of the solid (Wc(s)) and the work of cohesion of the liquid (Wc(l)), and the work of adhesion of the solid and liquid, i.e. Wc(s)+Wc(l)-Wa(sl).

The percentage increase in median diameter has been plotted against Wc(s)+Wc(l)-Wa(sl) in figure 4.7.4.

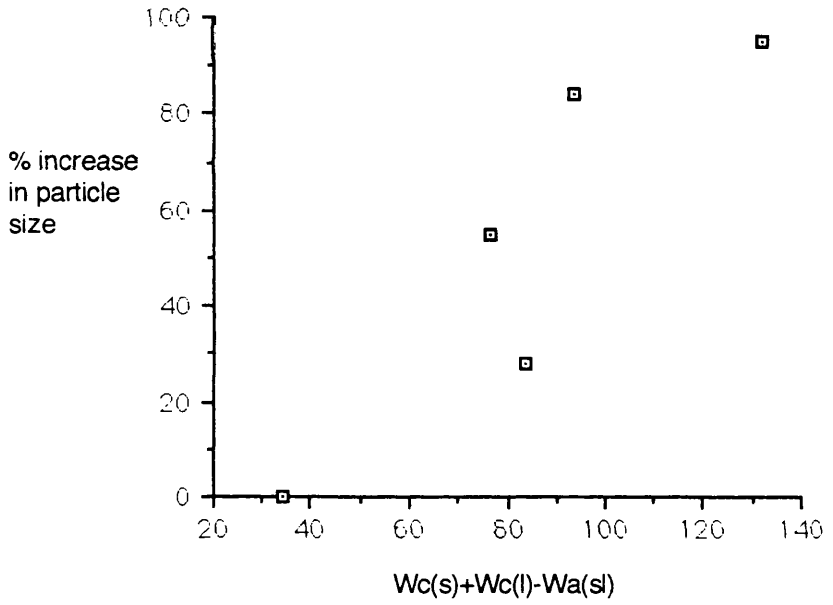

Figure 4.7.4. % increase in particle size of suspended solids as a function of Wc(s)+Wc(l)-Wa(sl).

It is clear from figure 4.7.4, however, that no correlation is readily apparent.

A relationship can be seen, however between the % increase in median particle size and the polarity of the solid surface (Figure 4.7.5).

The polarity of the powders ranges from 0% (PTFE, which does not aggregate) to 42.7% (isoprenaline which aggregates substantially). Thus for suspensions in a completely nonpolar liquid, the tendency to aggregate can be predicted on the basis of the polarity of the solid, and is unrelated to the surface energy of the liquid. Kanig and Cohn (1962) predicted that the relative polarity of the powder and the suspending medium will have an influence on the agglomeration of powders in suspension, suggesting that "the greater the difference in polarity between the powder and the liquid, the more difficult it is for the liquid to wet the surface of the solids and the greater the tendency for moisture to cause agglomeration".

While it is not necessarily the case that the larger the difference in polarity, the more difficult it is for the liquid to wet the surface of the solid, it is certainly the case that the extent of aggregation is related to the polarity of the powder. Since any water present in an essentially nonaqueous, nonpolar environment, will associate with polar components of the system, (for example the suspended solid or container wall) the problem of aggregation is likely to be

compounded for polar solids.

The extent of aggregation in nonaqueous nonpolar suspensions appears to be independent of the nonpolar liquid, and strongly dependent on the polarity of the solid. It therefore follows that manipulation of the solid surface by for example different milling or different crystallisation methods, with a subsequent effect on the solid surface polarity will have an effect on the physical stability of these suspensions.

Buckton et al. (1988) have shown that different milling techniques can produce powders with different surface energies. The tendency to aggregate is therefore likely to be highly dependent on powder processing history, changes in crystal morphology, and any other changes in the surface energy of the powder that occur with age.

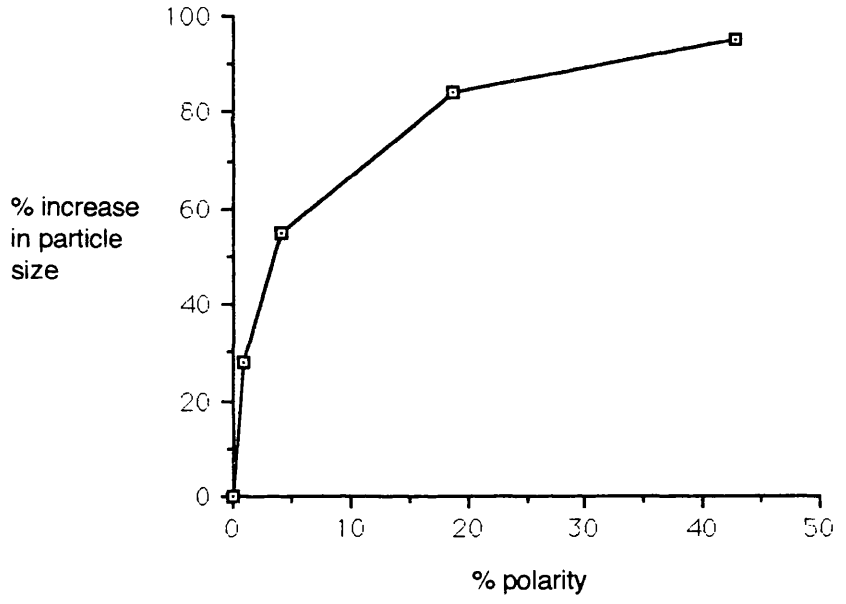

Figure 4.7.5 % increase in median particle size of various powders suspended in Arcton 113 as a function of powder polarity.

4.7.1.3. Extent of adhesion to the container wall.

The quantity of powder adhering to the container wall substrates varied considerably, depending upon the powder/substrate system (see tables 4.7.13.- 4.7.15.). For example, 3.21 ± 0.60mg Isoprenaline adhered to the clean glass container wall, while 0.06 ± 0.08mg PTFE adhered to the same surface.

The most obvious surface energy parameter to consider when assessing the extent of adhesion, is the work of adhesion, Wa. Figure 4.7.6 illustrates the relationship seen between the quantity of powder adhering to a clean glass surface and the work of adhesion between the powder and glass.

When the glass container is coated in order to change its surface energy and polarity, the amount of drug adhering is seen to change (tables 4.7.13.- 4.7.15). Coating with "repelcoat" yields a surface with a lower surface energy and polarity than glass (table 4.7.1.), and thus the calculated works of adhesion between the solids and repelcoated surface are lower.

A similar relationship can be seen for the adhesion of powders to a "repelcoat" coated container (figure 4.7.8.) to that seen for the glass wall, despite the fact that the the quantity of drug adhering is much lower.

Table 4.7.13. Extent of various powder particle adhesion to a clean glass container wall.

Solid	No. samples	mean weight gain, /mg	standard deviation
Indomethacin	20	0.33	0.10
Isoprenaline	20	3.21	0.60
Aspirin	20	1.04	0.24
PTFE	20	0.06	0.08
Beclomethasone	20	0.41	0.22

Table 4.7.14. Extent of various powder particle adhesion to a "Repelcoat" coated container wall.

Solid	No. samples	mean weight gain, /mg	standard deviation
Indomethacin	10	0.08	0.09
Isoprenaline	10	1.20	0.24
Aspirin	10	0.41	0.25
PTFE	10	0.01	0.08
Beclomethasone	10	0.08	0.04

Table 4.7.15. Extent of various powder particle adhesion to a ODTMCS coated container wall.

Solid	No. samples	mean weight gain, /mg	standard deviation
Indomethacin	10	0.00	0.11
Isoprenaline	10	0.16	0.09
Aspirin	10	-0.03	0.08
PTFE	10	0.05	0.06
Beclomethasone	10	0.06	0.10

The use of ODTMCS as a wall substrate reduces to zero the quantity of any of the powders adhering to the container wall (table 4.7.15). The ODTMCS surface has zero polarity and a very low surface energy (table 4.7.1), and consequently the values of W_a obtained for the drugs onto this surface are also very low. The resultant difference between W_a(powder/ODTMCS) and W_a(powder/Arcton 113) is negative in all cases. Consequently, it is not surprising that (within experimental error), no adhesion of particles was detected for the ODTMCS coated glass.

It is also worth considering, the perhaps more appropriate difference between the work of adhesion between the powder particles and Arcton 113, and the work of adhesion between the powder particles and the container wall substrate. These values have been calculated and the relationship between them and the extent of adhesion of the powders to clean glass and "repelcoat" surfaces is illustrated in figures 4.7.7. and 4.7.9. respectively. An approximately exponential relationship is seen, which passes through the origin. It is reasonable to conclude from this therefore that adhesion to the glass / "repelcoat" coated container walls will occur if W_a between the wall and the powder is greater than W_a between the powder and Arcton 113.

Further, if all of the data concerning adhesion to the container wall is compared (figures 4.7.10 and 4.7.11.), it is clear that a strong relationship exists between the quantity of powder adhering to the container

wall and the work of adhesion between the powder and the wall, independent of the wall coating.

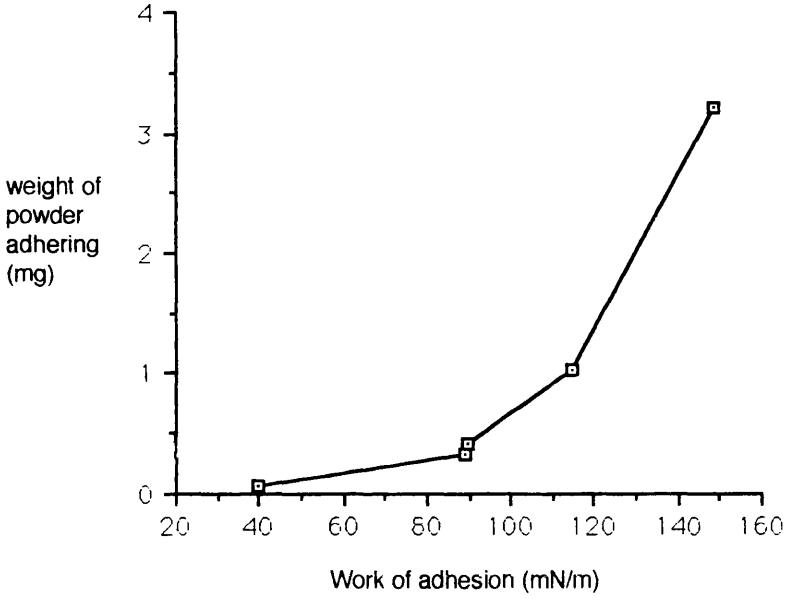

Figure 4.7.6. The extent of powder adhesion to a clean glass container wall as a function of the calculated work of adhesion between the powder and glass.

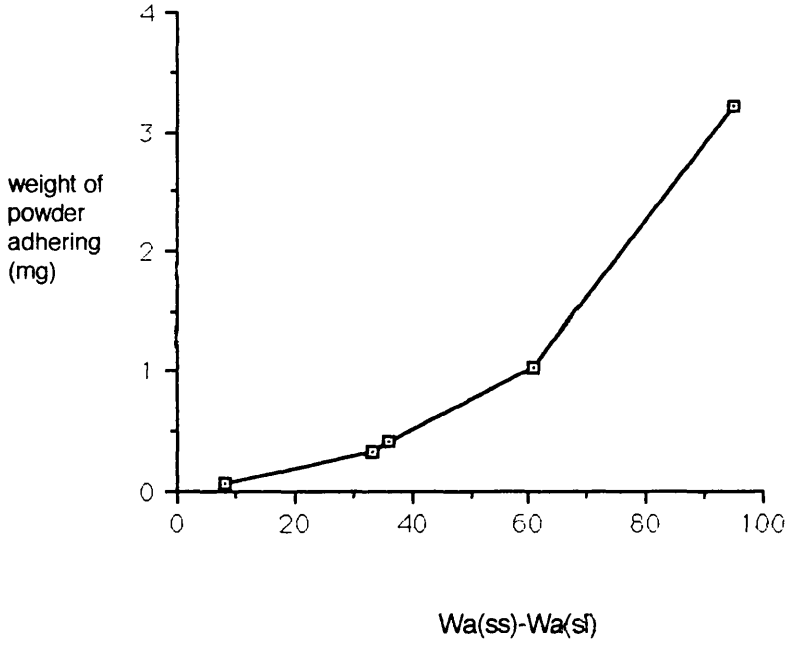

Figure 4.7.7. The extent of powder adhesion to a clean glass container wall as a function of Wa(ss)-Wa(sl).

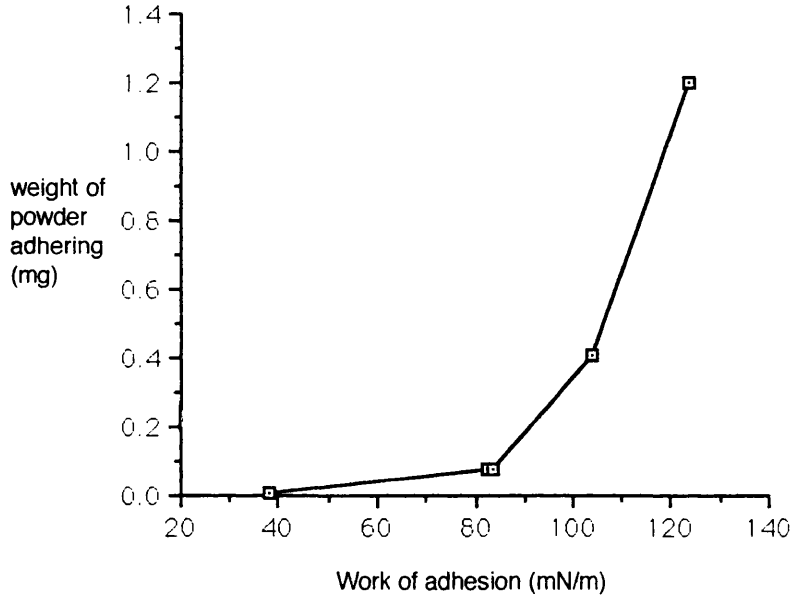

Figure 4.7.8. The extent of powder adhesion to a "repelcoat" coated container wall as a function of the calculated work of adhesion between the powder and surface.

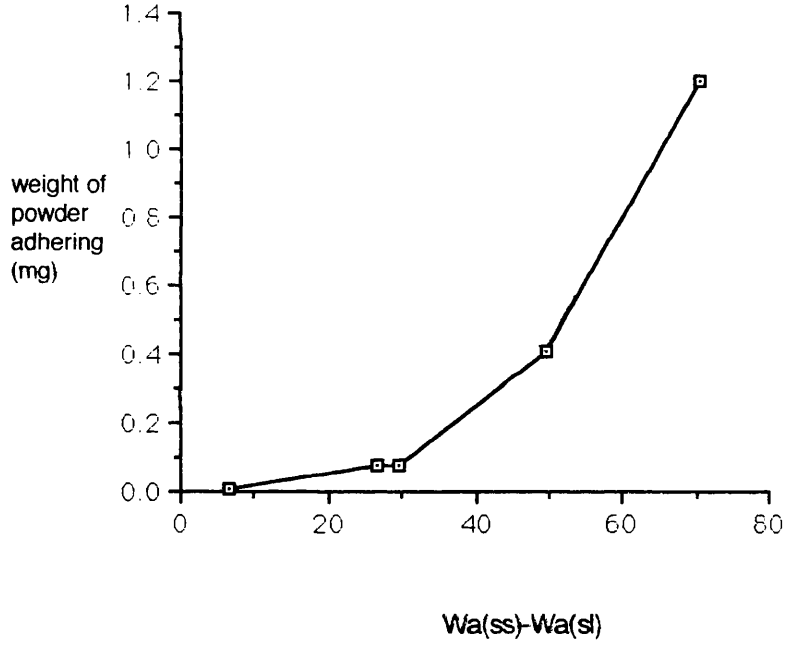

Figure 4.7.9. The extent of powder adhesion to a "repelcoat" coated container wall as a function of Wa(ss)-Wa(sl).

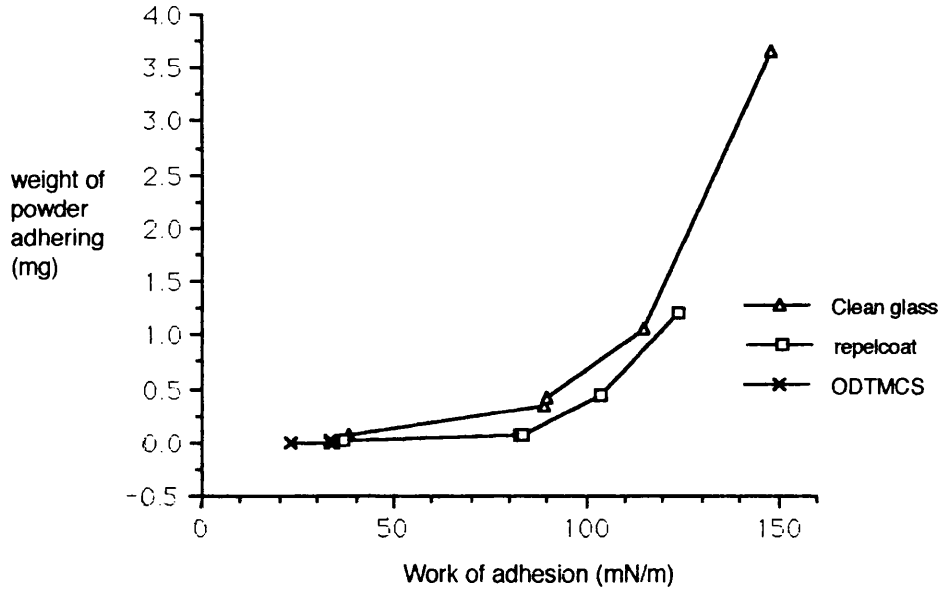

Figure 4.7.10. Relationship between the quantity of powder adhering to various container walls and the work of adhesion between the powder and the container wall.

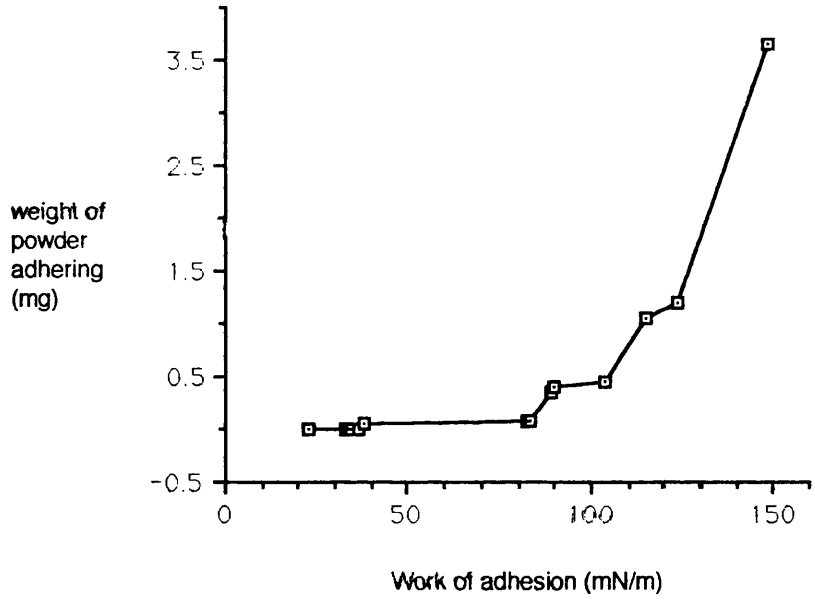

Figure 4.7.11. Relationship between the extent of powder adhesion to container walls and the work of adhesion between the powder and the container wall.

4.7.2. Application of the theory of nonadditive surface tension components (van Oss approach).

A drawback of the theory of nonadditive surface tension components approach (the van Oss approach) is that the characterisation of liquid surface tension parameters is, at present, extremely difficult.

Only a handful of the most commonly used probe liquids have been characterised by van Oss (1989). Consequently, whilst the determination of solid surface energies is relatively straightforward, the determination of interfacial interactions between solids and less commonly used liquids is not possible.

In this study therefore, the application of this approach to practical situations involving a solid/liquid interface has not been performed. However, a determination of the interaction between solid surfaces has been attempted.

4.7.2.1. Degree of aggregation.

The degree of aggregation observed in nonaqueous, nonpolar suspensions of the five powders studied was shown to be related to the polarity of the powder, as calculated by the harmonic mean approach.

Van Oss (1987) predicted that highly monopolar surfaces would exhibit a high degree of repulsion in aqueous media, which in turn would lead to improved dispersion. Van Oss (1987) set arbitrary levels for γ^{p+} and γ^{p-}, below which compounds could be considered a monopole of the opposite sign. For example, a compound

may be considered monopolar for γ^{p-} when its γ^{p+} value is significantly less than 1.

By this reasoning, only isoprenaline of the compounds used cannot be considered monopolar. Isoprenaline exhibits the greatest degree of aggregation of all of the compounds studied and it is therefore possible that monopolarity also leads to improved dispersion in nonaqueous media.

However, the remaining four compounds (indomethacin, aspirin, PTFE and beclomethasone) can all be considered γ^{p-} monopoles, and yet they exhibit varying degrees of aggregation, ranging from 0% increase in suspended particle size (PTFE) to 84% increase in suspended particle size (aspirin). In fact aspirin, by the van Oss (1987) definition is the most monopolar compound of all and yet exhibits the greatest degree of aggregation, after isoprenaline, which suggests that the extent of dispersion of solids in nonaqueous media is influenced by more than just the monopolarity of the solids.

Further, despite the fact that isoprenaline does not fall into the monopolar category as defined by van Oss et al. (1987), the difference between the level of γ^{p+} and γ^{p-} values for isoprenaline is significantly greater than for the other compounds studied (table 4.7.16), and would be expected to improve dispersion of the isoprenaline particles.

All of the compounds used exhibit a greater γ^{p-} value than γ^{p+} value. In the case of aspirin, the

difference is large (15.5) and yet the overall value of γ^{AB} for aspirin is 1.1, giving the impression that aspirin is relatively nonpolar despite the fact that aspirin has a large potential for polar interactions. Therefore, assuming that any water in the nonaqueous suspension will associate with polar solids (given that $\gamma^- = \gamma^+$ for water, which implies that water will associate with γ^+ monopoles to the same extent as γ^- monopoles) it is not surprising that aspirin aggregates to the extent it does.

The difference between the extent of aggregation of PTFE and both indomethacin and beclomethasone in the nonaqueous, nonpolar environment is more difficult to explain. Despite all three having very similar polar parameters of surface energy, indomethacin and beclomethasone both aggregated to a significant extent (table 4.7.12), whereas PTFE showed no sign of aggregating at all.

The magnitude of the apolar component of surface tension, γ^{LW}, may therefore also be exerting some influence on the aggregation process. The value of γ^{LW} is significantly lower for PTFE than for the other solids (table 4.7.12), which would make the solid/liquid interface more favourable for PTFE, reducing the thermodynamic "need" to aggregate.

Table 4.7.16. Components of surface energy for various solids, calculated by the van Oss approach

Solid	γ_s^{LW}	γ_s^{P+}	γ_s^{P-}	γ_s^{AB}	γ_s
Indomethacin	49.9	0.3	1.8	1.4	51.3
Isoprenaline	41.1	7.4	66.6	44.4	85.5
Aspirin	43.9	0.0	15.5	1.1	45.0
Beclomethasone	43.5	0.0	1.8	0.2	43.7
PTFE	21.1	0.1	2.4	0.7	21.8
ODTMCS	5.8	1.8	1.8	3.5	9.3
Repelcoat	32.9	2.7	20.5	14.9	47.8
Glass	38.5	3.0	48.4	24.0	62.5

4.7.2.2. Extent of adhesion to the container wall.

Values of works of adhesion (Wa) between the solids used and various container wall substrates are given in table 4.7.17.

The relationship between the quantity of drug adhering to the container walls (from tables 4.7.13.-4.7.15.) and the various values of Wa obtained from the van Oss approach to surface energy parameter determination is illustrated in figures 4.7.12 and 4.7.13.

The relationship is not as strong as that seen when the work of adhesion is calculated from harmonic mean surface energy data (figures 4.7.6. and 4.7.8.).

However, the similarity in shape of the two lines in figures 4.7.12 and 4.7.13 suggests that a relationship of some sort does exist. Unfortunately, it is not possible to manipulate the data further by taking into account concurrent interfacial interactions when applying van Oss' theory of nonadditive surface tension components since the liquid medium is not characterised.

Table 4.7.17 Estimated Work of Adhesion (W_a) between various solids and container wall substrates.(van Oss approach.)

Solid	Work of Adhesion (W_a) mN/m		
	Clean Glass	Repelcoat	ODTMCS.
Indomethacin	99.7	90.4	38.8
Isoprenaline	145.6	124.9	59.7
Aspirin	96.8	90.1	43.4
PTFE	66.4	80.3	35.4
Beclomethasone	86.5	60.3	26.8

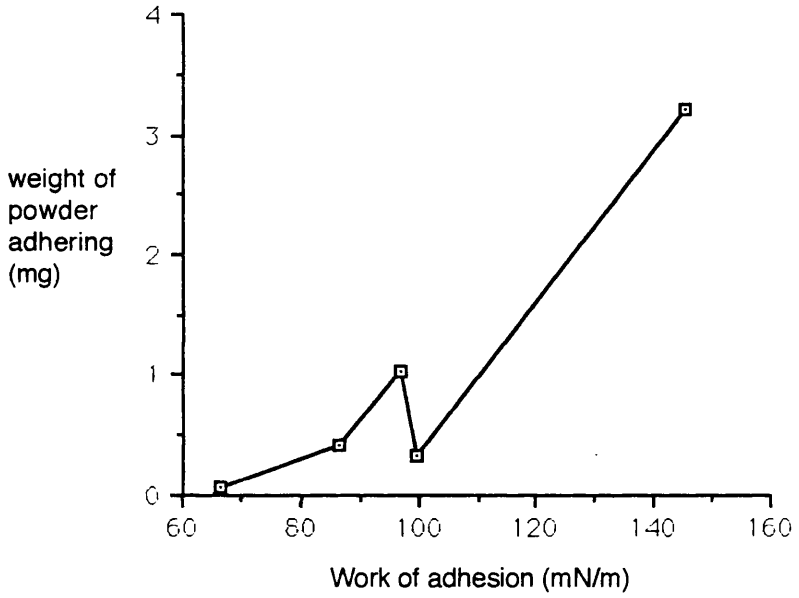

Figure 4.7.12 The extent of powder adhesion to a clean glass container wall as a function of the calculated work of adhesion between the powder and glass. (data from van Oss approach).

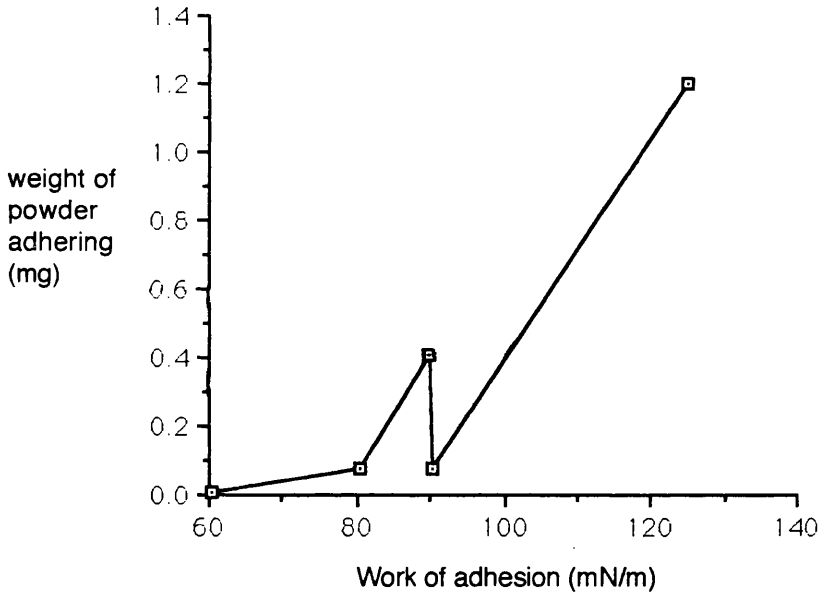

Figure 4.7.13. The extent of powder adhesion to a "Repelcoat" coated container wall as a function of the calculated work of adhesion between the powder and glass. (data from van Oss approach).

4.8. Conclusions

The outcome of various interfacial phenomena occuring in nonaqueous, nonpolar suspensions can be predicted through surface energy considerations.

It is important to recognise that many interfacial events are occuring simultaneously, and the interfacial interactions (e.g. aggregation of particles, adhesion of particles to the container wall) are not mutually exclusive.

Obviously, attempts can be made to eliminate various interfacial events so that others can be studied independently. For example, by coating the glass container with ODTMCS, adhesion to the container wall can be eliminated, allowing the extent of aggregation to be studied alone. However, pharmaceutical formulations are complex systems and for a knowledge of surface and interfacial energies to be a useful formulating tool, it must be possible to predict events in complete systems.

At present, this is not possible using the van Oss theory of nonadditive surface tension components since liquids are not easy to characterise by this method. The ultimate applicability of this method is therefore difficult to assess.

The use of solid surface energies and interfacial energies calculated by the harmonic mean approach, although empirical in origin (Wu, 1982), proved a successful basis for predicting various interfacial events. An aspect of solid surface energy or interfacial energy (or a combination of the two) could always be

found to relate to one of the interfacial phenomena studied (i.e. ease of dispersion, degree of aggregation or extent of adhesion to the container wall).

From the harmonic mean data, the ease of dispersion was found to be related to the work of cohesion for the powders, and the difference between the spreading coefficient of the liquid over the solid and the work of cohesion of the solid.

The degree of aggregation was shown to be unrelated to either the spreading coefficient of the liquid over the solid (and vice versa) or the works of adhesion and cohesion of the powders. Neither could a relationship be seen between the increase in suspended particle size and the difference between the sum of the works of cohesion for the solid and liquid and the work of adhesion between the solid and the liquid.

A relationship was however apparent between the degree of aggregation and the polarity of the solids.

The extent of powder adhesion to the container wall could be related to both the work of adhesion between the two solids, and the difference between the work of adhesion between the powder and suspending liquid and the work of adhesion between the powder and the container wall.

Chapter 5

Conclusions.

It is possible to quantify and potentially predict various interfacial phenomena occuring in nonaqueous nonpolar suspensions by considering the surface and interfacial energies involved.

Despite the indirect means of attaining values for solid surface energies (through measurements of contact angles), the derived values appear to correlate well with interfacial events involving the solid surface.

Contact angles on compressed plates of powder measured using the Wilhelmy plate technique are in good agreement with those obtained by the sessile drop method.

Contact angles obtained for the uncompressed powders using a liquid penetration technique are consistently higher than those generated by the Wilhelmy plate and sessile drop technique on compressed plates of powder, suggesting that the Washburn model for a packed powder bed of a bundle of parallel capillaries does not adequately describe penetration of a liquid through a powder bed.

The rate of liquid penetration through a packed bed of powder appears to be additionally dependent upon the pore geometry.

Using the contact angle data from the Wilhelmy plate technique, solid surface energy values derived for

the compressed plates of powder provide a useful measure of the surface energy of the uncompressed powder when employed empirically.

The harmonic and geometric mean variants of the theory of surface tension components, the theory of nonadditive surface tension components and an equation of state generate comparable values of γ_s for the solids studied.

The derivation of the polar (γ_s^p) and dispersion (γ_s^d) components of surface energy by the harmonic and geometric mean approaches requires contact angle determinations to be made with two liquids. Calculated values of γ_s^p were highly dependent upon the choice of liquid pair with which contact angles were made.

It is advisable to choose one nonpolar liquid of high surface energy along with one polar liquid of high surface tension as the liquid pair, as this increases the likelihood of encompassing the full magnitude of the solid surface interactive forces.

Various aspects of the stability of nonaqueous nonpolar suspensions can be satisfactorily correlated with derived surface and interfacial energy parameters.

Using the harmonic mean variant of the theory of surface tension components, the ease of dispersion of solids in nonaqueous nonpolar media was found to correlate with the work of cohesion of the solid, and the difference between the spreading coefficient of the

liquid over the solid and the work of cohesion of the solid.

The degree of aggregation of the solids in suspension was found to be related to the polarity of the solid surface. The extent of adhesion of the solids to the container wall could be related to both the work of adhesion between the solid and the container wall, and the difference between the work of adhesion between the powder and suspending liquid and the work of adhesion between the powder and the container wall.

Chapter 6

Further work.

6.1. Effect of pore geometry on the rate of liquid penetration.

The possibility of a relationship existing between the contact angles obtained by the Wilhelmy plate technique and those obtained from liquid penetration experiments has not previously been reported, and is worthy of further investigation.

Pore geometry can be altered by using ballotini of different, classified, sizes, coated with a suitable substrate, thus allowing the packing geometry to be changed whilst the surface energy remains constant. The use of a suitable range of probe liquids would allow the effect of pore geometry to be assessed in a controlled manner.

6.2. The theory of nonadditive surface tension components.

The van Oss theory of nonadditive surface tension components is an interesting extension of the fundamental theory that surface energy can be subdivided into components.

The theory of nonadditive surface tension components can, for example, justify the existence of monopolar solids and liquids which although apparently apolar are capable of strong interaction with bipolar compounds, or monopoles of the opposite sign.

The application of the theory of nonadditive surface tension components is, at present, limited by the lack of data available for liquids and the

difficulties associated with the elucidation of such information.

The potential exists, however, for the behaviour of two and three component systems to be critically assessed in terms of surface and interfacial energy by this method, particularly dispersion effects (due to monopolar repulsion/attraction), solubility and the mechanism of action of protective colloids.

6.3. Manipulation of the solid surface.

The influence of solid surface energy on the behaviour of various solids in suspension has been demonstrated in chapter 4 of this thesis.

The potential therefore exists for the surface energy of a solid to be altered in order to control its behaviour in certain situations.

Manipulation of the solid surface through different milling techniques has been shown by Buckton et al. (1988) to alter the solid surface energy.

The customisation of solid surface energy through controlled crystallisation may be a more manageable means of producing a solid with the desired surface characteristics.

Modifying the crystallisation media, adding impurities and using a variety of salting-out agents are all means by which the surface energy of the solid could potentially be altered in a controlable manner.

6.4. Pharmaceutical applications of surface energy values.

By definition, all pharmaceutical formulations consist of two of more excipients. Since all interactions begin with the meeting of surfaces to form an interface, the potential application of surface energy data in the pharmaceutical field is limitless.

Some of the more relevent applications may be to assess the adhesion of powders to powders in dry powder inhaler formulations or to investigate the adsorbtion of colloids onto solids in suspension. The often neglected interaction between excipients and packaging components can also be readily studied in terms of surface energies.

Ultimately, the interaction between drugs and the body may be quantifiable. For example, can the surface energy of a poorly bioavailable drug be altered to increase its solubility in vivo? Or, alternatively, can the adhesion to the gut mucosa of a poorly absorbed drug be influenced to increase the gastro-intestinal transit time?

References Cited.

REFERENCES CITED.

Adam, N. K., (1941), in: *The Physics and Chemistry of Interfaces*, 3rd. Edn., Lowe and Brydone, London.

Adam, N. K., (1964), Adv. Chem. Ser., **43**, 52-56.

Adam, N. K., Jessop, G, (1925), J. Chem. Soc., **127**, 1863-1868.

Adamson, A. W., (1982), in: *Physical Chemistry of Surfaces*, 4th edn., Wiley, New York.

Adamson, A. W., (1990), in: *Physical Chemistry of Surfaces*, 5th edn., Wiley, New York.

Andrade, J. D., Ma, S. M., King, R. N., Gregonis, D. E., (1979), J. Colloid Interface Sci., **72**, 488-494.

Aveyard, R., Heydon, D. A., (1973), in: *An Introduction to the Principles of Surface Chemistry*, Cambridge University Press, Cambridge.

Bargeman, D., (1972), J. Colloid Interface Sci., **40**, 344-348.

Bartell, F. E., Shepard, J. W., (1953), J. Phys. Chem., **57**, 211.

Bartell, F. E., Zuidema, H. H., (1936), J. Amer.Chem Soc., **58**, 1449-1456.

Becher, P., (1977), J. Colloid Interface Sci., **59**, 429-432.

Bernett, M. K., Zisman, W. A., (1959), J. Phys. Chem., **63**, 1241-1246.

Bikerman, J. J., (1950), J. Phys. Colloid Chem., **54**, 653.

Bikerman, J. J., (1957), Proc. 2nd. Int. Cong. Surface activity, London, **3**, 125.

Birdi, K. S., (1982), J. Colloid Interface Sci., **88**, 290-293.

Blake, P., Ralston, J., (1985), Colloids and Surfaces, **15**, 101-118.

Bleier, A., (1983a), J. Amer. Cer. Soc., **66**, C-79 - C-81.

Bleier, A., (1983b), J. Phys. Chem., **87**, 3493-3500.

Buckton, G., (1985), Ph.D. Thesis, London University.

Buckton, G., (1988), Int. J. Pharm., **44**, 1-8.

Buckton, G., (1990), Powder Technol, **61**, 237-249.

Buckton, G., Newton, J. M., (1985), J. Pharm. Pharmacol., **37**, 605-609.

Buckton, G., Newton, J. M., (1986a), J. Pharm. Pharmacol., **38**, 329-334.

Buckton, G., Newton, J. M., (1986b), Powder Technol., **46**, 201-208.

Buckton, G., Newton, J. M., (1986c) in Gorrod et al, *Development of drugs and modern medicines*, Ellis Horwood Ltd., Chichester, p421.

Buckton, G., (1988), Int. J. Pharm., **44**, 1-8.

Buckton, G., Choularton, A., Beezer, A. E., Chatham, S. M., (1988), Int. J. Pharm., **47**, 121-128.

Carli, F., Simioni, L., (1978), Pharm. Acta Helv., **53**, 320-326.

Carli, F., Simioni, L., (1979), J. Pharm. Pharmacol., B, 128.

Cassie, A. B. D., (1948), Discuss. Faraday Soc., **3**, 11-16.

Cassie, A. B. D., Baxter, S, (1944), Trans. Faraday Soc., **40**, 546-551.

Cazabat, A. M., Cohen Stuart, M. A., (1986), J. Phys. Chem., **90**, 5845-5849.

Cazabat, A. M., Heslot, F., (1990), Colloids and Surfaces, **51**, 309-322.

Cook, D. T., Grant, D. J. W., Newton, J. M., (1977), J. Pharm. Pharmacol., **29**, Suppl., 62P.

Crawford, R., Koopal, L. K., Ralston, J., (1987), Colloids and Surfaces, **27**, 57-64.

Cutie, A. J., Ertefaie, S., Sciarra, J. J., (1985), Aerosol Age, August 1985, 52-54.

Dalal, E., (1987), Langmuir, **3**, 1009-1015.

Dann, J. R., (1970a), J. Colloid Interface Sci., **32**, 302-320.

Dann, J. R., (1970b), J. Colloid Interface Sci., **32**, 321-331.

Davies, M. C., (1985), Ph.D. Thesis, London University

de Gennes, P. G., (1985), Rev. Mod. Phys., **57**, 827-862.

Dettre, R. H., Johnson, JR., R. E., Adv. Chem. Ser., **43**, 136-144.

Driedger, O., Neumann, A. W., Sell, P. J., (1965), Kolloid-Zeitschrift and Zeitschrift for polymers, **201**, 52-57.

Dullien, F. A. L., (1979), *Porous media; fluid transport and pore structure*, Academic Press, London.

Duncan-Hewitt, W.C. et al, (1989), Colloids and Surfaces, **42**, 391-403.

Dupré, A., (1869), *Theorie Mechanique de la Chaleur, Gaultier-Villars, Paris*. Through: Adamson, A. W., (1982).

Elliott, G. E. P., Riddiford, A. C., (1967), J. Colloid Interface Sci., **23**, 389-398.

El-Shimi, A., Goddard, E. D., (1974), J. Colloid Interface Sci., **48**, 242-248.

Erick, J. D., Good, R. J., Neumann, A. N., (1975), J. Colloid Interface Sci., **53**, 235-248.

Fell, J. T., Efentakis, E., (1979), Int. J. Pharm., **4**, 153-157.

Fisher, L. R., Lark, P. D., (1979), J. Colloid Interface Sci., **69**, 486-492.

Fisher, L. R., Lark, P. D., (1980), J. Colloid Interface Sci., **76**, 251-253.

Fort Jr., T., (1964), Adv. Chem. Ser., **43**, 302-309.

Fort Jr., T., Patterson, H. T., (1963), J. Colloid Sci., **18**, 217-222.

Fowkes, F. M., (1962a), J. Phys. Chem., **66**, 382.

Fowkes, F. M., (1962b), J. Phys. Chem., **66**, 1863-1866.

Fowkes, F. M., (1963), J. Phys. Chem., **67**, 2538-2541.

Fowkes, F. M., (1964), Adv. Chem. Ser., **43**, 99-111.

Fowkes, F. M., (1968) J. Colloid Interface Sci., **28**, 93-505.

Fowkes, F. M., (1968), J. Phys. Chem., **72**, 3700.

Fowkes, F. M., Riddle Jr., F. L., Pastore, W. E., Weber, A. A., (1990), Colloids and Surfaces, **43**, 367-387.

Fox, H. W., Zisman, W. A., (1950), J. Colloid Sci., **15**, 514-531..

Fox, H. W., Zisman, W. A., (1952a), J. Colloid Sci., **109**, 109-121.

Fox, H. W., Zisman, W. A., (1952b), J. Colloid Sci., **7**, 428-442.

Gaines Jr., G. L., J. Colloid Interface Sci., (1977), **62**, 191-192.

Gaydos, J., Moy, E., Neumann, A. W., (1990), Langmuir, **6**, 885-892.

Glasstone, S., Lewis, D., (1960), in: *Elements of Physical Chemistry*, 2nd Edn., Macmillan Co., Hong Kong.

Good, R. J., (1953), J. Phys. Chem., **74**, 5040-5042

Good, R. J., (1964), Adv. Chem. Ser., **43**, 74-87.

Good, R. J., (1977), J. Colloid Interface Sci., **59**, 398-419.

Good, R. J., (1979), in: *Surface and Colloid Science*, Vol.2, Eds. Good, R. J., Stromberg, R. R., Plenem Press, New York.

Good, R. J., Girifalco, L. A., Kraus, G., (1958), J. Phys. Chem., **62**, 1418-1421.

Good, R. J., Girifalco, L. A., (1957), J. Phys. Chem., **61**, 904-909.

Good, R. J., Girifalco, L. A., (1960), J. Phys. Chem., **64**, 561-565.

Good, R. J., (1973), J. Colloid Interface Sci., **42**, 473-477.

Good, R. J., (1952), J. Phys. Chem., **74**, 5041-5042.

Good, W. R., (1973), J. Colloid Interface Sci., **44**, 63-71.

Hansford, D. T., Grant, D. J. W., Newton, J. M., (1980a), Powder Technol., **26**, 119-126.

Hansford, D. T., Grant, D. J. W., Newton, J. M., (1980b), J. C. S. Faraday I, **76**, 2417-2431.

Heertjes, P. M., Kossen, N. W. F., (1967), Powder Technol., **1**, 33-42.

Heertjes, P. M., Witvoet, W. C., (1970), Powder Technol., **3**, 339-343.

Hiestand, E. N., (1966), J. Pharm. Sci., **55**, 1325-1344.

Jasper, J. J., (1972), J. Phys. Chem. Ref. Data, **1**, 841.

Jenson, W. B. (1980), In: *The Lewis Acid-Base Concepts*; Wiley-interscience: New York.

Johnson, Jr., R. E., Dettre, R. H., (1964), Adv. Chem. Ser., **43**, 112-135.

Johnson, Jr., R. E., Dettre, R. H., (1969), in: *Surface and Colloid Sci.*, Vol.2, Ed. Matijevic, E., Academic Press, New York.

Johnson, Jr., R. E., Dettre, R. H., (1989), Langmuir, **5**, 293-295

Kaeble, D. H., (1969), J. Adhes., **1**, 102-123.

Kaeble, D. H., (1971), in: Physical Chemistry of Adhesion, Wiley Interscience, New York.

Kanig, J. L., and Cohn, R. M., (1962), Proc. Sci. Sec. Am. Toil. Goods Ass., **37**, 19-26.

Kinloch, A. J., (1980), J. Mat Sci, **15**, 2141-2166.

Kitazaki, Y., Hata, T., (1972), J. Adhes., **4**, 123-130.

Ko, Y. C., Ratner, B. D., Hoffman, A. S., (1981), J. Coll. Int. Sci., **82**, 25-37.

Kollman, P., (1977), J. Am. Chem. Soc., **99**, 4875-4894.

Kossen, N. W. F., Heertjes, P. M., (1965) Chem. Eng. Sci., **20**, 593-599.

Lavielle, L., Schultz, J., (1985), J. Colloid Interface Sci.,**106**, 438-445.

Lerk, C. F., Lagas, M., Boelstra, J. P., Broersma, P., (1977), J. Pharm. Sci., **66**, 1480-1481.

Lerk, C. F., Schoonen, A. J. M., Fell, J. T., (1976), J. Pharm. Sci., **65**, 843-847.

Levine, S., Neale, G. H., (1975), Trans. Faraday Soc., **71**, 12-18.

Li, D., Neumann, A. W., (1992), J. Colloid Interface Sci., **148**, 190-200.

Liao, W-C., Zatz, J. L., (1979a), J. Pharm. Sci., **68**, 486-488.

Liao, W-C., Zatz, J. L., (1979b), J. Pharm. Sci., **68**, 488-494.

Lieberman, H. A., Rieger, M. M., Banker, G. S., (1989), in: *Pharmaceutical dosage forms: Disperse systems, Volume 2*, 1st Edn.,Marcel Dekker Inc., New York.

MacDougall, G., Ockrent, C., (1942), Proc. Royal Soc. A., **10**, 157-173.

Marmur, A., (1992), Adv. Coll. Int. Sci., **39**, 13-33.

Martin, A., Swarbrick, J., Cammarata, A., (1983), in: *Physical Pharmacy*, 3rd Edn., Lea & Febiger, Philadelphia.

Melrose, J. C., (1964), Adv. Chem. Ser., **43**, 158-179.

Melrose, J. C., (1965), J. Colloid Sci., **20**, 801-821.

Moy, E., Li, D., (1992), Adv. Coll. Int. Sci., **39**, 257-297.

Moy, E., Neumann, A. W., (1990), Colloids. Surf., **43**, 349-365.

Netzer, L., Sagiv, J., (1983), J. Amer. Chem. Soc., **105**, 674-688.

Neumann, A. W., (1974), Adv. Colloid Interface Sci., **4**, 105-191.

Neumann, A. W., (1978), in: *Wetting, Spreading and Adhesion*, Ed. Padday, J. F., Academic Press, London.

Neumann, A. W., Renzow, D. R., Reumuth, H., Richter, I. E., (1971), Fortschr. Kolloide Polymere, **55**, 49-54.

Neumann, A. W., Good, R. J., (1972), J. Colloid Interface Sci., **38**, 341-358.

Neumann, A. W., Good, R. J., (1979), in *Surface and Colloid Science*, Vol.2. Eds. Good R. J. and Stromberg, R. R., Plenem Press, New York.

Neumann, A. W., Good, R. J., Hope, C. J., Sejpal, M., (1974), J. Colloid Interface Sci., **49**, 291-304.

Neumann, A. W., Omenyi, S. N., van Oss, C. J., (1979), Colloid & Polymer Sci., **257**, 413-419.

Neumann, A. W., Spelt, J. K., Smith, R. P., Francis, D. W., Rotenberg, Y., Absolom, D. R., (1984), J. Colloid Interface Sci., **102**, 278-284.

Odidi, I. O., (1990), Ph.D. Thesis, London University.

Odidi, I. O., Newton, J. M., Buckton, G., (1991), Int. J. Pharm., **72**, 43-49.

Omenyi, S. N., Neumann, A. W., van Oss, C. J., (1981), J. Appl. Phys., **52**, 789-795.

Osterhof, H. J., Bartell, F. E. V., (1930), Phys. Chem., **34**, 1399.

Owens, D. K., Wendt, R. C., (1969), J. Appl. Polym. Sci., **13**, 1740-1747.

Padday, J. F., (1963), in: *Wetting, spreading and adhesion*, Ed. Padday, J.F., Academic Press, London.

Padday, J. F., (1969), in: Surface and Colloid Sci., Vol.I, Ed. Matijevic, E., Academic Press, New York.

Padday, J. F., Russell, D. R., (1960), J. Colloid Interface Sci., **15**, 503-511.

Parfitt, G. D., (1973), in: *Dispersion of Powders in Liquids*, 2nd Edn., Applied Science, England.

Parfitt, G. D., Sing, K. S. W., (1976), in: *Characterization of Powder Surfaces*, Academic Press, London.

Patton, T. C., (1966), in: *Paint Flow and Pigment Dispersion*, Interscience, London.

Pease, D. C., (1945), J. Phys. Chem., **49**, 107-110.

Penn, L. S., Miller, B., (1980a), J. Colloid Interface Sci.,**77**, 574-576.

Penn, L. S., Miller, B., (1980b), J. Colloid Interface Sci., **78**, 238-241.

Pyter, R. A., Zografi, G., Mukerjee, P., (1982), J. Colloid Interface Sci., **89**, 144-153.

Quincke, P., (1859), Ann. Physik., **108**, 326.

Ranucci, J. A., Dixit, S., Bray, Jr., R. N., Goldman, D., (1990), Pharm. Technol., April, 68-74.

Rowe, R. C., (1988a), Int. J. Pharm., **41**, 219-222.

Rowe, R. C., (1988b), Int. J. Pharm., **41**, 223-226.

Rowe, R. C., (1989), Int. J. Pharm., **52**, 149-154.

Rowe, R. C., (1990), Int. J. Pharm., **58**, 209-213.

Sanders, P. A., (1979), in: *Handbook of Aerosol Technology*, 2nd. Edn., van Nostrand Reinhold Co., New York.

Schroder, J., (1984), Prog. in Organic Coatings, **12**, 159-180.

Shafrin, E. G., Zisman, W. A., (1960), J. Phys. Chem., **64**, 519-524.

Shafrin, E. G., Zisman, W. A., (1964), Adv. Chem. Ser., **43**, 145-157.

Shepard, J. W., Bartell, F. E., (1953), J. Phys. Chem., **57**, 458.

Shuttleworth, R., Bailey, G. L. J., (1948), Discussions Faraday Soc., **3**, 16.

Spaarnay, M. J., (1983), J. Colloid Interface Sci., **91**, 307-319.

Spelt, J. K., (1990), Colloids and Surfaces, **43**, 389-411.

Spelt, J. K., Absolom, D. R., Neumann, A. W., (1986), Langmuir, **2**, 620-625.

Spelt, J. K., Neumann, A. W., (1987), Langmuir, **3**, 588-591.

Studebaker, M. L., Snow, C. W., (1955), J. Phys. Chem., **59**, 973-976.

Tabor, D., Winterton, R. H. S., (1968), Nature, **219**, 1120-1121.

Taylor, C. P. S., (1984), J. Colloid Interface Sci., **100**, 589-594.

van Damme, H. S., Hogt, A. H., Feijen, J., (1986), J. Colloid Interface Sci., **114**, 167-172.

van Oss, C. J., Chaudhury, M. K., Good, R. J., (1987), Adv. Coll. Int. Sci., **28**, 35-64.

van Oss, C. J., Giese, Jr., R. F., Good, R. J., (1990), Langmuir, **6**, 1711-1713.

van Oss, C. J., Good, R. J., (1989), J. Macromol. Sci. - Chem., **A26**, 1183-1203.

van Oss, C. J., Good, R. J., Chaudhury, M. K., (1986), J. Colloid Interface Sci., **111**, 378-390.

van Oss, C. J., Good, R. J., Chaudhury, M. K., (1988), Langmuir, **4**, 884-891.

van Oss, C. J., Ju, L., Chaudhury, M. K., Good, R. J., (1989), J. Colloid Interface Sci., **128**, 313-319.

Veale, C. R., (1972), in: *Fine Powders; preparation, properties and uses*, Applied Science, Barking.

Ward, C. A., Neumann, A. W., (1974), J. Colloid Interface Sci., **49**, 286-290.

Washburn, E. W., (1921), Phys. Rev., **17**, 273-283.

Weiser, H. B., (1949), in: *Colloid Chemistry*, 2nd Edn., Wiley, New York.

Wells, J. I., Walker, C. V., (1983), Int. J. Pharm., **15**, 97-111.

Wenzel, R. N., (1936), Ind. Eng. Chem., **28**, 988-994.

Wilhelmy, L., (1863), Ann. Physik., **119**, 177.

Wu, S., (1969), J. Phys. Chem., **74**, 632-638.

Wu, S., (1969), J. Colloid Interface Sci., **31**, 153-161.

Wu, S., (1971), J. Polym. Sci. Part C, **34**, 19-30.

Wu, S., (1973), J. Adhes., **5**, 39-55.

Wu, S., (1979), J. Coll. Int. Sci., **71**, 605-609.

Wu, S., Brzozowski, K. J., (1971), J. Colloid Interface Sci., **37**, 686-690.

Yang, Y-W., Zografi, G., (1986), J. Pharm. Sci., **75**, 719-721.

Yang, Y-W., Zografi, G., Miller, E. E., (1988), J. Colloid Interface Sci., **122**, 35-46.

Young, S. A., Buckton, G., (1990), Int. J. Pharm., **60**, 235-241.

Zajic, L., Buckton, G., (1990), Int. J. Pharm., **59**, 155-164.

Zatz, J. L., (1985), J. Soc. Cosmet. Chem., **36**, 393-411.

Zisman, W. A., (1964), Adv. Chem. Ser., **43**, 1-51.

Zisman, W. A., (1975), in: *Adhesion Science and Technology*, Ed. Lee, L. H., Plenem Press, New York.

Zografi, G., Johnson, B. A., (1984), J. Colloid Interface Sci., **22**, 159-176.

Zografi, G., Tam, S. S., (1976), J. Pharm. Sci., **65**, 1145-1149.

Zografi, G., Yalkowsky, S. H., (1974), J. Pharm. Sci., **63**, 1533-1536.